Targeting Mechanisms of Secretory Carrier Membrane Protein 1 in Tobacco BY-2 Cells

CAI, Yi

A Thesis Submitted in Partial Fulfillment

of the Requirements for the Degree of

Doctor of Philosophy

in

Biology

The Chinese University of Hong Kong

September 2010

Thesis/Assessment Committee

Prof. Yum Shing Wong	(Chair)
Prof. Liwen Jiang	(Thesis Supervisor)
Prof. Dianjing Guo	(Committee Member)
Prof. Jun Xia	(External Examiner)

Statement

All experiment works reported in this thesis were performed by the author, unless specially stated otherwise in the text.

CAI Yi

Abstract

Abstract of thesis entitled:

Targeting mechanisms of secretory carrier membrane protein 1 in tobacco BY-2 cells

Submitted by CAI, Yi

For the degree of Doctor of Philosophy

At the Chinese University of Hong Kong in September 2010

Little is known about the trafficking mechanism of plasma membrane (PM) proteins in the endomembrane system of plant cells that contain several membrane-bound organelles including the endoplasmic reticulum (ER), Golgi, trans-Golgi network (TGN) ot early endosome (EE), prevacuolar compartment (PVC) or late endosome (LE). Here, I study the transport pathway and sorting signals of secretory carrier membrane protein 1 (SCAMP1) by following its transient expression in tobacco BY-2 protoplasts and show that SCAMP1 reaches the PM via an ER-Golgi-TGN-PM pathway. Loss-of-function and gain-of-function analysis of various GFP fusions with SCAMP1 mutations further demonstrates that: 1) the cytosolic N terminus of SCAMP1 contains an ER export signal; 2) the transmembrane domain 2 (TMD2) and TMD3 of SCAMP1 are essential for Golgi export; and 3) SCAMP1 TMD1 is essential for TGN-to-PM targeting. Therefore, both the cytosolic N-terminus and TMD sequences of SCAMP1 play integral roles in mediating its transport to the PM via an ER-Golgi-TGN pathway.

Brefeldin A (BFA) has been a useful tool for studying organelle dynamics and protein trafficking in plant cells. Using several Golgi (MAN1 and GONST1) and TGN (SCAMP1 and SYP61) fluorescent protein markers as tools, I have showed that BFA-induced aggregates from Golgi apparatus and TGN are morphologically distinct in the same plant cells. In addition, the internalized endosomal marker FM4-64 colocalized with the TGN-derived aggregates but separated from the Golgi aggregates. In the presence of the endocytosis inhibitor tyrphostin A23, SCAMP1 and FM4-64 are largely excluded from the TGN SYP61-positive BFA-induced aggregates, indicating homotypic fusion of TGN rather than de novo endocytic trafficking is important for the formation of TGN/EE-derived BFA-induced aggregates. Since the TGN also serves as an EE receiving materials from plasma membrane continuously, these data therefore support the notion that the secretory Golgi organelle is distinct from the endocytic TGN/EE in response to BFA treatment in plant cells.

摘要

目前我们对于细胞膜蛋白运输机理的认知非常有限。在论文当中，我利用烟草原生质体研究了 SCAMP1 蛋白去细胞膜的运输途径，发现它是通过内质网-高尔基体-反式高尔基网的途径到细胞膜。通过缺失和突变分析，我发现 SCAMP1 具有多个信号序列：1) SCAMP1 蛋白的 N 端含有一段出内质网的信号；2) 第二和第三个跨膜区含有通过高尔基体的信号；3) SCAMP1 的第一个跨膜区对反式高尔基网到细胞膜的运输是必须的。因此，SCAMP1 蛋白定位于胞质区的 N 端和几个跨膜区都对它的运输非常重要。通过使用高尔基和反式高尔基网的蛋白标记，我发现布雷菲尔德菌素诱导的高尔基体和反式高尔基网是不同的聚集体。进一步使用内吞作用抑制剂酪氨酸磷酸化抑制剂 A23 处理细胞发现反式高尔基网聚集体的形成不依赖于内吞作用，而是通过反式高尔基网之间的相互聚集形成的。

Acknowledgements

First of all, I would like to take this opportunity to specially thank my supervisor, Prof. Liwen Jiang, for offering me the chance to study in his lab. I am grateful for his precious guidance, encouragement, kindly concern and patience throughout my postgraduate study.

I would also like to express my gratitude to the members of my thesis committee Prof. Dianjing Guo, Prof. Yum Shing Wong and Prof. Jun Xia, for their insightful advice and comments on my thesis.

The incessant support, sharing and assistance from all my labmates in CSLB LG101 and LG103 (Louise Lo, Dr. Junqi Wang, Dr. Yu Chung Tse, Angela Yu, Dr. Hongye Li, Dr. Yansong Miao, Dr. Jason Lam, Fudi Zhong, Dr. Lei Yang, Keith Li, Melody, Dr. Christine Yu, Angus, Caiji Gao, Yu Ding, Tianran Jia, Yong Cui, Pan Hu, Juan Wang, Xiangfeng Wang, Jinbo Shen, Hao Wang, Xiaohong Zhuang and Eric Suen) gave me great helps in conducting my researches. Moreover, my appreciation also goes to many parties in the department of biology (technicians in TeamA, C and D, especially Freddie Kwok) for their technical and emotional support.

Last but not least, I would like to thank my dearest parents (Lichen Yi and Guiying Cai), my wife (Yan Xue), my cousins (Li Cai, Lina Cai and Heng Cai) and my best friends (Sheng Wang) giving me strength to finish my study.

Table of Contents

List of Tables

List of Figures

List of Abbreviations

BFA	Brefeldin A
CCV	Clathrin coated vesicle
ConcA	Concanamycin A
CT	C-terminus
EE	Early endosome
ER	Endoplasmic reticulum
GFP	Green fluorescent protein
ImmunoEM	Immunocytochemical electron microscopy
LE	Late endosome
LV	Lytic vacuole
Man1	Mannosidase1
MVB	Multivesicular bodies
NT	N-terminus
PM	Plasma membrane
PVC	Prevacuolar compartment
RFP	Red fluorescent protein
SCAMP	Secretory carrier membrane protein
SN26	SCAMP1 N terminus 26 amino acid
SP	Signal peptide
TGN	*trans*-Golgi network
TMD	Transmembrane domain

VSR	Vacuolar sorting receptor
YFP	Yellow fluorescent protein

CHAPTER 1

General Introduction

1.1 The Plant Secretory and Endocytic Pathways

Plant cells contain three major compartments, the endoplasmic reticulum (ER), lytic vacuole (LV) and plasma membrane (PM), and a bunch of membrane bound organelles that are responsible for mediating the connection between them. Corresponding to the three major compartments, three major pathways (ER to LV, ER to PM and PM to LV) coexist in the same plant cell.

Among these pathways, protein trafficking from ER to LV is best established. It has been generally accepted that proteins destined for the plant secretory pathway are synthesized in the ER and transported to the Golgi apparatus where they could get various kinds of modifications such as glycosylation and methylation. To reach the LV, proteins leaving from the Golgi have to travel through an intermediate organelle termed prevacuolar compartment (PVC). However, how the Golgi apparatus is connected with the PVC remains unclear. Vacuolar sorting receptors (VSRs) are type I transmembrane proteins that involved in the transport of hydrolytic enzymes from Golgi to LV. VSRs are initially purified from clathrin coated vesicles (CCVs) of pea and later on proved to be localized on the *trans*-Golgi cisternae and the PVC (Kirsch et al., 1994; Sanderfoot et al., 1998; Li et al., 2002; Tse et al., 2004; Hinz et al., 2007). The biological function of VSRs and their unique localizations suggest that VSRs are transported from the Golgi to the PVC via CCV. Interestingly, recent ultrastructural studies found that CCVs are not directly initiated from the Golgi but from the *trans*-Golgi network (TGN) (Lam et al., 2007b; Staehelin and Kang, 2008), leading to the popular notion that TGN could be the intermediate organelle between Golgi

and PVC.

The PM to LV pathway, also known as the endocytic pathway, is less well clarified. Following the uptake of a lipophilic styryl dye, FM4-64, plant TGN has been proved to be the first endocytic compartment labeled with the internalized FM4-64, whereas the labeling of the dye on the PVC and LV appears to be much slower (Dettmer et al., 2006; Lam et al., 2007b; Chow et al., 2008). Based on the order of FM4-64 labeling, TGN was put upstream of the PVC in the endotytic pathway and termed as the early endosome (EE) while PVC was designated as a downstream organelle and termed as the late endosome (LE). However, although such concept is generally accepted by the plant biologists, we could not exclude the possibility that the plant TGN is not actually functional upstream of PVC but the trafficking of FM4-64 to TGN is achieved by a different route and simply faster than that of the PVC.

The biosynthetic pathway from ER to PM is the most controversial one among these three pathways. Based on the current data, proteins can reach the PM from either the Golgi apparatus, the TGN or even the PVC (Foresti and Denecke, 2008). Concanamycin A (ConcA) is a V-ATPase inhibitor that could affect the function of VHA-a1 at the TGN (Dettmer et al., 2006). In the ConcA treatment, an integrated PM protein, BRI1, was significantly trapped within some intracellular organelles, thus indicating that the TGN could directly communicate with the PM (Dettmer et al., 2006; Viotti et al., 2010). However, when subcellular localization studies were performed with RabE1d and RabA4b, small GTPases involingd in the secretion of

soluble cargoes in plant cells (Preuss et al., 2004; Zheng et al., 2005), these two molecules were located to the Golgi apparatus but not the TGN (Preuss et al., 2004; Zheng et al., 2005). Moreover, when a PVC-localized syntaxin PEP12/SYP21 was overexpressed, Amy-spo, a soluble cargo aiming at the LV, was partially secreted (Foresti et al., 2006). Therefore, it remains controversial about the detailed pathway from ER to PM.

1.2 Sorting signals of PM proteins

PM is a major compartment in plant cells that harbors thousands of proteins for various biological functions such as cell-cell or cell-environment communication (Alexandersson et al., 2004; Marmagne et al., 2004; Nuhse et al., 2007). To maintain a proper function of PM, its protein content is regulated by both biosynthetic and degradative pathways.

For the biosynthetic pathway of PM proteins, when single transmembrane domain (TMD) with different lengths of 17, 20 or 23 amino acids was fused with a soluble reporter, the green fluorescent protein (GFP), the resulting chimera reached the ER, Golgi or PM respectively (Brandizzi et al., 2002). Such observation indicated that the length of TMD could provide the minimal information deciding the final destination of proteins along the synthetic pathway of PM owing to the thickness and composition of different membranes (Brandizzi et al., 2002). However, sorting of polytopic PM proteins may follow a different way, since special sequences are required for their export from ER or Golgi (Lefebvre et al., 2004; Sieben et al., 2008;

Zelazny et al., 2008).

For the degradative pathway of PM proteins, sorting signals regulating this process are largely unknown. Following the internalization of FLAGELLIN SENSITIVE2 (FLS2), it has been suggested that the internalization of FLS2 is regulated by the ubiquitin signal (Robatzek et al., 2006; Gohre et al., 2008). However, this may only be specific for ligand-induced PM protein degradation but not the constitutive degradation of other PM proteins.

1.3 Secretory carrier membrane protein 1 (SCAMP1)

Secretory carrier membrane proteins (SCAMPs) were initially identified in mammalian cells from rat parotid secretion granule membranes (Brand et al., 1991). Later on, they were also found in the PM, TGN and vesicles that are internalized from and recycled back to the PM (Brand and Castle, 1993; Castle and Castle, 2005). When SCAMP1 was knocked out from the mice, the execution of stable exocytosis was affected in mast cells, suggesting that it may function in the formation of stable fusion pores (Fernandez-Chacon et al., 1999). Moreover, the N-terminus of SCAMP1 could bind to intersectin 1, which is involved in endocytic budding at the plasma membrane, and gamma-synergin, which may mediate the budding of vesicles in the TGN. Expression of SCAMP1 lacking the N-terminal NPF repeats inhibited transferrin uptake by endocytosis (Fernandez-Chacon et al., 2000). Therefore, both the localization and functional studies point out an important role of SCAMP1 in endomembrane trafficking of mammalian cells.

Recently, we have cloned the rice SCAMP1 cDNA which shares high similarity with the animal SCAMPs (Lam et al., 2007b). Drug treatment, confocal immunofluorescent and immunocytochemical electron microscopy (immunoEM) studies demonstrated that YFP-SCAMP1 and SCAMP1-YFP fusions as well as SCAMP1 localized to both the PM and TGN (Lam et al., 2007b). Further studies with two protein trafficking inhibitors, tyrphostin A23 and brefeldin A (BFA), that influence the endocytic or recycling pathway respectively in plant cells, showed that SCAMP1 is actively recycling between these two compartments (Lam et al., 2009). Thus, our previous studies suggest that SCAMP1 could be an excellent marker to be used for understanding the trafficking mechanism of polytopic PM proteins.

1.4 Project Objectives

PM is the biological membrane of plant cells that separates the interior of a cell from the extracellular environment. It contains a wide variety of biological molecules, mainly proteins and lipids that are involved in a vast array of cellular processes such as cell signaling and ion channel conductance (Komatsu, 2008). To properly respond to the challenging environment and full fill the biological functions of PM, the protein composition of PM should be dynamically controlled. Although the biosynthetic and degradative pathways of PM proteins are crucial for their biological functions, little is known about the underling mechanisms. Therefore, the major goal of this thesis research is to use SCAMP1 protein as a tool to characterize the biosynthetic pathway of polytopic PM proteins. Sepcific objectives are as follows:

1. To study the biosynthetic pathway of SCAMP1 in transiently expressed tobacco BY-2 protoplasts.
2. To study the nature of BFA compartments using SCAMP1 as a marker.

CHAPTER 2

Multiple Cytosolic and Transmembrane Determinants Are Required for the Trafficking of SCAMP1 via an ER-Golgi-TGN-PM Pathway

2.1 Introduction

The secretory pathway of eukaryotic cells contains a network of membrane-bound organelles that are defined by their unique proteins with special functions. These organellar compartments include the endoplasmic reticulum (ER), Golgi apparatus, trans-Golgi network (TGN), prevacuolar compartment (PVC), and plasma membrane (PM). The latter separates the interior of a cell from its extracellular environment; it harbors thousands of proteins that function in essential cellular processes such as the transport of molecules into and out of the cell, communication with the external environment, and defense against the pathogens (Alexandersson et al., 2004; Marmagne et al., 2004; Nuhse et al., 2007). Newly synthesized proteins that are essential to the function of the PM must travel along a secretory pathway in order to reach their destination in this membrane. In mammalian and yeast cells, PM proteins are incorporated via an ER-Golgi-TGN pathway, in which the TGN functions as the sorting center, and delivers newly-synthesized proteins to either the PM or lysosome/vacuole (Mellman and Warren, 2000; Bard and Malhotra, 2006; De Matteis and Luini, 2008). However, little is known about the transport of, or sorting signals for, PM proteins in plant cells.

There is evidence that the TGN in plant cells is a compartment, which is distinct from the Golgi apparatus, e.g., the location of various TGN markers (SYP61, SYP41 and SCAMP1) is different from that of Golgi markers in the same cell (Uemura et al., 2004; Lam et al., 2007b; Foresti and Denecke, 2008). Similarly, Brefeldin A (BFA)-induced compartments derived from the Golgi apparatus are morphologically

and functionally distinct from those derived from the TGN in the same Arabidopsis and tobacco BY-2 cells (Lam et al., 2009). In addition, in several plant cell types, the plant TGN is early endosome-like because the internalized endocytic tracker FM4-64 reaches the TGN prior to the PVC (a multivesicular body [MVB] that functions as a late endosome (Tse et al., 2004)), en route to the tonoplast (Dettmer et al., 2006; Chow et al., 2008). Therefore, TGN may merge the secretory and endocytic pathways in plant cells but its roles in transport pathways remain debatable.

Relative little is known about the targeting mechanisms of integral membrane proteins in plant cells. Several studies using GFP fusion approaches have been carried out, including the use of GFP to replace the luminal N-terminus of vacuolar sorting receptor (VSR) proteins and its expression in protoplasts of tobacco and Arabidopsis cells. The transmembrane domain (TMD) and cytoplasmic tail (CT) of type I integral membrane VSRs were found to be both essential and sufficient to target VSRs to PVCs (Jiang and Rogers, 1998; Tse et al., 2004; Miao et al., 2006). Interestingly, GFP fusions with different synthetic TMD sequences of 17, 20 or 23 amino acids in length showed distinct subcellular localization to the ER, Golgi or PM, respectively, when expressed in these plant cells (Brandizzi et al., 2002). This indicates that the different lengths of the TMD of a type I integral membrane protein can provide minimal information to determine its final destination in different membranes of varying in thickness and composition (Brandizzi et al., 2002). However, much less is known about the sorting determinants of polytopic PM proteins in plant cells.

As in other eukaryotes, the plant ER has been suggested to be the first checking point for the trafficking of membrane proteins to the downstream organelles (Hanton et al., 2006). Indeed, the cytosolic sequences of several polytopic PM proteins are important for their export from the ER (Lefebvre et al., 2004; Sieben et al., 2008; Zelazny et al., 2008). However, little is known about their targeting signals and mechanisms of post-ER trafficking in plant cells, e.g. it is not known if polytopic PM proteins follow a default pathway in a similar manner to soluble proteins secreted into the apoplast (Phillipson et al., 2001; Pimpl et al., 2006).

Secretory carrier membrane proteins (SCAMPs) belong to a family of integral membrane proteins with four TMDs; it is ubiquitously expressed in cells of higher eukaryotes (Castle and Castle, 2005; Lam et al., 2007b; Toyooka et al., 2009). Recently, we have used yellow fluorescent protein (YFP) fusion to study the subcellular localization of rice SCAMP1 in transgenic tobacco BY-2 cells. Both SCAMP1 and SCAMP1-YFP or YFP-SCAMP1 fusions are localized to PM and cytosolic punctuate structures identified as TGN (Lam et al., 2007b; Lam et al., 2009). In addition, SCAMP1 also highlighted the cell plate during cytokinesis, suggestive of the involvement of endocytic trafficking in cell plate formation (Lam et al., 2008). However, since SCAMP1 does not contain a predicted N-terminal signal peptide required for import into the ER (Lam et al., 2007b), it is thus unclear if it enters the ER prior to reaching PM.

As a first step to understand the targeting mechanism of polytopic PM proteins in plants, here I study the transport pathway and sorting signals of SCAMP1 using

transient expression in tobacco BY-2 protoplasts. Using several specific vesicle trafficking inhibitors as tools, I demonstrate that SCAMP1 reaches PM via an ER-Golgi-TGN-PM pathway. Further studies using a loss-of-function approach with various C- or N-terminal SCAMP1 deletions demonstrate that both the specific cytosolic sequences and TMDs play important roles in regulating the proper trafficking steps of SCAMP1 along the secretory pathway. I propose that the targeting of SCAMP1 to PM is spatially controlled in the ER, Golgi and TGN.

2.2 Materials and Methods

General methods for construction and characterization of recombinant plasmids, maintenance of suspension-cultured tobacco (Nicotiana tabacum) BY-2 cells have been described previously (Tse et al., 2004; Lam et al., 2007b).

2.2.1 Plasmid construction

All SCAMP1 mutation constructs (Figure 1) were prepared in a pBI221 vector that contained the 35S promoter, the nopaline synthase 3' terminator and the GFP gene. Primers used to generate various SCAMP1 deletion cDNAs are shown in Table 1. All SCAMP1 mutants were generated by PCR, double-digested with restriction enzymes and inserted into the pBI221 transient expression cassette. After verification by sequencing, all plasmids were prepared on a large scale (5-10mg) for transient expression.

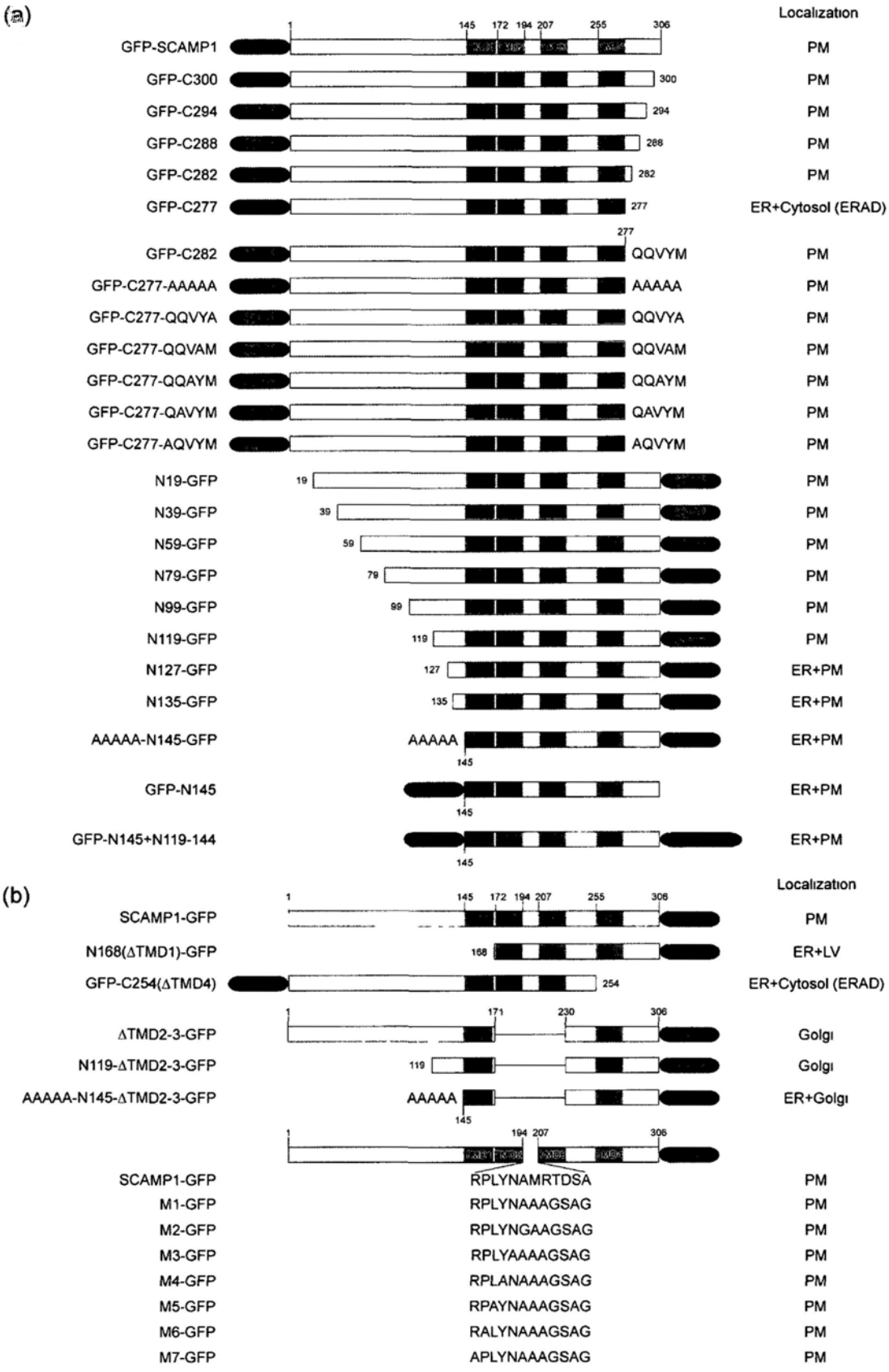
(a)
Localization
GFP-SCAMP1
PM
GFP-C300
PM
GFP-C294
PM
GFP-C288
PM
GFP-C282
PM
GFP-C277
ER+Cytosol (ERAD)
GFP-C282
QQVYM
PM
GFP-C277-AAAAA
AAAAA
PM
GFP-C277-QQVYA
QQVYA
PM
GFP-C277-QQVAM
QQVAM
PM
GFP-C277-QQAYM
QQAYM
PM
GFP-C277-QAVYM
QAVYM
PM
GFP-C277-AQVYM
AQVYM
PM
N19-GFP
PM
N39-GFP
PM
N59-GFP
PM
N79-GFP
PM
N99-GFP
PM
N119-GFP
PM
N127-GFP
ER+PM
N135-GFP
ER+PM
AAAAA-N145-GFP
AAAAA
ER+PM
GFP-N145
ER+PM
GFP-N145+N119-144
ER+PM
(b)
Localization
SCAMP1-GFP
PM
N168(ΔTMD1)-GFP
ER+LV
GFP-C254(ΔTMD4)
ER+Cytosol (ERAD)
ΔTMD2-3-GFP
Golgi
N119-ΔTMD2-3-GFP
Golgi
AAAAA-N145-ΔTMD2-3-GFP
AAAAA
ER+Golgi
SCAMP1-GFP
RPLYNAMRTDSA
PM
M1-GFP
RPLYNAAAGSAG
PM
M2-GFP
RPLYNGAAGSAG
PM
M3-GFP
RPLYAAAAGSAG
PM
M4-GFP
RPLANAAAGSAG
PM
M5-GFP
RPAYNAAAGSAG
PM
M6-GFP
RALYNAAAGSAG
PM
M7-GFP
APLYNAAAGSAG
PM

Figure 1. Constructs used for SCAMP1 mutation analysis.
Shown are constructs of GFP fusions with various SCAMP1 mutants. The wild type (WT) GFP-SCAMP1 fusion contains the full-length SCAMP1 with a 29-AA C-terminus (from 278 to 306) and 144-AA N-terminus (from 1 to 144). Arabic numbers indicate the amino acid positions of TMD or both ends of the mutants. Blue boxes represent the TMDs of SCAMP1. The name of the corresponding mutants is shown on the left panel. The localization of each mutant is given on the right panel. ER, endoplasmic reticulum; ERAD, ER-associated protein degradation; LV, lytic vacuole; PM, plasma membrane; TMD, transmembrane domain.

Table 1. Detailed information and primer sequences for each construct.

GFP-C300	P1 (XbaI) 35s Pro GFP SCAMP1 mutant NOS P2 (XhoI)
	P1: 5'-GGG TCT AGA ATG GCG GGG CGC TAC GAC AGC AA-3' P2: 5'-GGG CTC GAG TTA ACC CCT AGT TGC ATA CGC CTT CAT CTC-3'
GFP-C294	P1 (XbaI) 35s Pro GFP SCAMP1 mutant NOS P2 (XhoI)
	P1: 5'-GGG TCT AGA ATG GCG GGG CGC TAC GAC AGC AA-3' P2: 5'-GGG CTC GAG TTA CTT CAT CTC AGC AGC TTT TCC ACT TCC T-3'
GFP-C288	P1 (XbaI) 35s Pro GFP SCAMP1 mutant NOS P2 (XhoI)
	P1: 5'-GGG TCT AGA ATG GCG GGG CGC TAC GAC AGC AA-3' P2: 5'-GGG CTC GAG TTA TCC ACT TCC TCG GAA GTA CAT GTA CAC T-3'
GFP-C282	P1 (XbaI) 35s Pro GFP SCAMP1 mutant NOS P2 (XhoI)
	P1: 5'-GGG TCT AGA ATG GCG GGG CGC TAC GAC AGC AA-3' P2: 5'-GGG CTC GAG TTA CAT GTA CAC TTG CTG GAT AAC CCA GAT GC-3'
GFP-C277	P1 (XbaI) 35s Pro GFP SCAMP1 mutant NOS P2 (XhoI)
	P1: 5'-GGG TCT AGA ATG GCG GGG CGC TAC GAC AGC AA-3' P2: 5'-GGG CTC GAG TTA GAT AAC CCA GAT GCT GAG CAA TGA TTC GAC-3'

GFP-C277-AAAAA	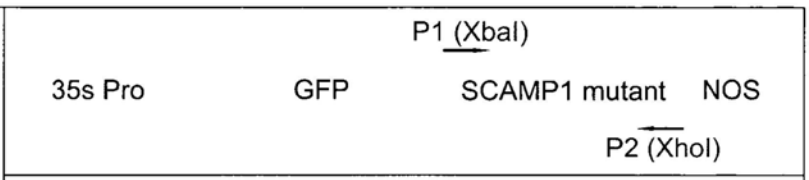
	P1: 5'-GGG TCT AGA ATG GCG GGG CGC TAC GAC AGC AA-3' P2: 5'-GGG CTC GAG TTA TGC AGC TGC AGC CTT GAT AAC CCA GAT GCT GAG CAA TGA TTC GAC-3'
GFP-C277-QQVYA	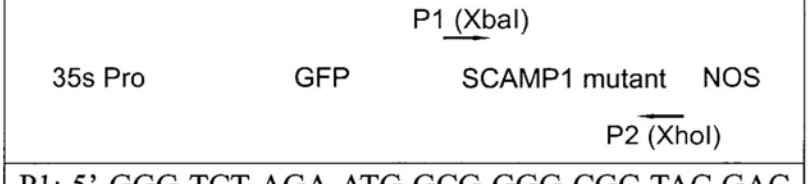
	P1: 5'-GGG TCT AGA ATG GCG GGG CGC TAC GAC AGC AA-3' P2: 5'-GGG CTC GAG TTA TGC GTA CAC TTG CTG GAT AAC CCA GAT GCT GA-3'
GFP-C277-QQVAM	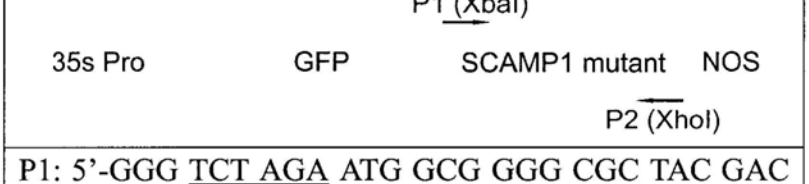
	P1: 5'-GGG TCT AGA ATG GCG GGG CGC TAC GAC AGC AA-3' P2: 5'-GGG CTC GAG TTA CAT TGC CAC TTG CTG GAT AAC CCA GAT GCT GAG C-3'
GFP-C277-QQAYM	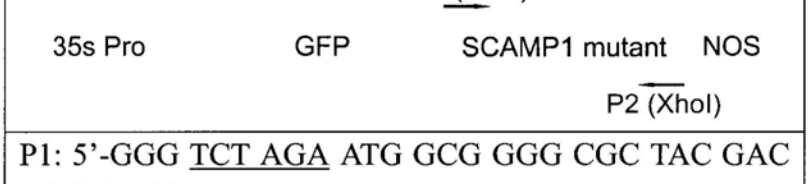
	P1: 5'-GGG TCT AGA ATG GCG GGG CGC TAC GAC AGC AA-3' P2: 5'-GGG CTC GAG TTA CAT GTA TGC TTG CTG GAT AAC CCA GAT GCT GAG CAA T-3'
GFP-C277-QAVYM	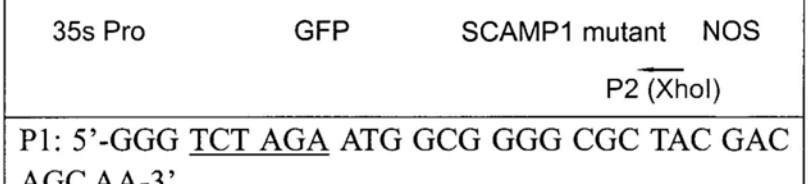
	P1: 5'-GGG TCT AGA ATG GCG GGG CGC TAC GAC AGC AA-3' P2: 5'-GGG CTC GAG TTA CAT GTA CAC TGC CTG GAT AAC CCA GAT GCT GAG CAA TGA TTC-3'
GFP-C277-AQVYM	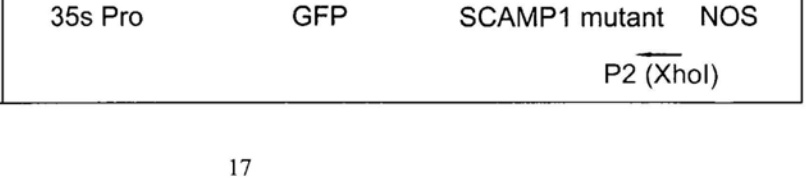

	P1: 5'-GGG TCT AGA ATG GCG GGG CGC TAC GAC AGC AA-3' P2: 5'-GGG CTC GAG TTA CAT GTA CAC TTG TGC GAT AAC CCA GAT GCT GAG CAA TGA TTC GAC-3'
N19-GFP	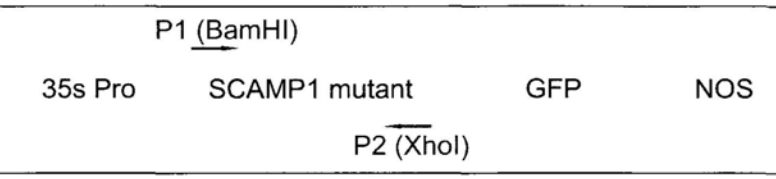
	P1: 5'-GGG GGA TCC ATG TCG GAA CAA GCG CGT GGT AAG GCT-3' P2: 5'-GGG CTC GAG AAA AGC TGC CCG CAT AGC ACC CCT-3'
N39-GFP	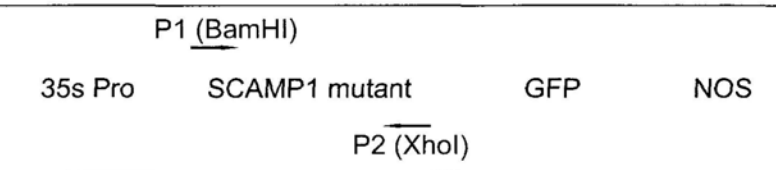
	P1: 5'-GGG GGA TCC ATG CCG AAT CCA CGG AAT GTG CC-3' P2: 5'-GGG CTC GAG AAA AGC TGC CCG CAT AGC ACC CCT-3'
N59-GFP	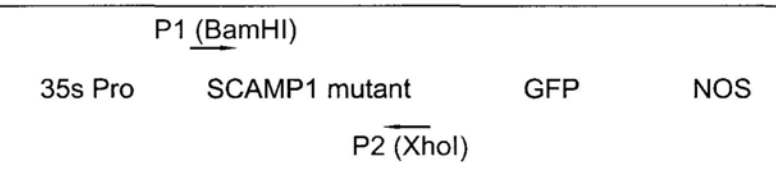
	P1: 5'-AAA GGA TCC ATG CCT GAG CCC GCA GCT TTT GGG-3' P2: 5'-GGG CTC GAG AAA AGC TGC CCG CAT AGC ACC CCT-3'
N79-GFP	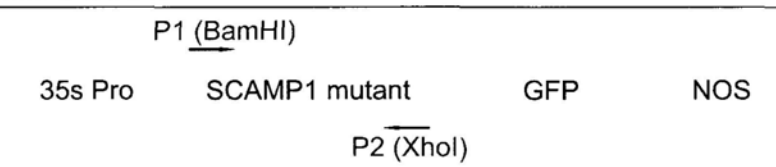
	P1: 5'-GGG GGA TCC ATG AAG AAT AGG GAA AAG GAG CTG CAA GCT-3' P2: 5'-GGG CTC GAG AAA AGC TGC CCG CAT AGC ACC CCT-3'
N99-GFP	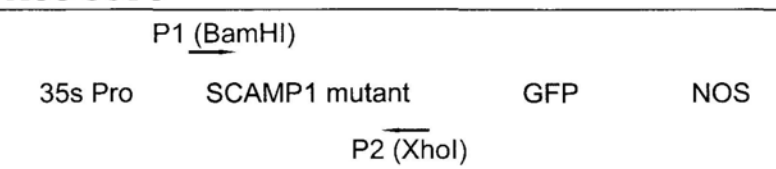
	P1: 5'-GGG GGA TCC ATG CTA AAA AGG AGG GAG GAG GCT GCA G-3' P2: 5'-GGG CTC GAG AAA AGC TGC CCG CAT AGC ACC CCT-3'

N119-GFP	P1 (BamHI) 35s Pro SCAMP1 mutant GFP NOS P2 (XhoI)
	P1: 5'-GGG GGA TCC ATG CCT CCA TTT CTG CCA CTC ATC CAT CA-3' P2: 5'-GGG CTC GAG AAA AGC TGC CCG CAT AGC ACC CCT-3'
N127-GFP	P1 (BamHI) 35s Pro SCAMP1 mutant GFP NOS P2 (XhoI)
	P1: 5'-GGG GGA TCC ATG CAT GAT ATC ACC AAT GAG ATA CCG AGT CAC CTT C-3' P2: 5'-GGG CTC GAG AAA AGC TGC CCG CAT AGC ACC CCT-3'
N135-GFP	P1 (BamHI) 35s Pro SCAMP1 mutant GFP NOS P2 (XhoI)
	P1: 5'-GGG GGA TCC ATG AGT CAC CTT CAA AGA ATG CAA TAT-3' P2: 5'-GGG CTC GAG AAA AGC TGC CCG CAT AGC ACC CCT-3'
AAAAA-N145-GFP	P1 (XbaI) 35s Pro SCAMP1 mutant GFP NOS P2 (XhoI)
	P1: 5'-GGG TCT AGA ATG GCA GCT GCA GCT GCA TTT GCA TCA TTT CTT GGA TTG GCT TGC-3' P2: 5'-GGG CTC GAG AAA AGC TGC CCG CAT AGC ACC CCT-3'
GFP-N145	P1 (XbaI) 35s Pro GFP SCAMP1 mutant NOS P2 (XhoI)
	P1: 5'-GGG TCT AGA TTT GCA TCA TTT CTT GGA TTG GCT TGC TGT-3' P2: 5'-GGG CTC GAG TTA AAA AGC TGC CCG CAT AGC ACC CCT-3'
GFP-N145+N119-144	P1 (XbaI) 35s Pro GFP SCAMP1 mutant NOS P2 (XhoI)

	P1: 5'-GGG TCT AGA TTT GCA TCA TTT CTT GGA TTG GCT TGC TGT-3' P2: 5'-GGG CTC GAG TTA AGG TGG AAA CAG TGG GAG GAT ATG ATG ATC GAT GGT ATT CTC TAT CGG ACT GTG AAG TTG TCT CAT TTG ATA AAC TGC AAA AGC TGC CCG CAT AGC ACC CCT-3'
N168(ΔTMD1)-GFP	P1 (BamHI) 35s Pro SCAMP1 mutant GFP NOS P2 (XhoI)
	P1: 5'-GGG GGA TCC ATG CAA TAT GTT GCA TTT GCA TCA TTT-3' P2: 5'-GGG CTC GAG AAA AGC TGC CCG CAT AGC ACC CCT-3'
GFP- C254(ΔTMD4)	P1 (XbaI) 35s Pro GFP SCAMP1 mutant NOS P2 (SacI)
	P1: 5'-GGG TCT AGA ATG GCG GGG CGC TAC GAC AGC AA-3' P2: 5'-GGG GAG CTC TTA CAA AGC ATT CTT GCT GAT GAG ATC A-3'
ΔTMD2-3-GFP	P1 (XbaI) P3 (BamHI) 35s Pro SCAMP1 mutant GFP NOS P2 (BamHI) P4 (XhoI)
	P1: 5'-GGG TCT AGA ATG GCG GGG CGC TAC GAC AGC AA-3' P2: 5'-GGG GGA TCC GCC TTC CCC CTT GAC CCA AGC-3' P3: 5'-GGG GGA TCC GTG GGG ATC TTC TAC TTT GTT GGA TTT GGA-3' P4: 5'-GGG CTC GAG AAA AGC TGC CCG CAT AGC ACC CCT-3'
N119-ΔTMD2-3-GFP	P1 (XbaI) P3 (BamHI) 35s Pro SCAMP1 mutant GFP NOS P2 (BamHI) P4 (XhoI)
	P1: 5'-GGG TCT AGA ATG CCT CCA TTT CTG CCA CTC ATC CAT CA-3' P2: 5'-GGG GGA TCC GCC TTC CCC CTT GAC CCA AGC-3' P3: 5'-GGG GGA TCC GTG GGG ATC TTC TAC TTT GTT GGA TTT GGA-3'

	P4: 5'-GGG CTC GAG AAA AGC TGC CCG CAT AGC ACC CCT-3'
AAAAA-N145-ΔTM D2-3-GFP	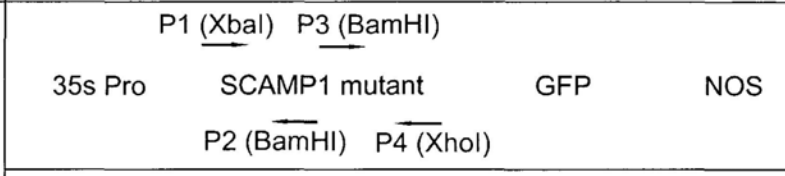
	P1: 5'-GGG TCT AGA ATG GCA GCT GCA GCT GCA TTT GCA TCA TTT CTT GGA TTG GCT TGC-3' P2: 5'-GGG GGA TCC GCC TTC CCC CTT GAC CCA AGC-3' P3: 5'-GGG GGA TCC GTG GGG ATC TTC TAC TTT GTT GGA TTT GGA-3' P4: 5'-GGG CTC GAG AAA AGC TGC CCG CAT AGC ACC CCT-3'
M1-GFP	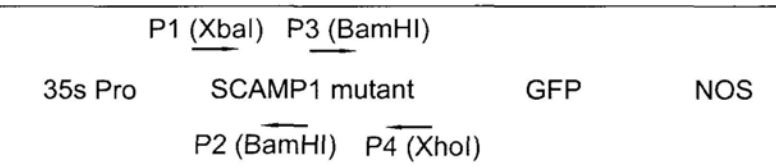
	P1: 5'-GGG TCT AGA ATG GCG GGG CGC TAC GAC AGC AA-3' P2: 5'-GGG GGA TCC AGC TGC AGC ATT ATA CAG AGG TCG ATA CCA TAA AAC ATA TGC ACC-3' P3: 5'- GGG GGA TCC GCA GGT TTG AAG TTT GGA TTG TTC TTC TTG GTT TAC CTG TT-3' P4: 5'-GGG CTC GAG AAA AGC TGC CCG CAT AGC ACC CCT-3'
M2-GFP	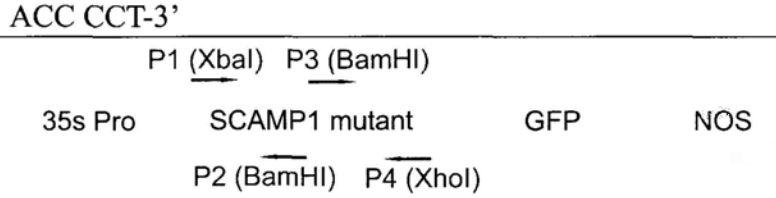
	P1: 5'-GGG TCT AGA ATG GCG GGG CGC TAC GAC AGC AA-3' P2: 5'-GGG GGA TCC AGC TGC ACC ATT ATA CAG AGG TCG ATA CCA TAA AAC ATA TGC ACC-3' P3: 5'- GGG GGA TCC GCA GGT TTG AAG TTT GGA TTG TTC TTC TTG GTT TAC CTG TT-3' P4: 5'-GGG CTC GAG AAA AGC TGC CCG CAT AGC ACC CCT-3'
M3-GFP	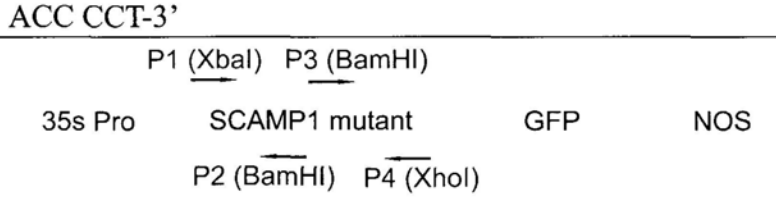
	P1: 5'-GGG TCT AGA ATG GCG GGG CGC TAC GAC AGC AA-3'

	P2: 5'- GGG GGA TCC AGC TGC AGC TGC ATA CAG AGG TCG ATA CCA TAA AAC ATA TGC ACC AG-3' P3: 5'- GGG GGA TCC GCA GGT TTG AAG TTT GGA TTG TTC TTC TTG GTT TAC CTG TT-3' P4: 5'-GGG CTC GAG AAA AGC TGC CCG CAT AGC ACC CCT-3'
M4-GFP	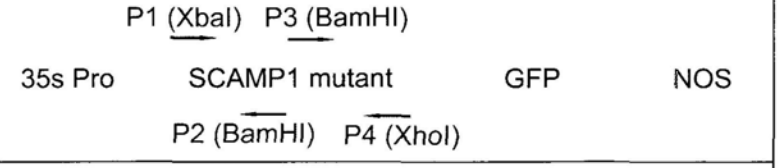
	P1: 5'-GGG TCT AGA ATG GCG GGG CGC TAC GAC AGC AA-3' P2: 5'-GGG GGA TCC AGC TGC AGC ATT TGC CAG AGG TCG ATA CCA TAA AAC ATA TGC ACC AG-3' P3: 5'- GGG GGA TCC GCA GGT TTG AAG TTT GGA TTG TTC TTC TTG GTT TAC CTG TT-3' P4: 5'-GGG CTC GAG AAA AGC TGC CCG CAT AGC ACC CCT-3'
M5-GFP	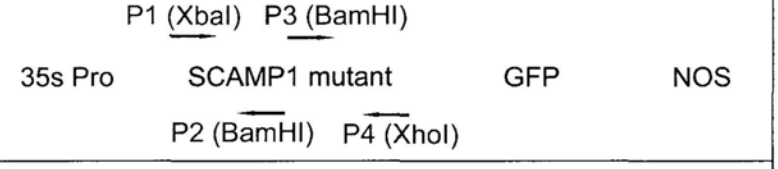
	P1: 5'-GGG TCT AGA ATG GCG GGG CGC TAC GAC AGC AA-3' P2: 5'- GGG GGA TCC AGC TGC AGC ATT ATA TGC AGG TCG ATA CCA TAA AAC ATA TGC ACC AG-3' P3: 5'- GGG GGA TCC GCA GGT TTG AAG TTT GGA TTG TTC TTC TTG GTT TAC CTG TT-3' P4: 5'-GGG CTC GAG AAA AGC TGC CCG CAT AGC ACC CCT-3'
M6-GFP	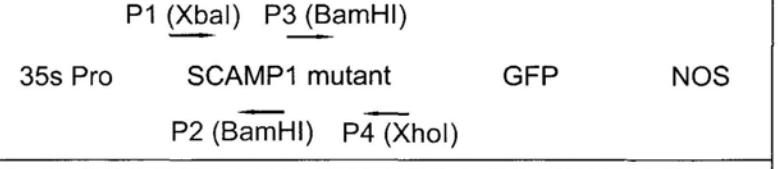
	P1: 5'-GGG TCT AGA ATG GCG GGG CGC TAC GAC AGC AA-3' P2: 5'- GGG GGA TCC AGC TGC AGC ATT ATA CAG TGC TCG ATA CCA TAA AAC ATA TGC ACC AG-3' P3: 5'- GGG GGA TCC GCA GGT TTG AAG TTT GGA TTG TTC TTC TTG GTT TAC CTG TT-3' P4: 5'-GGG CTC GAG AAA AGC TGC CCG CAT AGC ACC CCT-3'

M7-GFP	P1 (XbaI) P3 (BamHI) 35s Pro SCAMP1 mutant GFP NOS P2 (BamHI) P4 (XhoI)
	P1: 5'-GGG TCT AGA ATG GCG GGG CGC TAC GAC AGC AA-3' P2: 5'- GGG GGA TCC AGC TGC AGC ATT ATA CAG AGG TGC ATA CCA TAA AAC ATA TGC ACC AGG AAC-3' P3: 5'- GGG GGA TCC GCA GGT TTG AAG TTT GGA TTG TTC TTC TTG GTT TAC CTG TT-3' P4: 5'-GGG CTC GAG AAA AGC TGC CCG CAT AGC ACC CCT-3'

Name of each construct is given on the left panel. Detailed information of the construct including the restriction sites is given on the top right panel. Primer sequences are given on the bottom right panel. The introduced restriction sites of the primers are underlined.

2.2.2 Drug treatments

For drug treatment experiments, aliquots of ConcA (Sigma-Aldrich; C-9705; stock at 1mM in DMSO) solution were added to tobacco BY-2 protoplasts to a final concentration of 2 μM.

2.2.3 Transient expression and confocal imaging

Transient expression with tobacco BY-2 protoplasts was carried out essentially as described previously (Miao and Jiang, 2007). Confocal images were collected at about 13 hrs or specific time points after transformation using an Olympus FV1000 system (http://www.olympusconfocal.com). Images were processed using Adobe Photoshop software (http://www.adobe.com) (Jiang and Rogers, 1998). REF was obtained using ImageJ software on a non-saturating confocal image of 1024X1024 pixels. Ten circles of 6 pixels in diameter were randomly picked out on either the ER or PM and quantified. REF was calculated as a percentage of the total ER signal intensity against the total PM signal intensity: REF = (ER signal intensity/PM signal intensity) X 100.

2.3 Results

2.3.1 SCAMP1 localizes to both PM and TGN in transiently expressed BY-2 protoplasts

SCAMP1 and SCAMP1-YFP or YFP-SCAMP1 are localized to both the PM and TGN in transgenic tobacco BY-2 cells (Lam et al., 2007b). Transient expression using protoplasts is a powerful tool for studying protein localization and organelle dynamics in plant cells (Miao and Jiang, 2007); hence this approach was used to study SCAMP1 targeting, with GFP-SCAMP1 being co-expressed with either the TGN marker RFP-SYP61 or the Golgi marker Man1-RFP in tobacco BY-2 protoplasts. As shown in Figure 2a, GFP-SCAMP1 localizes on both PM and cytosolic punctate dots containing RFP-SYP61, but is separate from Man1-RFP, a result consistent with the PM and TGN localization of YFP-SCAMP1 in stably transformed tobacco BY-2 cells (Lam et al., 2007b). In addition, when co-expressed together with RFP-SCAMP1, both GFP-SCAMP1 and SCAMP1-GFP were largely colocalized with this in the same cells (Figure 2b), indicating neither the GFP fusions at the C-terminus or the N-terminus of SCAMP1 nor the types of fluophores (GFP or RFP) used affected its correct subcellular localization. These results using BY-2 protoplasts are consistent with those obtained using transgenic BY-2 cells (Lam et al., 2007b), validating the use of protoplasts to analyze the SCAMP1 targeting mechanisms.

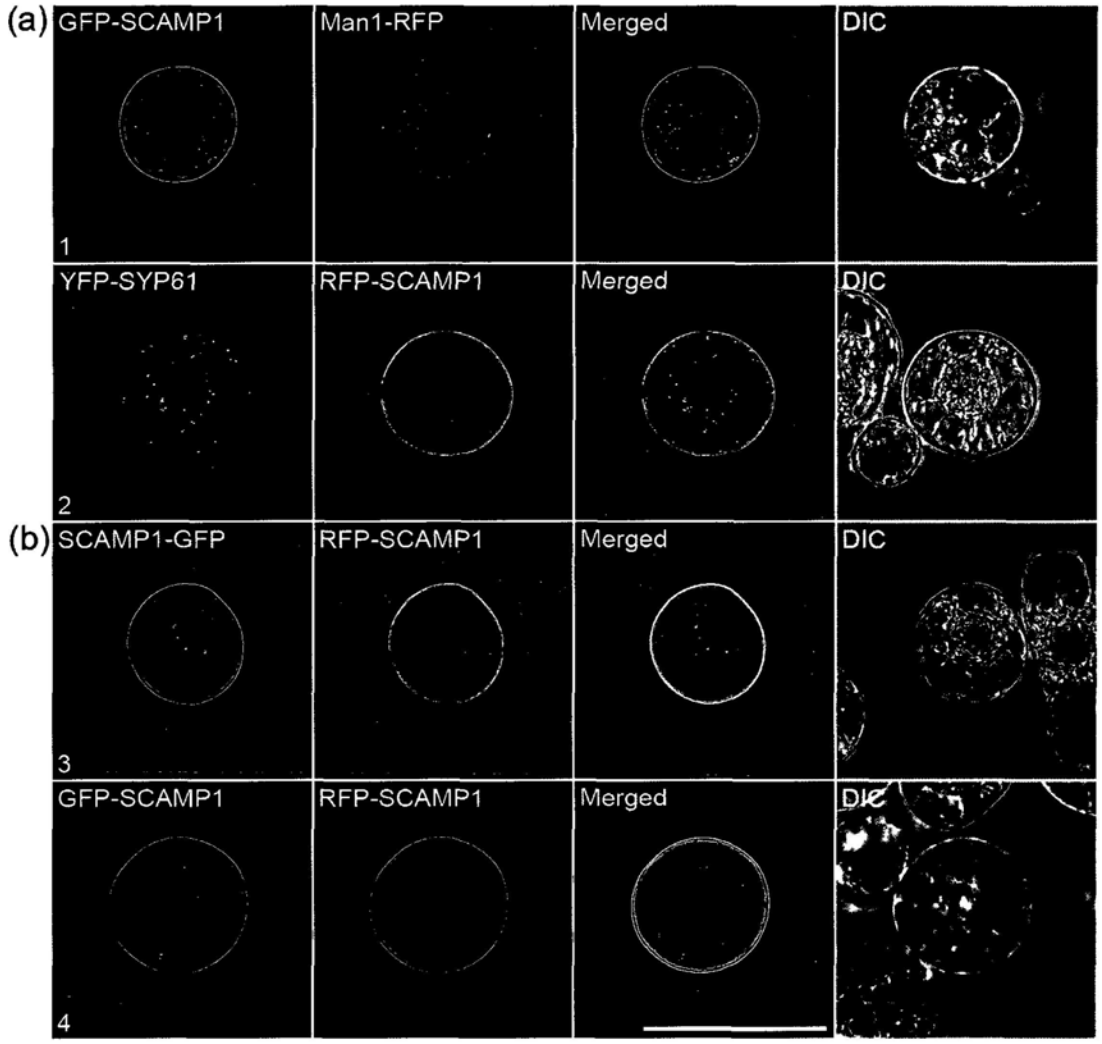

Figure 2. SCAMP1 reaches the PM and TGN in BY-2 protoplasts.
(a) Transient coexpression of GFP-SCAMP1 or RFP-SCAMP1 with either the Golgi marker Man1-RFP (panel 1) or the TGN marker YFP-SYP61 (panel 2) in BY-2 protoplasts.
(b) Transient coexpression of GFP-SCAMP1 or SCAMP1-GFP with RFP-SCAMP1.
DIC, differential interference contrast. Scale bar = 50 μm.

2.3.2 SCAMP1 reaches the PM via an ER-Golgi-TGN pathway

SCAMP1 is predicted to be a polytopic PM protein with its N- and C-terminus facing towards the cytosol (Lam et al., 2007b). Sequence analysis using TMHMM (http://www.cbs.dtu.dk/services/TMHMM-2.0/) shows that SCAMP1 does not contain an N-terminal signal peptide (Lam et al., 2007b). Therefore, I determined if SCAMP1 is synthesized in the ER and trafficks through the secretory pathway prior to reaching the PM.

Initially I tested whether the transport of SCAMP1 requires COPII vesicles, using Sec12p and ARF1 mutants of Arabidopsis. Sec12p is a Sar1p-specific guanosine nucleotide exchange factor that is involved in the formation of COPII vesicles (Phillipson et al., 2001), whereas ARF1 (ADP ribosylation factor) functions at the cis-Golgi cisternae to initiate the budding of COPI vesicles (Pimpl et al., 2000; Pimpl et al., 2003). Overexpression of Sec12p or ARF1 mutants can disrupt the inter-transport between ER and Golgi, thus trapping the newly synthesized proteins in the ER (Phillipson et al., 2001; Pimpl et al., 2003; Langhans et al., 2008). Therefore, if SCAMP1 reaches the PM from its origin in the ER (Figure 3a), by blocking the ER-to-Golgi transport pathway via overexpression of Sec12p or ARF1 mutant, SCAMP1 should be trapped in the ER (Figure 3b). Indeed, when co-expressed in BY-2 protoplasts with Sec12p or ARF1 (Q71L) (ARF1 GTP mutant) or ARF1 (T31N) (ARF1 GDP mutant), GFP-SCAMP1 was trapped in the ER together with Man1-RFP, a Golgi marker known to traffic from the ER (Figure 3c, panels 1-3). The effect was specific because overexpression of ARF1 wild type did

not cause GFP-SCAMP1 or Man1-RFP to be retained in the ER (Figure 3c, panel 4). Thus GFP-SCAMP1 is synthesized in the ER and trafficks through the Golgi apparatus.

The next step was to find out if SCAMP1 trafficks through the TGN prior to reaching the PM. Concanamycin A (ConcA) is a V-ATPase inhibitor that prevents post-TGN trafficking (Robinson et al., 2004; Takano et al., 2005; Dettmer et al., 2006; Kleine-Vehn et al., 2008; Viotti et al., 2010). Therefore if SCAMP1 reaches the TGN prior to the PM (Figure 4a), inhibition of post-TGN trafficking by ConcA will trap SCAMP1 in the TGN between the ER and PM (Figure 4b). Indeed, when tobacco BY-2 protoplasts were treated with the inhibitor for 10 hrs, the GFP-SCAMP1 signals were mainly in the cytosolic punctate or in aggregate structures that were largely separated from the Golgi marker Man1-RFP (Figure 4c, panel 1). But they did colocalize with the TGN marker RFP-SYP61 (Figure 4c, panel 2), indicating that GFP-SCAMP1 was trapped into the TGN aggregates. After washing off the ConcA for 10 hrs, the GFP-SCAMP1 signals were on both the PM and cytosolic TGN, spatially distinct from the Golgi marker Man1-RFP (Figure 4d, panel 3), indicating that the drug treatment was not toxic to the cells because there was recovery of the normal GFP-SCAMP1 signals. Taken together, these results demonstrate that GFP-SCAMP1 reaches the PM via an ER-Golgi-TGN-PM pathway.

To find out if other known PM proteins follow the same transport pathway, I also performed similar experiments using FLAGELLIN SENSITIVE2 (FLS2)-GFP, a type I integral membrane protein that locates on the PM (Robatzek et al., 2006).

Identical results were obtained (Figure 5), indicating that an ER-Golgi-TGN-PM pathway might be conserved for certain PM-localized proteins in plant cells.

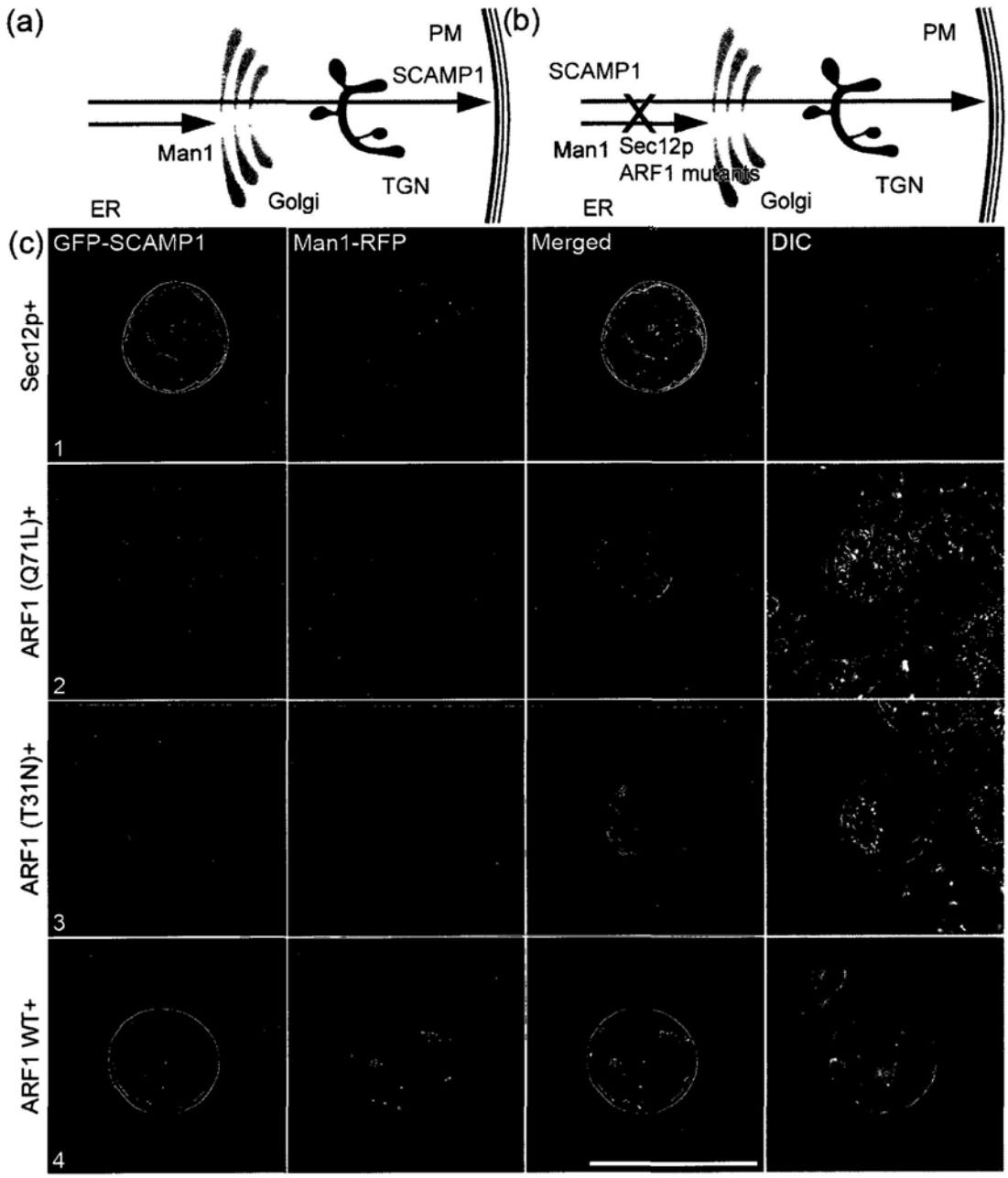
(a)
PM
SCAMP1
Man1
ER
Golgi
TGN
(b)
PM
SCAMP1
Man1
Sec12p
ARF1 mutants
ER
Golgi
TGN
(c)
GFP-SCAMP1
Man1-RFP
Merged
DIC
Sec12p+
ARF1 (Q71L)+
ARF1 (T31N)+
ARF1 WT+
1
2
3
4

Figure 3. SCAMP1 is synthesized in the ER and trafficks through the Golgi apparatus.

(a). Hypothetical trafficking pathway of SCAMP1 from ER-Golgi-TGN-PM in plant cells.

(b) Use of the ER-Golgi transport inhibitors Sec12p or ARF1 mutants to study the SCAMP1 transport pathway. Blocking of ER-to-Golgi traffic traps both Man1 and SCAMP1 in the ER.

(c) ER export inhibitors trap both Man1-RFP and GFP-SCAMP1 in the ER. GFP-SCAMP1 and Man1-RFP were coexpressed together with individual protein trafficking inhibitors of Sec12p, ARF1 (Q71L), ARF1 (T31N) or its control ARF1 WT respectively (panels 1-4 as indicated).

DIC, differential interference contrast; ER, endoplasmic reticulum; PM, plasma membrane; TGN, *trans*-Golgi network. Scale bar = 50 μm.

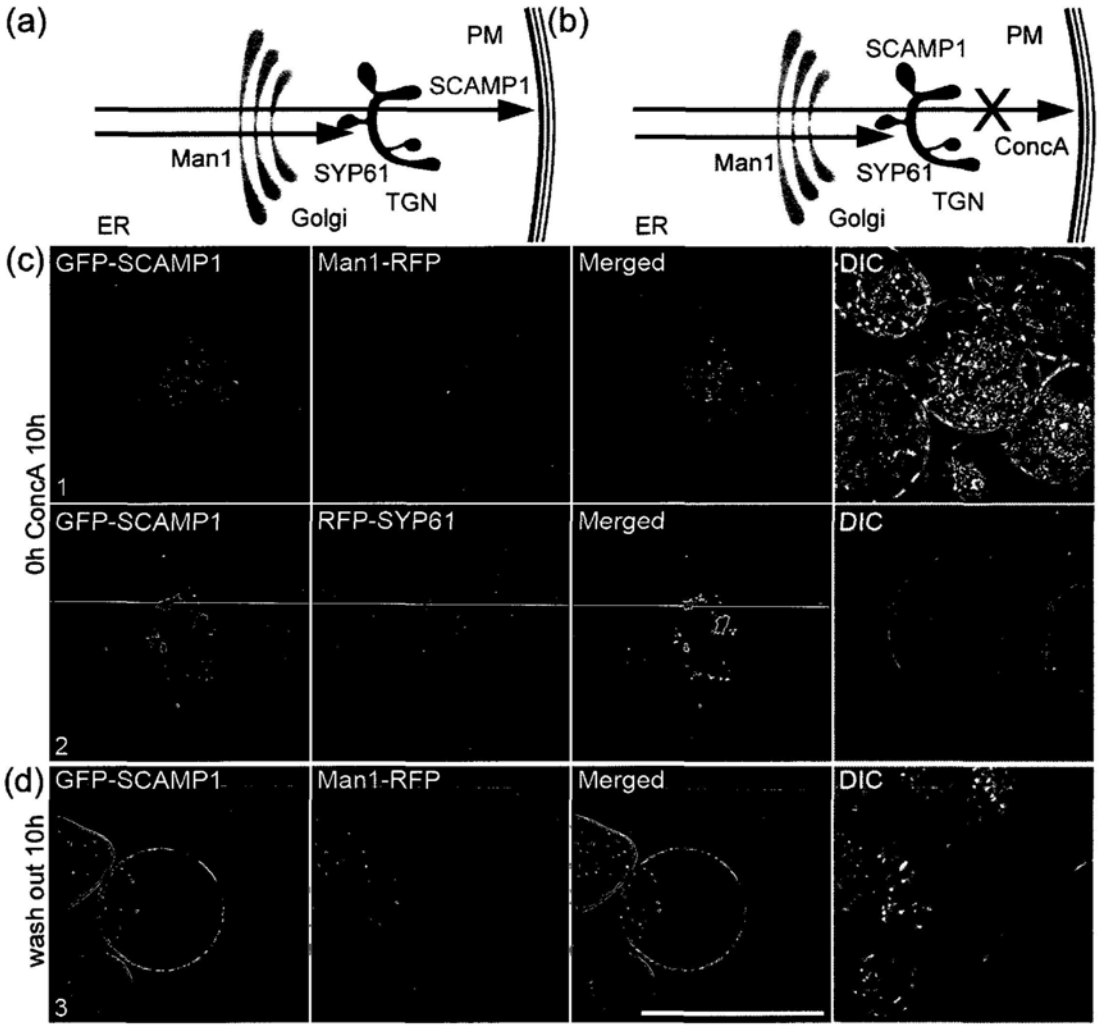

Figure 4. SCAMP1 reaches TGN prior to the PM.

(a) Hypothetical trafficking pathway of SCAMP1 from ER-Golgi-TGN-PM along with the Golgi-localized Man1 and TGN-localized SYP61 in plant cells.

(b) Blocking of post-Golgi protein traffic by ConcA would trap SCAMP1 in the TGN.

(c) ConcA treatment trapped GFP-SCAMP1 in TGN. Tobacco BY-2 protoplasts coexpressing GFP-SCAMP1 either with the Golgi marker Man1-RFP or the TGN marker RFP-SYP61 were treated with ConcA immediately after transformation, followed by incubation for 10 hrs before confocal imaging.

(d) GFP-SCAMP1 trapped in TGN recovered to PM upon washing off ConcA. BY-2 protoplasts coexpressing GFP-SCAMP1 and Man1-RFP were first treated with ConcA for 10 hrs as indicated, followed by washing off the drug and incubating for another 10 hrs before confocal imaging.

DIC, differential interference contrast; ConcA, Concanamycin A; ER, endoplasmic reticulum; PM, plasma membrane; TGN, *trans*-Golgi network. Scale bar = 50 μm.

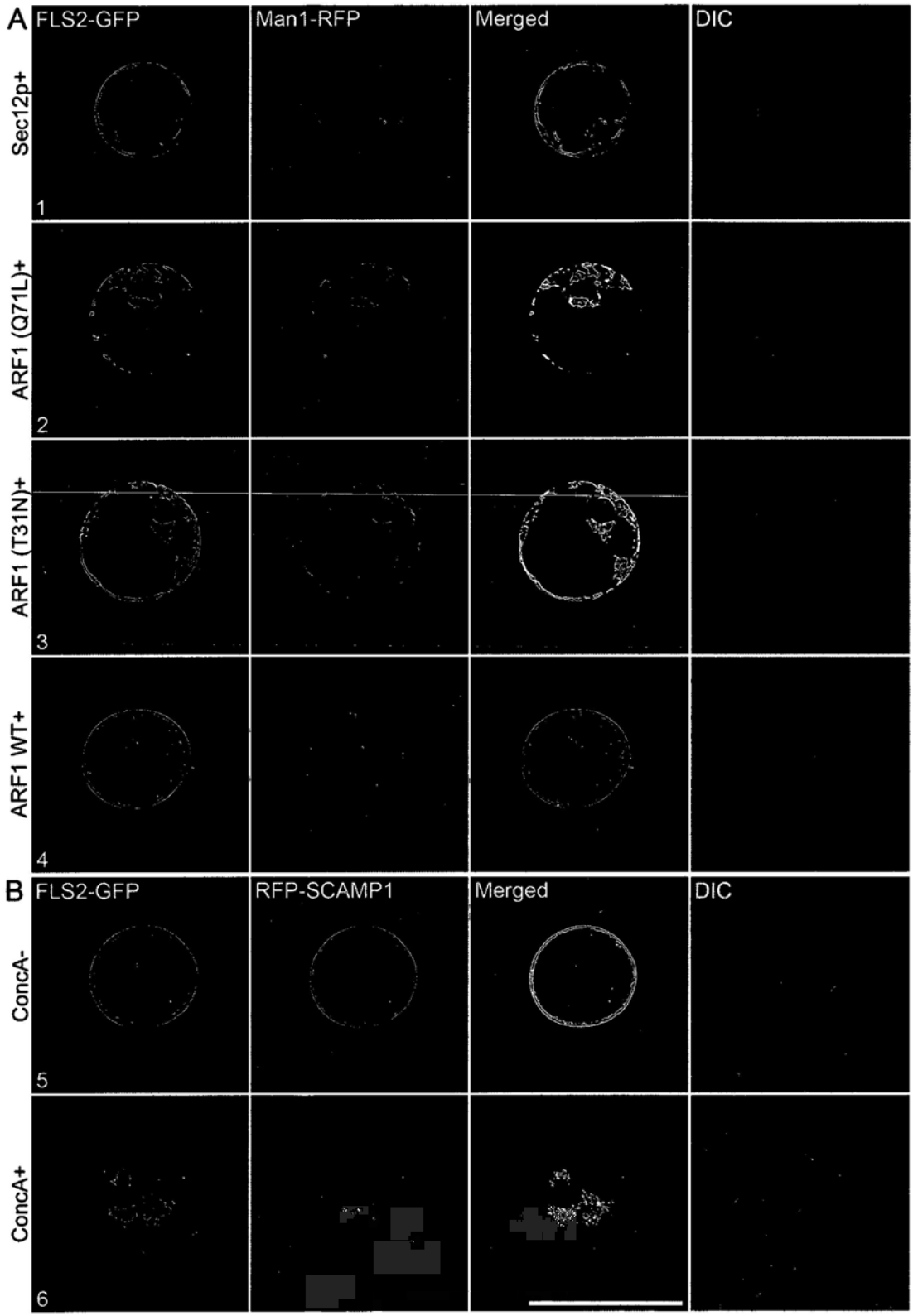
A
FLS2-GFP
Man1-RFP
Merged
DIC
Sec12p+
1
ARF1 (Q71L)+
2
ARF1 (T31N)+
3
ARF1 WT+
4
B
FLS2-GFP
RFP-SCAMP1
Merged
DIC
ConcA-
5
ConcA+
6

Figure 5. Trafficking pathway of FLS2-GFP in tobacco BY-2 protoplasts.
(a) FLS2-GFP and Man1-RFP were co-expressed with Sec12p, ARF1 (Q71L), ARF1 (T31N) or ARF1 WT in tobacco BY-2 protoplasts.
(b) Tobacco BY-2 protoplasts transiently co-expressing FLS2-GFP and RFP-SCAMP1 were treated with ConcA immediately after electroporation and incubated for 10 hrs before confocal imaging.
Scale bar = 50 μm.

2.3.3 Analysis of the SCAMP1 cytosolic C-terminus

SCAMP1 is predicted to contain a 144 amino acid N-terminus and a 29 amino acid C-terminus, and four transmembrane domains (TMDs). To determine if either the N- or C-terminus contain any targeting signals for the correct PM localization of SCAMP1, I conducted a loss-of-function study by making series C- and N-terminal deletions of the protein while maintaining the four TMDs intact and expressed their fusions with GFP in tobacco BY-2 protoplasts (Figure 1).

As shown in Figure 6a, deletion at the C-terminus up to amino acid position 282 (e.g. from GFP-C300 to GFP-C282 in Figure 1a) did not affect the correct PM localization of the GFP-SCAMP1 fusions (Figure 6a, panel 1). However, further deletion of the last 5 amino acids at the C-terminus (GFP-C277) caused the GFP-SCAMP1 fusion to be retained in the ER at 13 hrs after expression, while most of the GFP signal was relocated from the ER to the cytosol, with obviously decreasing signal intensity at 24 hrs (Figure 6b). When GFP-C277, RFP-SCAMP1 and ARF1 GDP mutant were coexpressed together and observed at 13 and 24 hrs after transformation, RFP-SCAMP1 was completely trapped in the ER between these two times, while GFP-C277 showed a similar ER to cytosol patterns at both times (Figure 6c). This indicates that GFP-C277 was directly retro-translocated from the ER to the cytosol independently of post-ER trafficking (Figures 6d, e).

The relative instability of GFP-C277 when transiently-expressed in BY-2 protoplasts suggested that GFP-C277 is not correctly folded and thus recognized for destruction by the cells. ER-associated protein degradation (ERAD) is one cellular

pathway, which targets misfolded proteins of the ER for ubiquitination and subsequently degradation in the proteosome (Liu et al., 2003; Meusser et al., 2005; Romisch, 2005). This type of protein quality control machinery was first demonstrated in yeast and mammals and more recently in plants (Brandizzi et al., 2003; Muller et al., 2005; Hong et al., 2008; Marshall et al., 2008). While such dislocation of GFP-C277 from the ER to the cytosol, followed by its degradation is typical of the ERAD pathway (Tsai et al., 2002; Brandizzi et al., 2003; Nakatsukasa et al., 2008), western blot analysis using UBQ antibodies failed to detected polyubiquitination of GFP-C277 in transiently expressed BY-2 cells; this could be due to low expression of this proteins, however (data not shown).

Further amino acid substitution analysis was carried out for the last five C-terminal amino acids QQVYM (Figure 1a). However, none of the deletions of these terminal amino acids altered the PM localization of the appropriate GFP fusion proteins (Figure 7). Thus while the five C-terminal amino acids adjacent to the TMD4 may be important for maintaining the correct structure of SCAMP1 they are not essential for its targeting. Indeed, membrane topological analysis using TMHMM program indicates that the TMD positions of GFP-C277 were altered from the normal topology of GFP-SCAMP1 (data not shown).

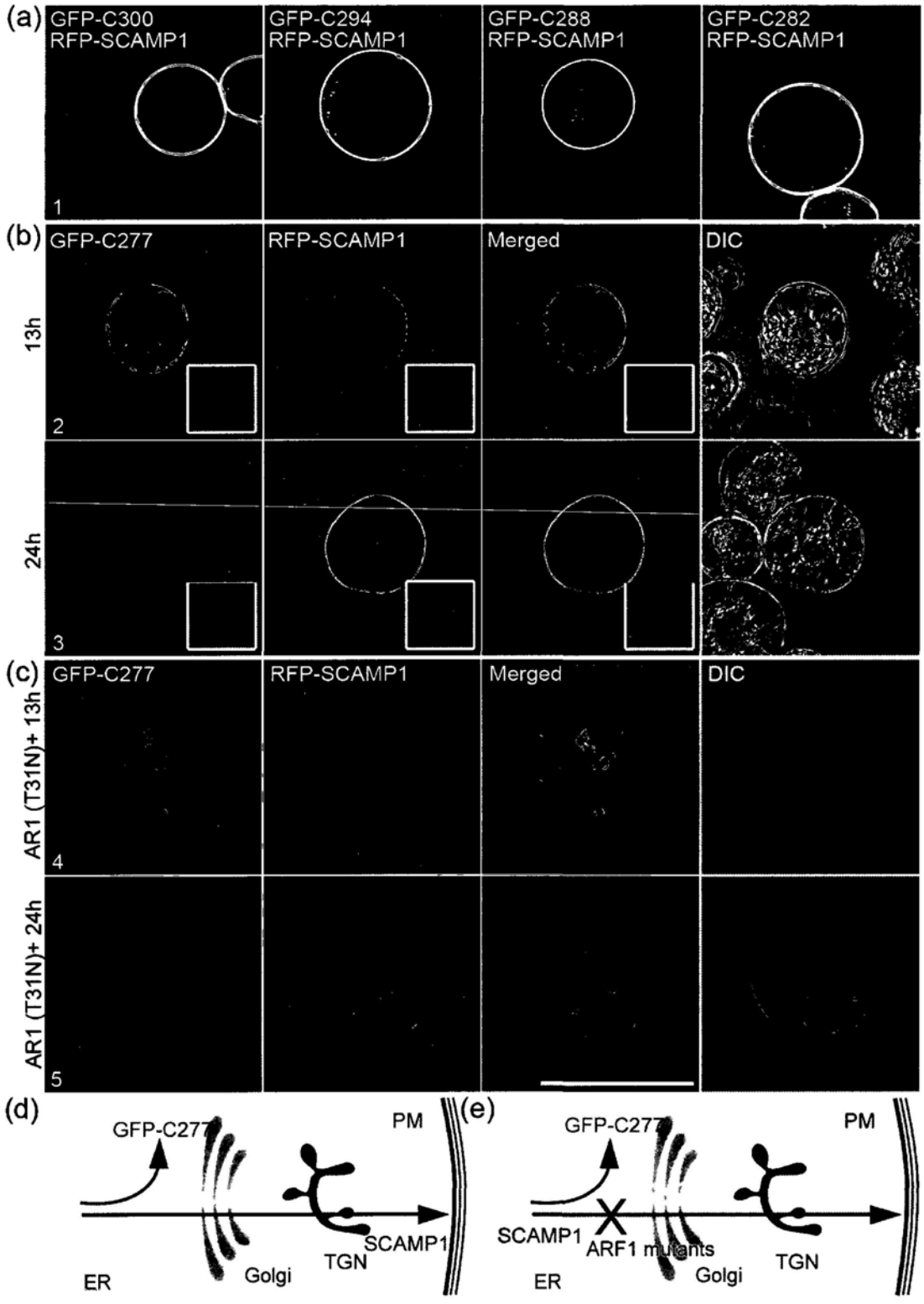
(a)
GFP-C300
RFP-SCAMP1
GFP-C294
RFP-SCAMP1
GFP-C288
RFP-SCAMP1
GFP-C282
RFP-SCAMP1
1
(b)
GFP-C277
RFP-SCAMP1
Merged
DIC
13h
2
24h
3
(c)
GFP-C277
RFP-SCAMP1
Merged
DIC
AR1 (T31N)+ 13h
4
AR1 (T31N)+ 24h
5
(d)
GFP-C277
PM
SCAMP1
TGN
ER
Golgi
(e)
GFP-C277
PM
SCAMP1
ARF1 mutants
TGN
ER
Golgi

Figure 6. The last five amino acids of SCAMP1 C-terminus have an important structure role.

(a) Coexpression and colocalization of GFP-C300, GFP-C294, GFP-C288 or GFP-C282 with RFP-SCAMP1 in BY-2 protoplasts.

(b) GFP-C277 was trapped in the ER and degraded. GFP-C277 was transiently coexpressed with RFP-SCAMP1 in BY-2 protoplasts, followed by confocal imaging at 13 hrs or 24 hrs respectively as indicated.

(c) GFP-C277 was trapped in the ER and degraded without reaching Golgi. GFP-C277 and RFP-SCAMP1 were coexpressed together with ARF1 (T31N), followed by confocal imaging at 13 hrs or 24 hrs respectively as indicated.

(d) and (e) Possible account for the degradation of GFP-C277 via an ERAD pathway in BY-2 protoplasts.

DIC, differential interference contrast; ER, endoplasmic reticulum; PM, plasma membrane; TGN, *trans*-Golgi network. Scale bar = 50 μm.

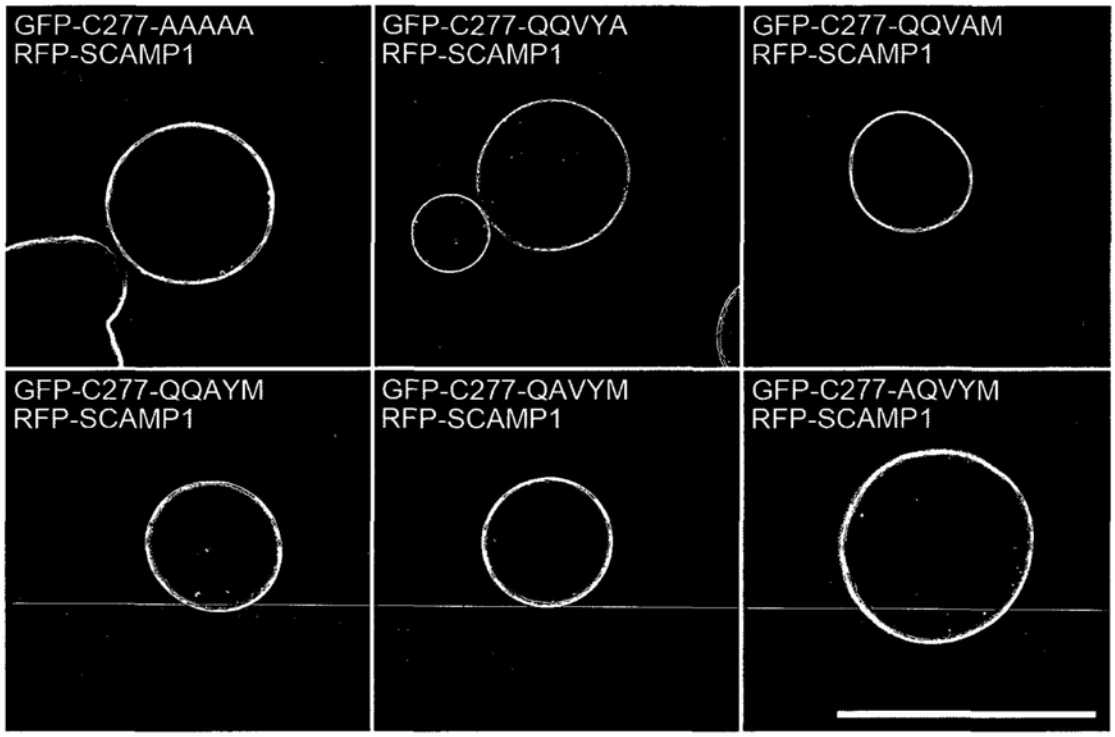

Figure 7. Subcellular localization of SCAMP1 C-terminal deletion mutants. Co-expression of RFP-SCAMP1 with GFP-C277-AAAAA, GFP-C277-QQVYA, GFP-C277-QQVAM, GFP-C277-QQAYM, GFP-C277-QAVYM or GFP-C277-AQVYM in tobacco BY-2 protoplasts. Scale bar = 50 μm.

2.3.4 Analysis of SCAMP1 cytosolic N-terminus

To further elucidate the possible roles of the cytosolic N-terminus in SCAMP1 targeting, a series of deletions were made in this region and used for the generation of GFP fusions (Figure 1a). For most of the mutants, the GFP gene was directly fused to the C-terminus of SCAMP1. An AAAAA-N145-GFP fusion protein construct was also used (five Ala fused to the N-terminus) to maintain an identical membrane topology as full length SCAMP1. As shown in Figure 6a, deletions at the cytosolic N-terminus up to 118 AA (e.g. from N19-GFP to N119-GFP in Figure 4b) did not change the expected PM localization in BY-2 cells (Figure 8a). However, complete deletion of the N-terminus AAAAA-N145-GFP resulted in ER retention (Figure 8b), indicating the possible existence of an ER export signal within the 26 amino acid (PPFLPLIHHDITNEIPSHLQRMQYVA) region adjacent to the first TMD1 of SCAMP1. Further deletion and mutation analyses within this 119-144 amino acid region were thus carried out (Figure 1a). As shown in Figure 9a, in cells expressing N119-GFP, typical PM and punctate TGN signals were already detected within 13 hrs after the start of transient expression, and the signal patterns remained unchanged by 24 hrs (Figure 9a, panels 1-2). However, in cells expressing N127-GFP, N135-GFP or AAAAA-N145-GFP, increasing GFP signals in the ER network were detected within 13 hrs after transient expression, although they gradually declined as the PM signals increased by 24 hrs (Figure 9a, panels 3-8). To quantify these changes, I calculated the fluorescence intensity ratio of ER to PM (see Materials and Methods). As shown in Figure 9b, the relative ER fluorescence (REF) of N119-GFP was similar

to that of SCAMP1-GFP; however, the REF for N127-GFP, N135-GFP and AAAAA-N145-GFP increased gradually at either 13 or 24 hrs after transient expression. In addition, when the N-terminus N119-144 amino acid region was attached to the C-terminus of GFP-N145 (Figure 1a), the resulting GFP-N145+N119-144 fusion showed higher ER export efficiency than that of AAAAA-N145-GFP and GFP-N145 (Figure 9a, panels 5, 6, 9, 10 and Figure 10a). Also, GFP-N145+N119-144 followed the identical ER-Golgi-TGN-PM pathway as RFP-SCAMP1, because these two fusion proteins had similar responses in both Arf1 mutants and after ConcA treatment (Figures 10b, c). Taken together, these results indicate that the cytosolic N-terminus 119-144 amino acid region of SCAMP1 contains signals controlling its efficient export from the ER.

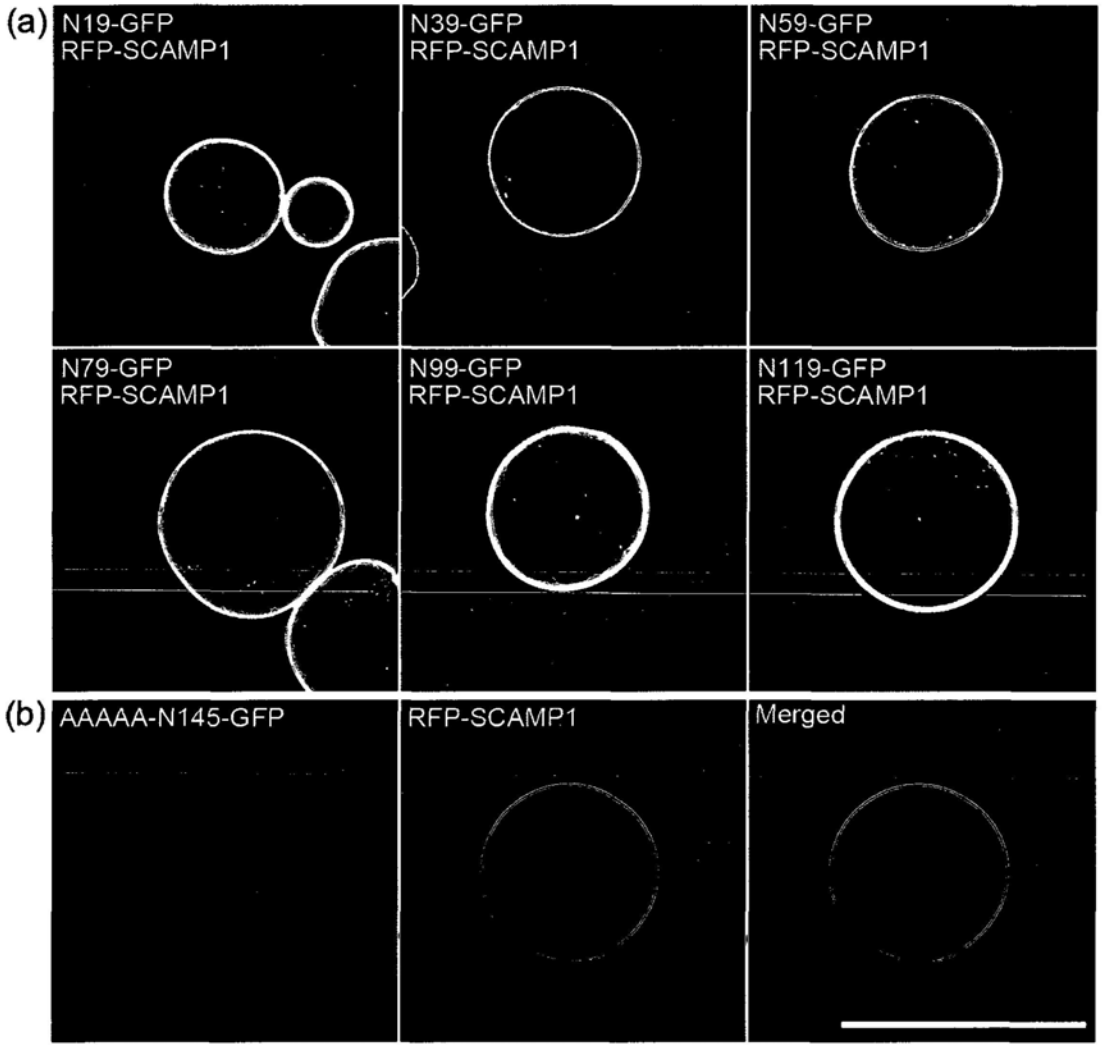

Figure 8. The cytosolic N-terminus of SCAMP1 contains an ER export signal. RFP-SCAMP1 was transiently coexpressed with N19-GFP, N39-GFP, N59-GFP, N79-GFP, N99-GFP, N119-GFP (a) or AAAAA-N145-GFP (b) respectively in BY-2 protoplasts, followed by confocal imaging. Scale bar = 50 μm.

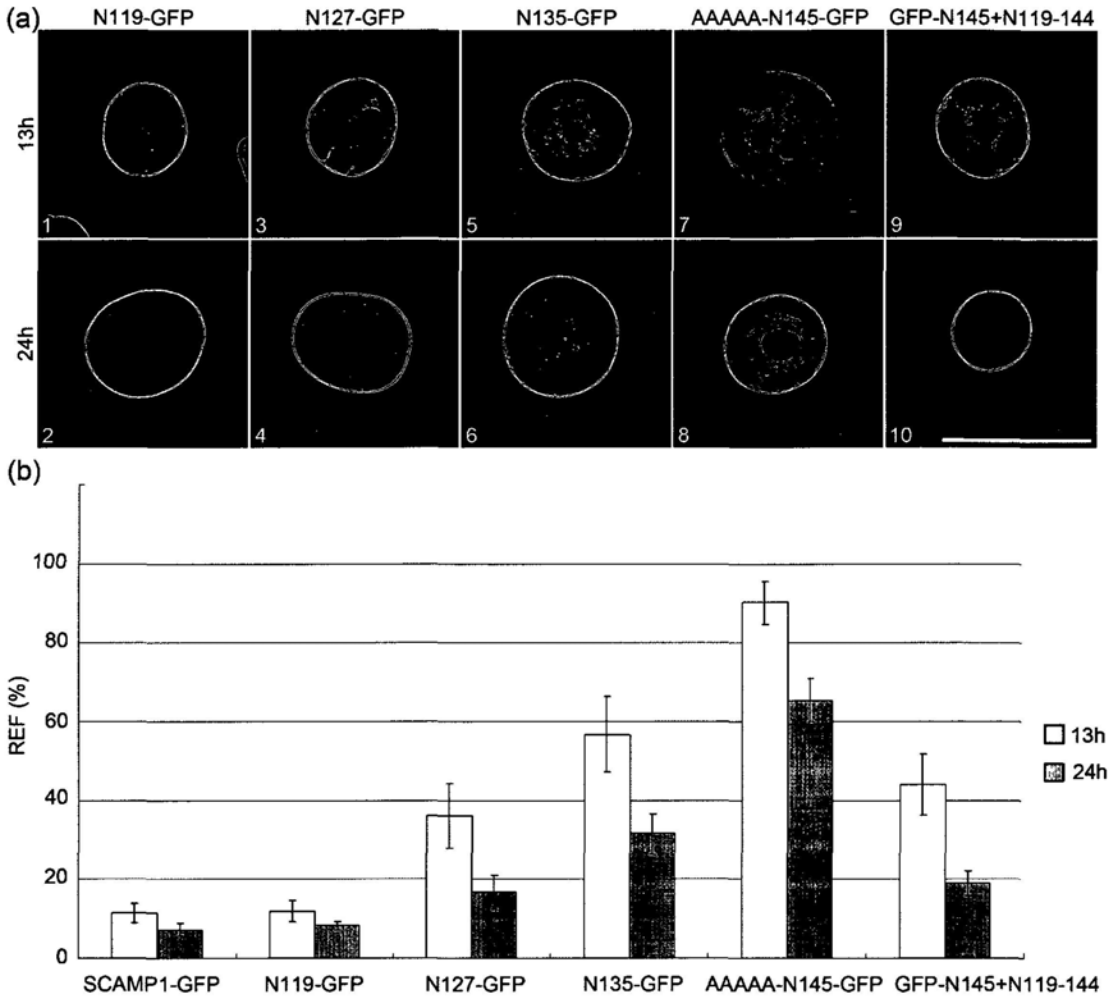

Figure 9. The N-terminal N119-144 region of SCAMP1 is a conformational ER export signal.

(a) Individual N-terminal deletion constructs of N119-GFP, N127-GFP, N135-GFP, AAAAA-N145-GFP or GFP-N145+N119-144 were expressed in BY-2 protoplasts, followed by confocal imaging at 13 hrs or 24 hrs as indicated.

(b) Quantitative analysis of the N-terminus deletion constructs for their relative ER fluorescence (REF) upon their expression in BY-2 protoplasts at 13 hrs and 24 hrs. REF is calculated as percentage of the ER signal intensity against the PM signal intensity (see Methods). Error bars represent SD for analysis of 40 individual cells.

Scale bar = 50 μm.

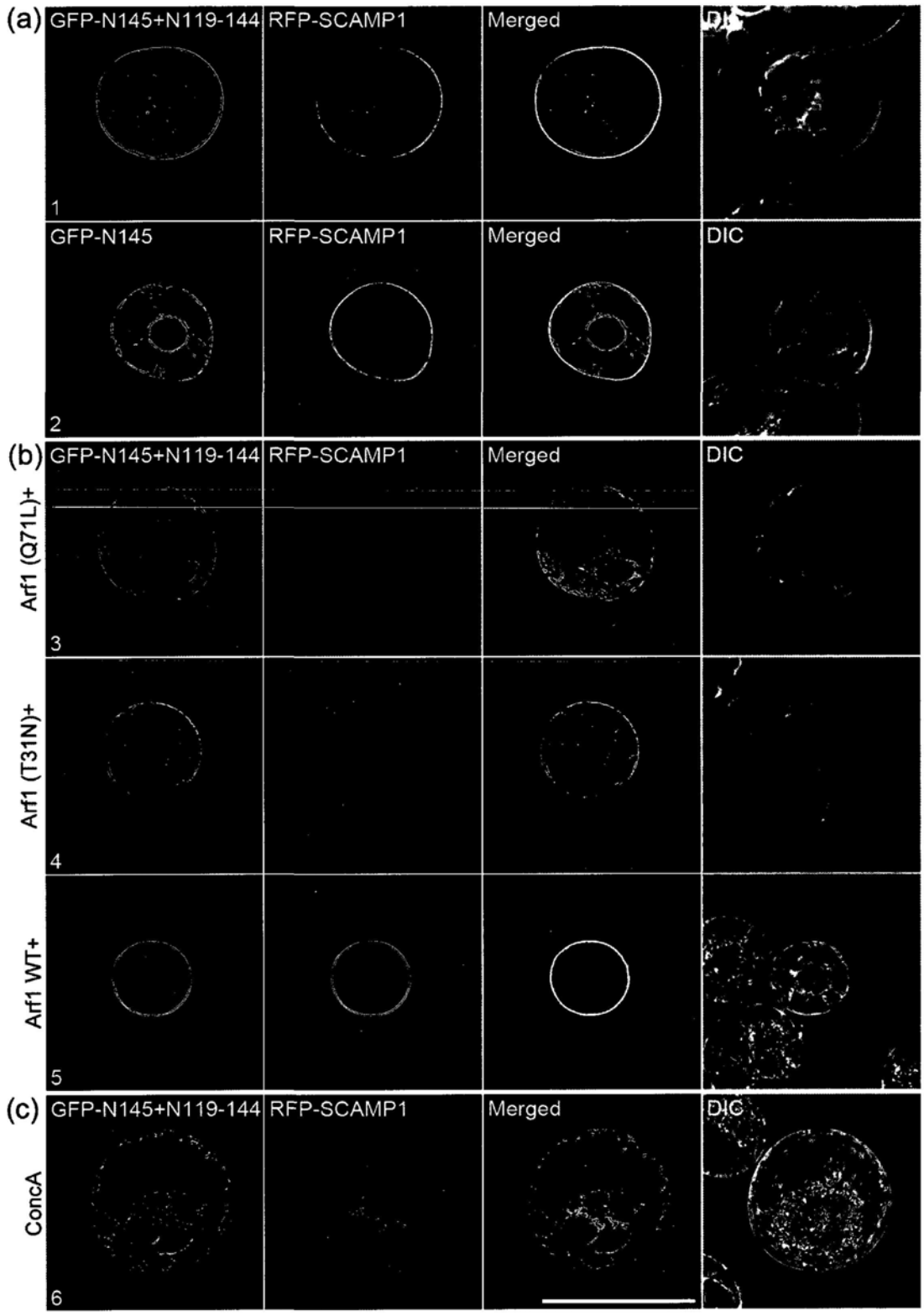
(a)
GFP-N145+N119-144
RFP-SCAMP1
Merged
DIC
1
GFP-N145
RFP-SCAMP1
Merged
DIC
2
(b)
GFP-N145+N119-144
RFP-SCAMP1
Merged
DIC
Arf1 (Q71L)+
3
Arf1 (T31N)+
4
Arf1 WT+
5
(c)
GFP-N145+N119-144
RFP-SCAMP1
Merged
DIC
ConcA
6

Figure 10. GFP-N145+N119-144 and SCAMP1 share the identical ER-Golgi-TGN-PM transport pathway.

(a) Coexpression of RFP-SCAMP1 with either GFP-N145+N119-144 (panel 1) or GFP-N145 (panel 2) in tobacco BY-2 protoplasts.

(b) Coexpression of RFP-SCAMP1 and GFP-N145+N119-144 together with ARF1 (Q71L), ARF1 (T31N) or ARF1 WT respectively (panels 3-5) in BY-2 protoplasts.

(c) ConcA trapped both GFP-N145+N119-144 and RFP-SCAMP1 in TGN. Tobacco BY-2 protoplasts transiently coexpressing GFP-N145+N119-144 and RFP-SCAMP1 were treated with ConcA immediately after transformation and incubated for 13 hrs prior to confocal imaging.

DIC, differential interference contrast. Scale bar = 50 μm.

2.3.5 SCAMP1 TMD1 is essential for TGN-to-PM targeting

The possible roles of TMDs in SCAMP1 targeting were next tested. First, N168(ΔTMD1)-GFP that lacks the first TMD of SCAMP1 (Figure 1b) was expressed in BY-2 cells. N168(ΔTMD1)-GFP was largely trapped in the ER (Figure 11, panels 1, 3), but in contrast to AAAAA-N145-GFP, it still slowly reached the PM, N168(ΔTMD1)-GFP no longer reached the PM but increasing GFP signal was detected in the lytic vacuole (LV) within 24 hrs from the start of transient expression (Figure 11, panels 2, 4).

When transiently expressed together in BY-2 protoplasts, N168(ΔTMD1)-GFP and the prevacuolar compartment (PVC) marker RFP-AtVSR2 colocalized in both punctate PVC and vacuole (Figure 11b), indicating that N168(ΔTMD1)-GFP may reach the vacuole via the PVC. In contrast, N168(ΔTMD1)-GFP was spatially separated from both the Golgi marker Man1-RFP and the TGN marker RFP-SYP61 (Figure 12a). The two vesicle trafficking inhibitors, ARF1 mutants and ConcA, also trapped N168(ΔTMD1)-GFP in the ER (Figure 12b) or TGN-derived aggregates (Figure 12c), respectively, indicating that the former trafficks through an ER-Golgi-TGN-PVC-LV pathway. Taken together, these results indicate that TMD1 is essential for TGN-to-PM targeting of SCAMP1 in BY-2 protoplasts (Figures 12d, e).

When the TMD4 of SCAMP1 was deleted (Figure 1b) and the resulting GFP-C254(ΔTMD4) fusion transiently expressed in BY-2 protoplasts, the GFP signals were mainly found in both the ER and cytosol after 13 hrs, but the GFP

signals were completely in the cytosol after 24 hrs from the start of expression, unlike RFP-SCAMP1 (Figure 13a). In addition, overexpression in the ARF1 GDP mutant trapped the RFP-SCAMP1 within the ER but did not prevent the translocation of GFP-C254(ΔTMD4) from the ER, at 13 hrs, to the cytosol at 24 hrs (Figure 13b). Thus the ER-to-cytosol change of GFP-C254(ΔTMD4) signal is independent of post-ER trafficking (Figures 13c, d). Therefore, the fourth TMD of SCAMP1 may play an important structural role.

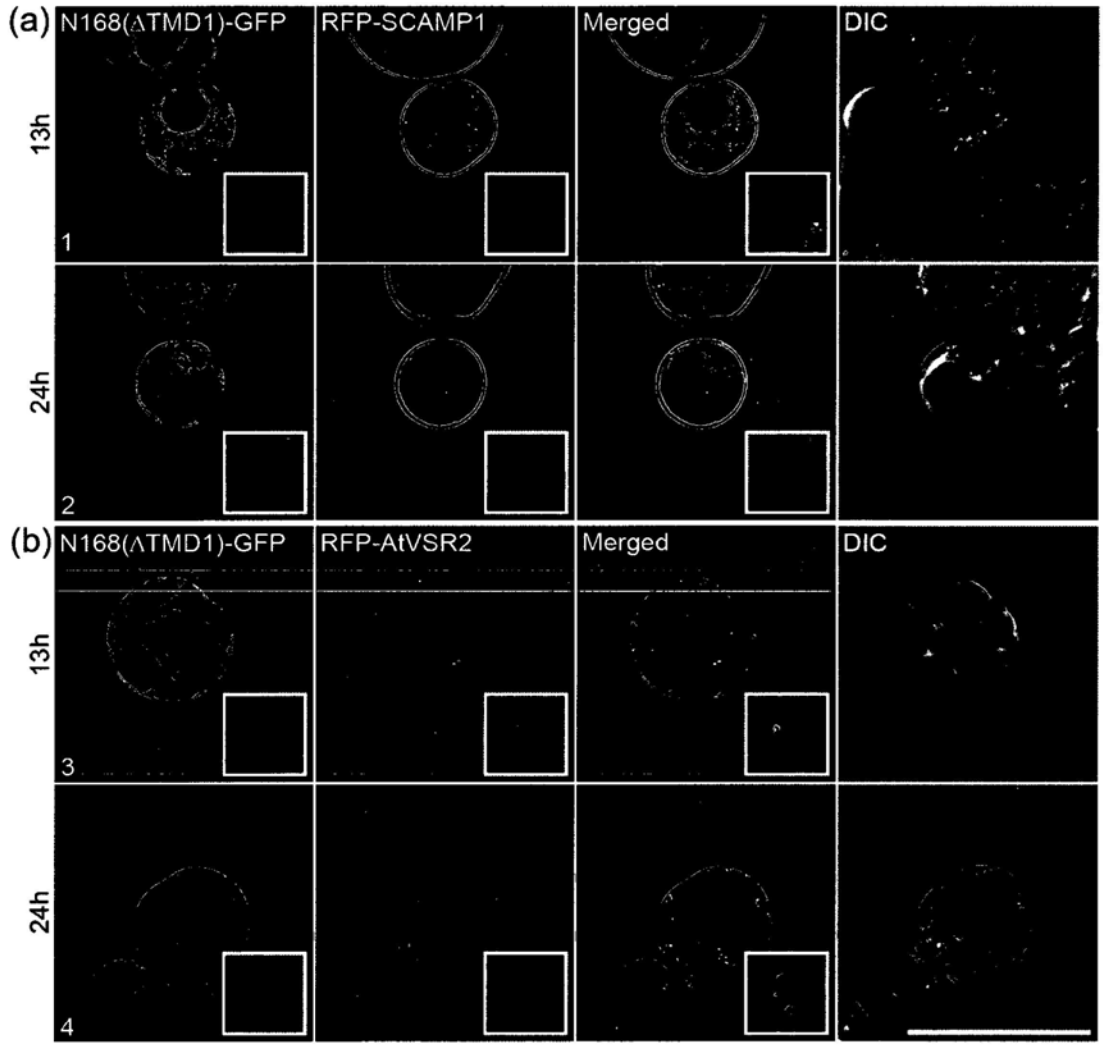

Figure 11. N168(ΔTMD1)-GFP reaches vacuole via the PVC.
N168(ΔTMD1)-GFP was coexpressed with either RFP-SCAMP1 (a) or RFP-AtVSR2 (b) respectively in tobacco BY-2 protoplasts, followed by confocal imaging at either 13 hrs or 24 hrs as indicated. DIC, differential interference contrast. Scale bar = 50 μm.

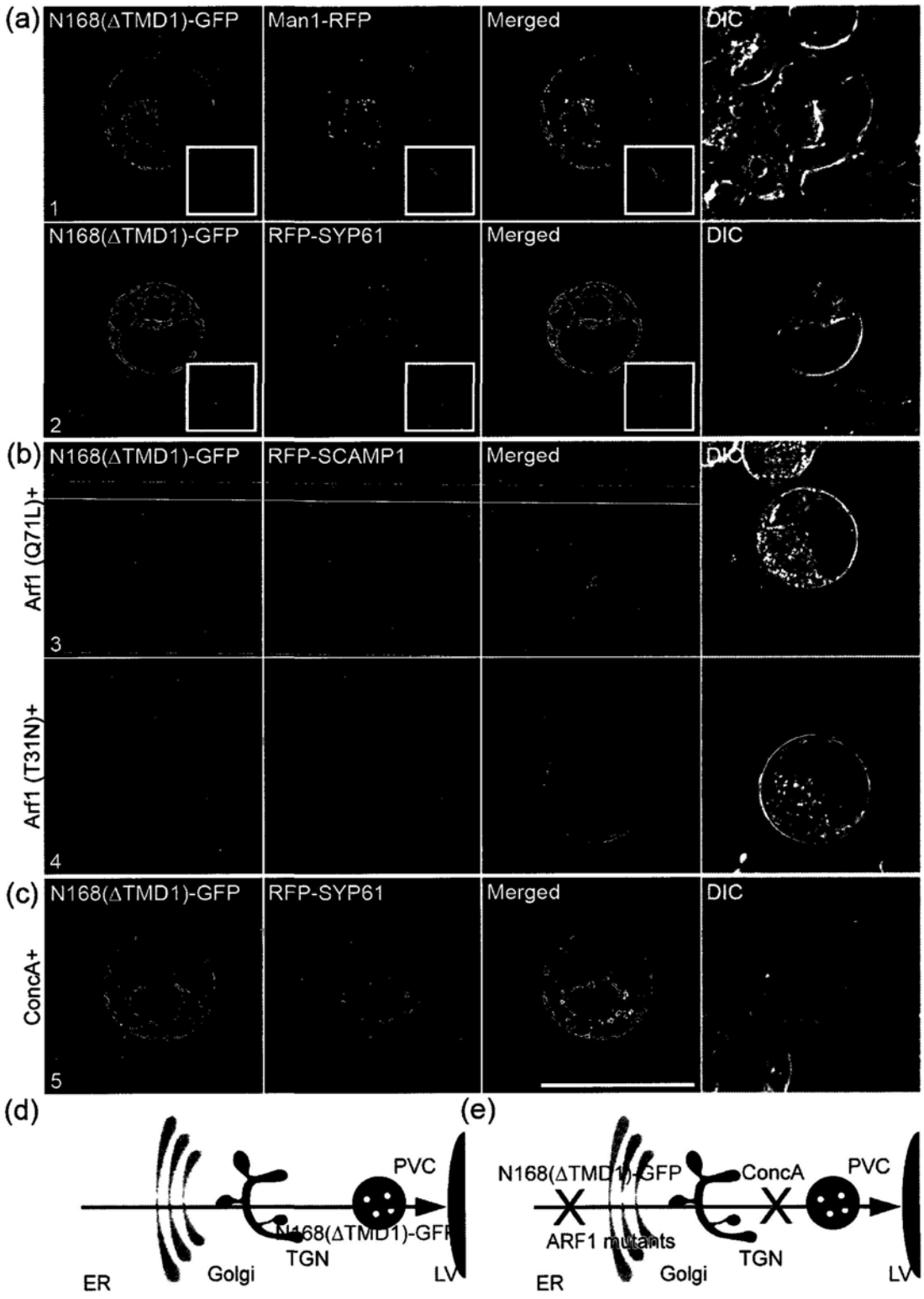
(a)
N168(ΔTMD1)-GFP
Man1-RFP
Merged
DIC
1
N168(ΔTMD1)-GFP
RFP-SYP61
Merged
DIC
2
(b)
N168(ΔTMD1)-GFP
RFP-SCAMP1
Merged
DIC
Arf1 (Q71L)+
3
Arf1 (T31N)+
4
(c)
N168(ΔTMD1)-GFP
RFP-SYP61
Merged
DIC
ConcA+
5
(d)
PVC
N168(ΔTMD1)-GFP
TGN
ER
Golgi
LV
(e)
N168(ΔTMD1)-GFP
ConcA
PVC
ARF1 mutants
TGN
ER
Golgi
LV

Figure 12. N168(ΔTMD1)-GFP reaches PVC/LV via an ER-Golgi-TGN pathway.

(a) N168(ΔTMD1)-GFP was coexpressed with Man1-RFP or RFP-SYP61 in tobacco BY-2 protoplasts, followed by confocal imaging.

(b) N168(ΔTMD1)-GFP and RFP-SCAMP1 were coexpressed with ARF1 (Q71L) or ARF1 (T31N), followed by confocal imaging.

(c) Tobacco BY-2 protoplasts transiently coexpressing N168(ΔTMD1)-GFP and RFP-SYP61 were treated with ConcA immediately after transformation and incubated for 13 hrs before confocal imaging.

(d) and (e) Normal transport of N168(ΔTMD1)-GFP is affected by ARF1 mutants (d) and ConcA (e) in plant cells.

DIC, differential interference contrast; ER, endoplasmic reticulum; LV, lytic vacuole; PM, plasma membrane; PVC, prevacuolar compartment; TGN, *trans*-Golgi network. Scale bar = 50 μm.

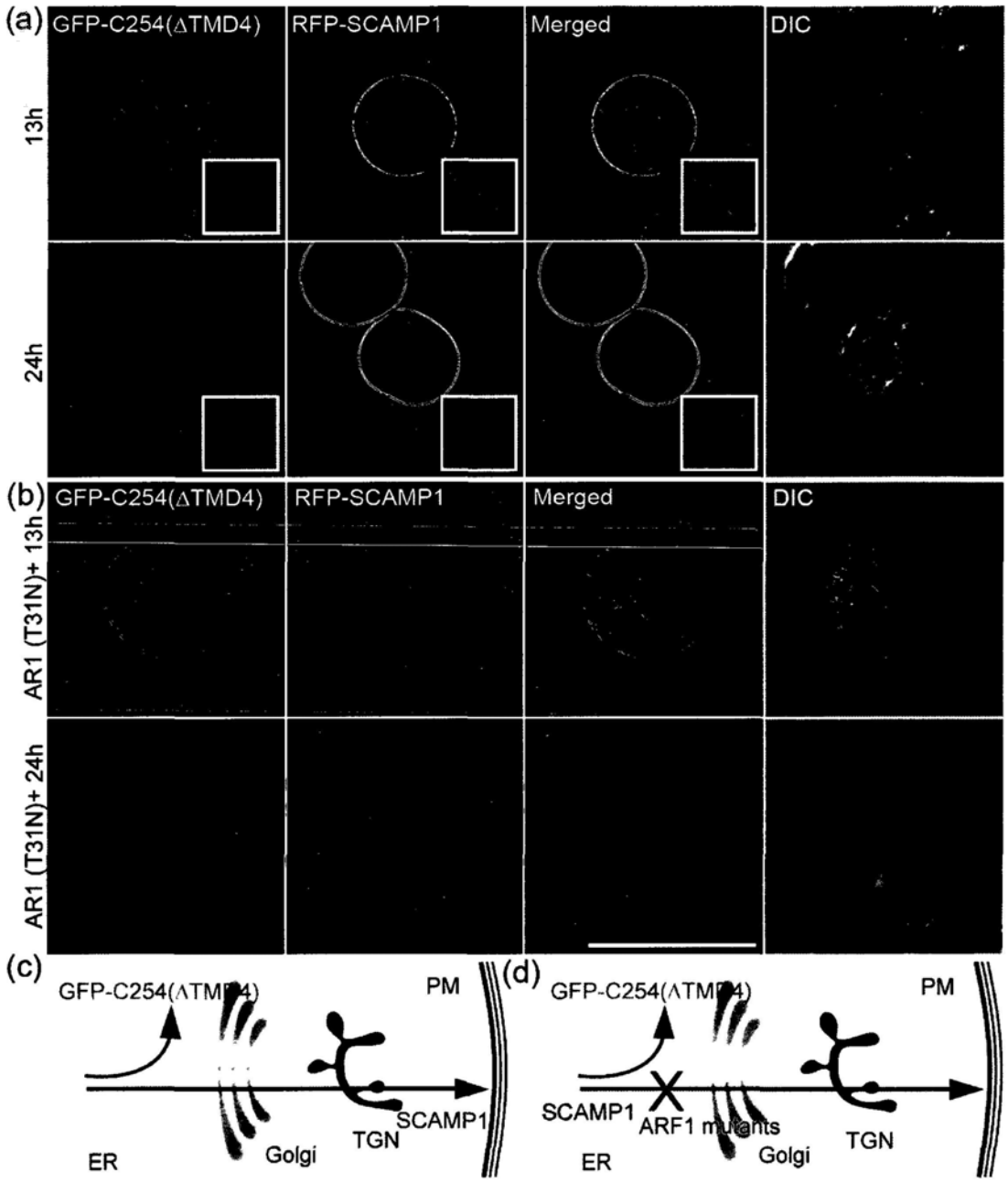

Figure 13. TMD4 of SCAMP1 has an important structure role.
(a) GFP-C254(ΔTMD4) was coexpressed with RFP-SCAMP1 in tobacco BY-2 protoplasts, followed by confocal imaging at either 13 hrs or 24 hrs as indicated.
(b) GFP-C254(ΔTMD4) and RFP-SCAMP1 were coexpressed with ARF1 (T31N) in tobacco BY-2 protoplasts, followed by confocal imaging at 13 hrs or 24 hrs as indicated.
(c) and (d) Possible translocation of GFP-C254(ΔTMD4) from ER to cytosol and the effect of ARF1 (T31N) on the location of GFP-C254(ΔTMD4) or SCAMP1.
DIC, differential interference contrast; ER, endoplasmic reticulum; PM, plasma membrane; TGN, *trans*-Golgi network. Scale bar = 50 μm.

2.3.6 The TMD2 and TMD3 of SCAMP1 are essential for Golgi export

Since TMD4 has an important structural role, and TMD1 is essential for TGN-to-PM trafficking of SCAMP1, I determined if these two TMD domains are sufficient for mediating SCAMP1 targeting to the PM. A chimeric GFP fusion ΔTMD2-3-GFP containing the SCAMP1 N terminus, TMD1, TMD4 and the C terminus was generated (Figure 1b). When coexpressed with various organelle markers in pairs, ΔTMD2-3-GFP colocalized with the Golgi marker Man1-RFP (Figure 14a), but separately from the PM marker RFP-SCAMP1, TGN marker RFP-SYP61 and PVC marker RFP-AtVSR2 (Figure 15), indicating that ΔTMD2-3-GFP is trapped within the Golgi apparatus, and not reaching any post-Golgi compartments. In addition, truncation of the N terminus of ΔTMD2-3-GFP from amino acid 1 to 118 (N119-ΔTMD2-3-GFP) (Figure 1b) did not affect the Golgi-localization of the resulting N119-ΔTMD2-3-GFP fusion protein (Figure 14b). However, complete N-terminal deletion from amino acid 119 to 144 caused the resulting AAAAA-N145-ΔTMD2-3-GFP fusion protein (Figure 1b) to be trapped mainly within the ER at 13 hrs, with some signals reaching the Golgi apparatus by 24 hrs after transformation (Figure 14c). Here, the AAAAA was included to ensure the proper structural conformation of N145-ΔTMD2-3-GFP. The trafficking pathway of ΔTMD2-3-GFP remained the same as that for full-length SCAMP1 because overexpression of ARF1 mutants caused both ΔTMD2-3-GFP and the Golgi marker Man1-RFP to be trapped within the ER (Figure 16).

To determine if the cytosolic sequences between TMD2 and TMD3 are essential

for Golgi export of SCAMP1, mutagenic analysis was carried out on this region (Figure 1b). To facilitate the cloning process, a BamHI restriction site (encoding Gly-Ser) was first introduced and this region mutated from RPLYNAMRTDSA to AAAAAGAAGSAG; no visible signal was detected upon transient expression (data not shown). Therefore, a series of amino acid substitutions or point mutations were then introduced into this region and the resulting mutated constructs M1-GFP to M7-GFP (Figure 1b) were analyzed via transient expression. As shown in Figure 17, all the GFP fusions were found in both the PM and cytosolic punctate organelles, distinct from the Golgi marker Man1-RFP (Figure 17), indicating that the cytosolic sequences between TMD2 and TMD3 did not play any role in SCAMP1 Golgi export. Taken together, since ΔTMD2-3-GFP did not reach any post-Golgi compartments (Figures 14a and 15), and the cytosolic region between TMD2 and TMD3 did not contain any Golgi export signals (Figure 17), TMD2 and TMD3 are thus likely essential for Golgi export of SCAMP1.

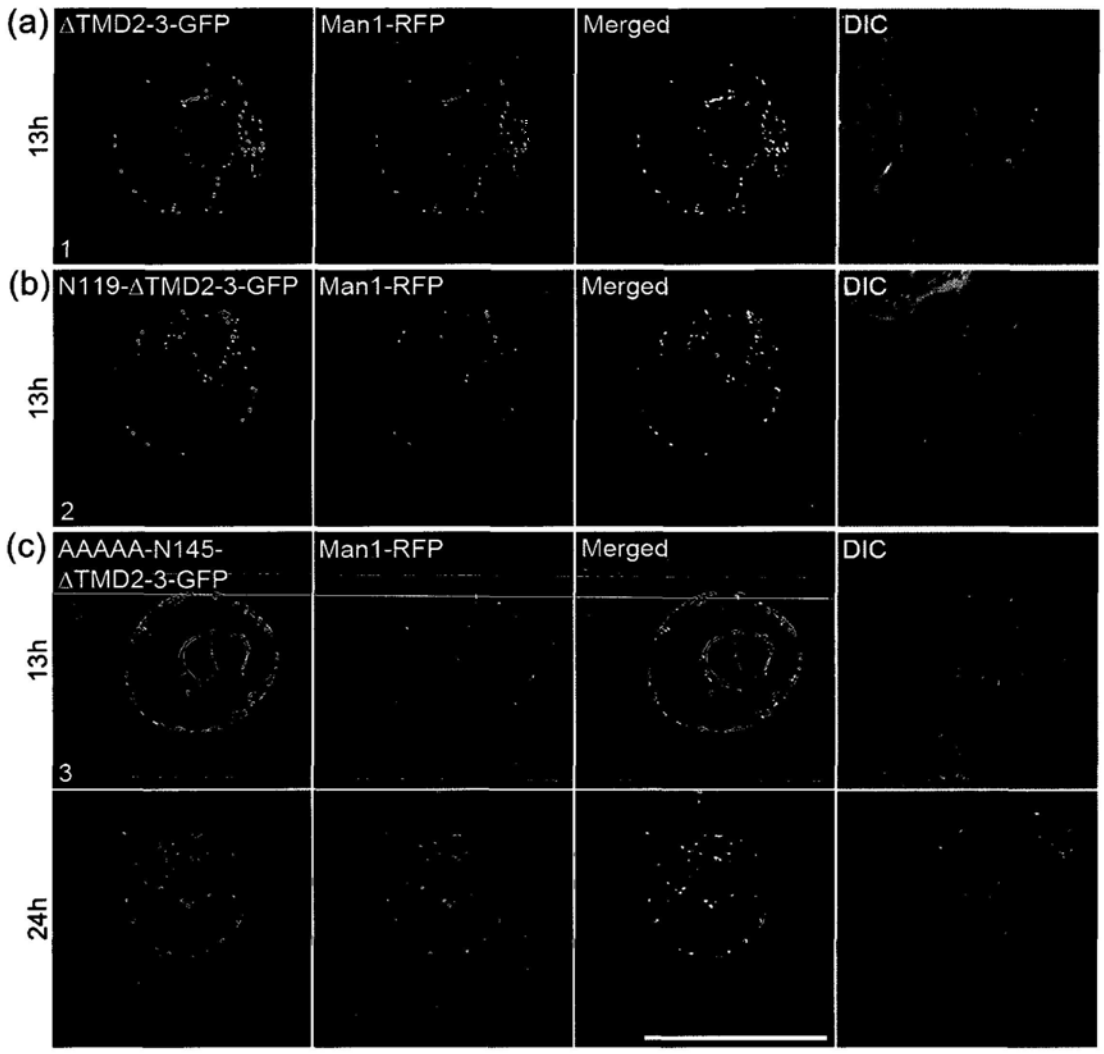

Figure 14. TMD2-3 is essential for post-Golgi traffic of SCAMP1.
The Golgi marker Man1-RFP was coexpressed with ΔTMD2-3-GFP (a), N119-ΔTMD2-3-GFP (b) or AAAAA-N145-ΔTMD2-3-GFP (c) in tobacco BY-2 protoplasts, followed by confocal imaging at either 13 hrs or 24 hrs as indicated. DIC, differential interference contrast. Scale bar = 50 μm.

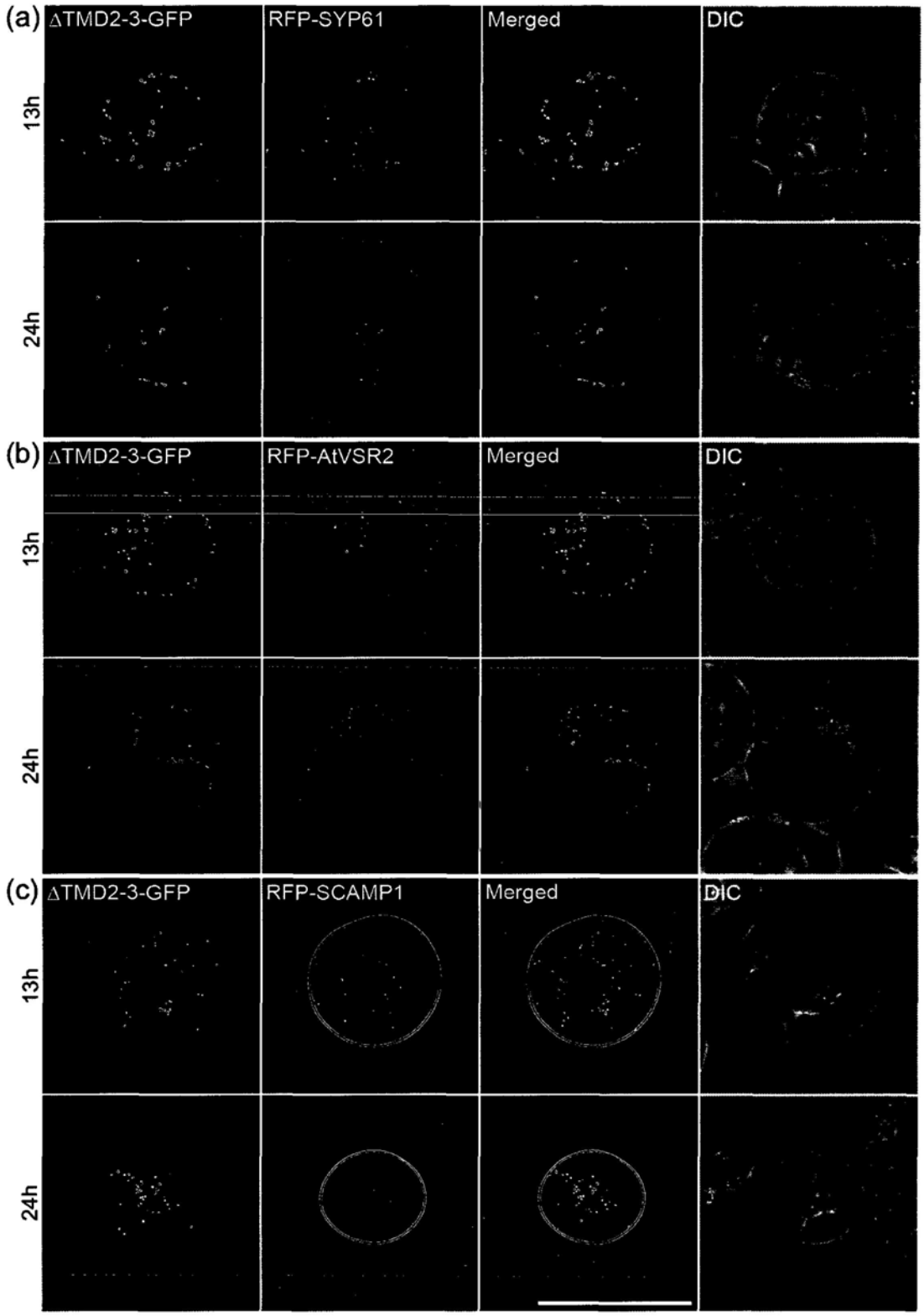

Figure 15. N168(ΔTMD1)-GFP did not reach any post Golgi organelles. N168(ΔTMD1)-GFP was transiently coexpressed with RFP-SYP61 (a), RFP-AtVSR2 (b) or RFP-SCAMP1 (c) in tobacco BY-2 protoplasts. Images were taken at either 13 hrs or 24 hrs as indicated. Scale bar = 50 μm.

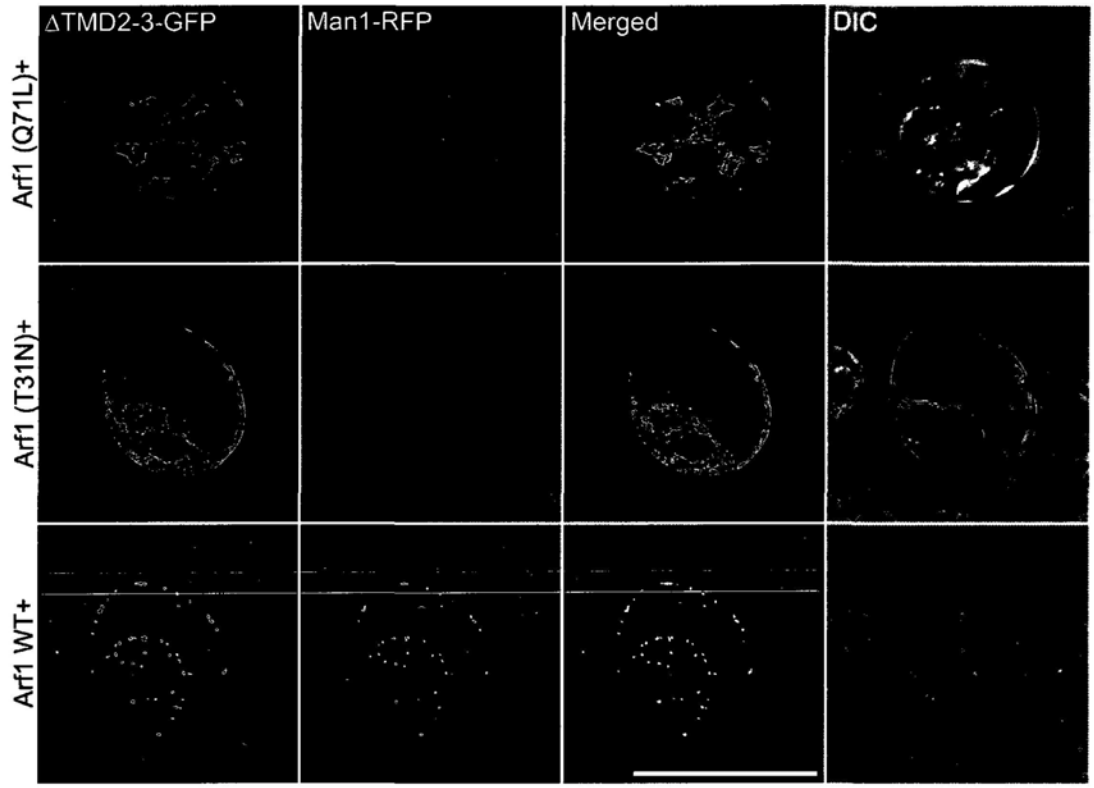

Figure 16. ΔTMD2-3-GFP follows the identical trafficking pathway as SCAMP1.

ΔTMD2-3-GFP and Man1-RFP were coexpressed with ARF1 (Q71L), ARF1 (T31N) or ARF1 WT in tobacco BY-2 protoplasts. Scale bar = 50 μm.

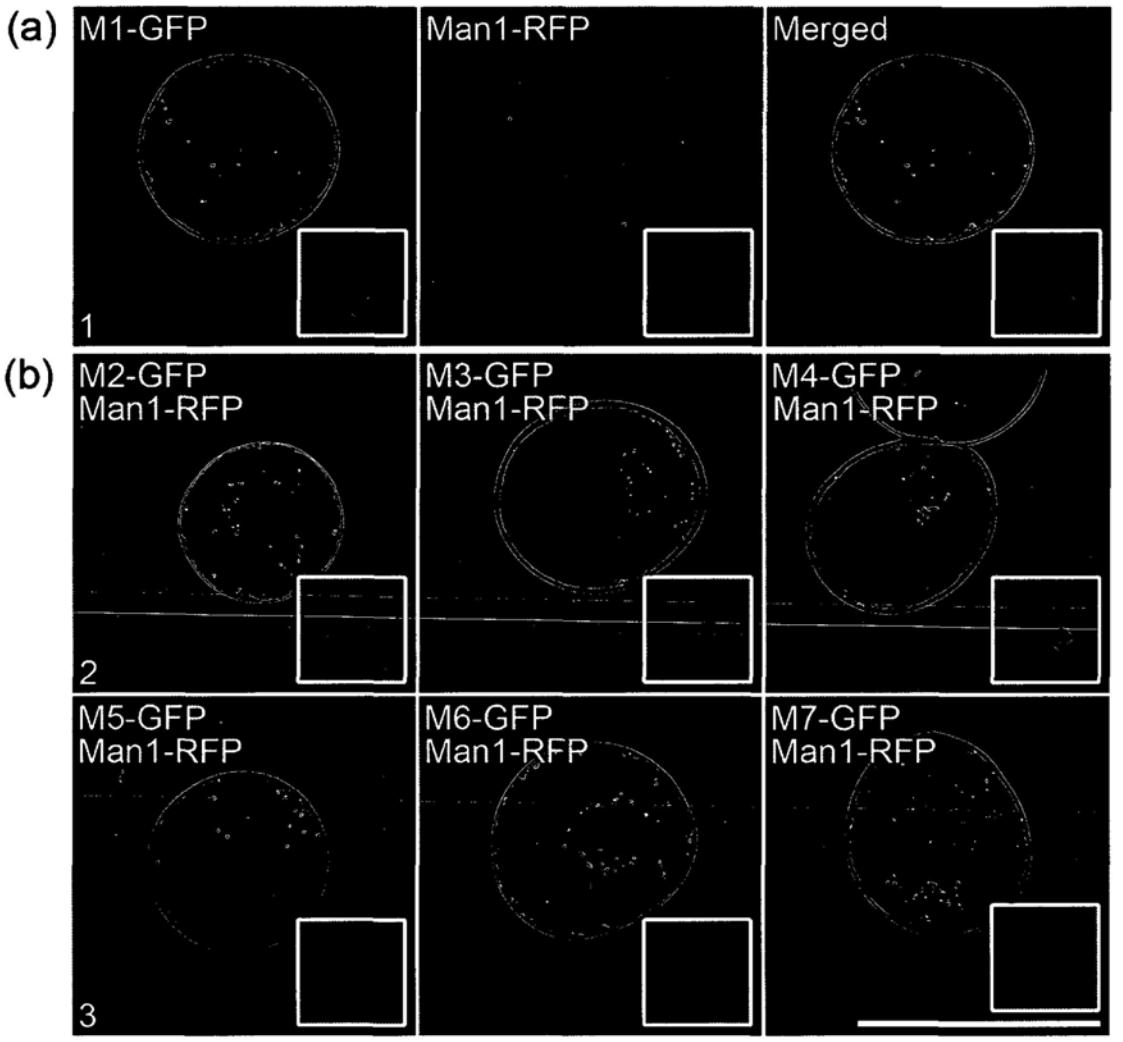

Figure 17. The cytosolic flanking sequences between TMD2 and TMD3 do not contain any targeting signals.

Man1-RFP was coexpresssed with either M1-GFP (a), M2-GFP, M3-GFP, M4-GFP, M5-GFP, M6-GFP or M7-GFP (b) in tobacco BY-2 protoplasts followed by confocal imaging. Scale bar = 50 μm.

2.4 Discussion

2.4.1 SCAMP1 reaches the PM via an ER-Golgi-TGN-PM pathway in plant cells

The PM is one of the major compartments in the endomembrane system of eukaryotic cells that harbors thousands of proteins for various biological functions. It has been well established in yeast and mammalian cells that both soluble and membrane proteins destined for the PM reach their final destination via an ER-Golgi-PM pathway. However, relatively little is known about the transport pathways of integral membrane proteins destined for the PM in plant cells.

Several recent studies on plant cells point to the distinct roles of the Golgi and TGN in mediating secretion of soluble and membrane proteins, respectively. For example, when Arabidopsis root cells are treated with ConcA, a V-ATPase inhibitor affecting the function of VHA-a1 at the TGN (Dettmer et al., 2006), the integrated PM protein BRI1 is trapped within intracellular organelles in a cycloheximide-sensitive manner (Dettmer et al., 2006). These BRI1 positive aggregates are now known to be derived from the TGN (Viotti et al., 2010), indicating the direct involvement of this network in transporting PM proteins to their final destination. In contrast, when subcellular localization studies were carried out for RabE1d and RabA4b, two small GTPases involved in the secretion of a green fluorescent marker and cell wall components, respectively (Preuss et al., 2004; Zheng et al., 2005), these two molecules located to the Golgi apparatus rather than the TGN (Preuss et al., 2004; Zheng et al., 2005). In addition, overexpression of a PVC-localized Arabidopsis syntaxin PEP12/SYP21 caused the partial secretion of a

vacuolar soluble cargo protein Amy-spo without affecting the Golgi structure (Foresti et al., 2006). These results together demonstrate that soluble cargo proteins can reach the apoplast via Golgi apparatus or PVC.

In this study, I used the BY-2 protoplasts transient expression system and several protein trafficking inhibitors as tools to study the trafficking pathway of SCAMP1, a polytopic PM protein. The results provide direct evidence that SCAMP1 reaches the PM via an ER-Golgi-TGN-PM pathway (Figures 3 and 4). Moreover, the single transmembrane protein FLS2-GFP also follows the identical pathway to reach the PM (Figure 5).

2.4.2 Central role of TGN in endomembrane trafficking

In the recent models of plant endomembrane trafficking, TGN has been proposed to be the main sorting station where secretory (biosynthetic) and endocytic pathways converge (Hanton et al., 2007; Lam et al., 2007a; Foresti and Denecke, 2008; Hwang, 2008; Otegui and Spitzer, 2008; Robinson et al., 2008; Richter et al., 2009). However, among these pathways, only a functional role for TGN in the endocytic pathway has been well established (Dettmer et al., 2006; Lam et al., 2007b; Chow et al., 2008; Tanaka et al., 2009), whereas the pathways from the ER to PM or LV remain debatable (Foresti and Denecke, 2008; Richter et al., 2009). A recent immunogold EM study on the transport of BOR1-GFP and BRI1-GFP showed that at least in Arabidopsis root cells, newly synthesized GFP-tagged PM proteins reach the TGN prior to the PM (Viotti et al., 2010).

Here, I used both full-length SCAMP1 and SCAMP1 truncation mutants as tools to characterize the transport pathways of PM proteins in tobacco BY-2 cells. The former follows an ER-Golgi-TGN-PM pathway (Figures 3 and 4), whereas the latter, as N168(ΔTMD1)-GFP, reaches the vacuole via an ER-Golgi-TGN-PVC-LV pathway (Figures 11 and 12). Therefore, the sorting of proteins destined for either the PM or PVC-vacuole occurs at the TGN; this organelle may serve as a central sorting station with multiple domains to determine the fate or transport pathway of proteins between the Golgi and PM (Figure 18).

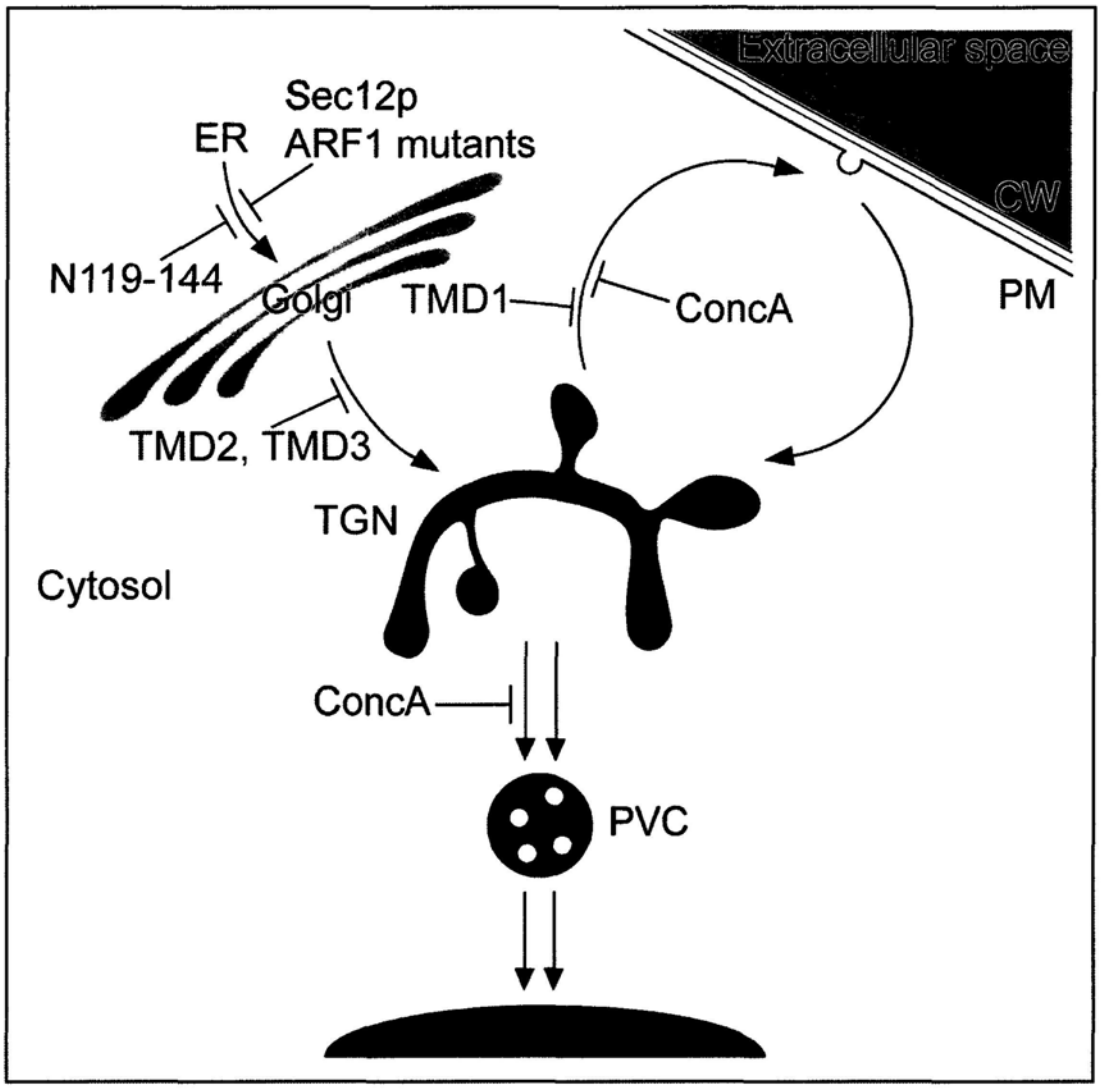

Figure 18. Working model of SCAMP1 trafficking and the roles of its targeting determinants or signals for an ER-Golgi-TGN-PM pathway.
Multiple targeting signals are required for the transport of SCAMP1 via an ER-Golgi-TGN-PM pathway. Such pathway is sensitive to several protein trafficking inhibitors including ConcA and Sec12p/ARF1 mutants as indicated by the red characters. Blue characters indicate the defined SCAMP1 signals required for proper traffic of SCAMP1 along the ER-Golgi-TGN-PM pathway.
ConcA, concanamycin A; CW, cell wall; ER, endoplasmic reticulum; LV, lytic vacuole; PM, plasma membrane; PVC, prevacuolar compartment; TGN, *trans*-Golgi network; TMD, transmembrane domain.

2.4.3 ER export signals

In the secretory pathway, proteins with an N-terminal signal peptide are usually cotranslationally inserted into the ER for further transport to the Golgi via COPII vesicles. In yeast and mammalian cells, membrane cargoes are recognized by different COPII coats before being packaged into COPII vesicles for ER-to-Golgi transport. Such selective ER export machinery allows the cells to control the protein composition of post-Golgi organelles such as PM (Mancias and Goldberg, 2005; Sato and Nakano, 2007; Achour et al., 2008). However, relatively little is known about the molecular mechanism of ER export in plant cells even though all COPII components have also been identified in plants (Hawes et al., 2008).

In this study, I have defined a conformational ER export signal residing in the N119-144 region of the cytosolic N-terminus of SCAMP1 (Figures 8-10). Interestingly, this region does not contain any classical diacidic motif ((D/E)x(D/E) that functions as the ER export signal for several membrane proteins (Hanton et al., 2005; Mikosch et al., 2006; Dunkel et al., 2008; Sieben et al., 2008; Zelazny et al., 2008). Since the amino acid sequence of N119-144 is only conserved within the SCAMP family, it is likely that the ER export signal in SCAMP1 is unique to this family. Such protein-specific ER export signals occur in several other plant membrane proteins including the Arg/Lys residues in the cytoplasmic tail of plant glycosylation enzymes (Schoberer et al., 2009), and MELAD in SYP31 (Chatre et al., 2009). Thus, there are various ER export signals in plant cells that mediate the efficient export from the ER of membrane proteins.

2.4.4 Golgi export signals

Sorting of soluble proteins via the Golgi apparatus is considered to be a default process; however, export from the Golgi of membrane proteins with single transmembrane domain (TMD) may be mediated by the TMD length or cytosolic motifs (Phillipson et al., 2001; Brandizzi et al., 2002; daSilva et al., 2006). In addition, a study on the targeting mechanism of the plasma membrane H+-ATPase (PMA), which contains ten TMDs, demonstrated that GFP fusions with TMDs 1-4 or 5-10 truncations were trapped in the Golgi apparatus, not reaching the PM, thus providing the first evidence in plant cells that export of multi-transmembrane proteins from Golgi is also signal-dependent (Lefebvre et al., 2004).

In this study, when both TMD2 and TMD3 of SCAMP1 were truncated, the resulting ΔTMD2-3-GFP was trapped in the Golgi apparatus (Figure 14a). Since mutation analysis in the cytosolic region between TMD2 and TMD3 did not affect the PM localization of SCAMP1 (Figure 17), the TMD2/3 sequences may act as export signals from the Golgi. A recent study on the targeting mechanism of tandem-pore potassium (TPK) channel family proteins demonstrated that the C terminus of TPK1 is critical for both export from the ER and Golgi sorting (Dunkel et al., 2008). Thus, both TMD and cytosolic sequences of multi-transmembrane proteins may play important roles in plant cells in mediating export from the Golgi.

2.4.5 TGN sorting

The TGN has recently been proposed to be the central sorting or recycling station for proteins destined for or from the PM and PVC-LV (Lam et al., 2007a). Experimental evidence came from recent studies on the trafficking pathway of several PM proteins including BOR1, BRI1, SCAMP1 and FLS2 (Viotti et al., 2010). Studies on the trafficking mechanism of single transmembrane proteins, including the human lysosomal protein LAMP1 and the plant vacuolar sorting receptor (VSR) BP-80, suggest that the PM is likely the default destination for these proteins, whereas specific transmembrane or cytosolic motifs are required for TGN-to-PVC transport (Brandizzi et al., 2002; daSilva et al., 2006). However, in this study, the first TMD of SCAMP1 was found to be essential for PM targeting because N168(ΔTMD1)-GFP, which lacks the SCAMP1 TMD1, did not reach the PM but instead reached the vacuole via the TGN and PVC (Figures 11 and 12), Possibly, therefore, the vacuole is the default location for multi-transmembrane proteins in plant cells.

2.4.6 Roles of TMDs

Cytosolic sequences of membrane proteins have been suggested to play a major role in determining the fate of the protein in the secretory pathway in eukaryotic cells (Mancias and Goldberg, 2005; Seaman, 2008). However, recent studies in yeast and mammalian cells also point to the important roles of TMDs in sorting of the membrane proteins (Letourneur and Cosson, 1998; Barman and Nayak, 2000; Dunbar et al., 2000; Reggiori et al., 2000; Martin et al., 2001; Bulbarelli et al., 2002; Wang et al., 2002; Nufer et al., 2003; Schamel et al., 2003; Hong et al., 2004; Ronchi

et al., 2008). For example, the first two TMDs of human latent membrane protein 1 are essential for PM targeting and partitioning to specific lipid rafts for cell signaling (Coffin et al., 2003; Lee and Sugden, 2007).

In this study, I show that trafficking of SCAMP1 along the secretory pathway is spatially controlled at the ER, Golgi and TGN by either the cytosolic or individual TMDs sequences within this protein (Figure 18).

How does the TMD function as sorting signal? Two possible mechanisms may exist: protein-protein or protein-lipid interactions. First, the retrieval of sec71p from Golgi to ER relies on the physical interaction of its transmembrane domain with Rer1p, a Golgi membrane protein required for the retrieval of various ER membrane proteins (Sato et al., 2003). Second, reporters with TMD of different lengths (17 and 22 amino acids) locate to different microdomains of ER, demonstrating that the physical-chemical features of the TMD alone may determine the fate of membrane proteins (Ronchi et al., 2008).

CHAPTER 3

BFA-induced Compartments From the Golgi Apparatus and Trans-Golgi network/Early endosome Are Distinct in Plant Cells

3.1 Introduction

All eukaryotic cells have an endomembrane system for protein trafficking and secretion that consists of several morphologically and functionally distinct membrane-bound organelles, each with characteristic proteins for their unique functions that can also be used as markers for their identity. These organelles include the endoplasmic reticulum (ER), Golgi apparatus, *trans*-Golgi network (TGN), prevacuolar compartment (PVC), plasma membrane (PM), various endosomal compartments, and vacuole or lysosome. Several recent studies on the post-Golgi trafficking in plant cells have demonstrated that the plant PVC had a characteristic of multivesicular body (MVB) in the secretory pathway (Tse et al., 2004; Haas et al., 2007) while the TGN, identified as tubular-vesicular structures at the *trans*-Golgi with clathrin coats that are distinct from the Golgi apparatus in tobacco BY-2 cells (Lam et al., 2007b), also served as an early endosome (EE) connecting the secretory and endocytic pathways in plant cells (Dettmer et al., 2006; Lam et al., 2007b; Lam et al., 2007a; Robinson et al., 2008).

Proteins are often transported through multiple compartments via distinct transport vesicles before reaching their final destinations in the plant secretory and endocytic pathways (Lam et al., 2007a; Robinson et al., 2008). Several approaches have been used to identify and define specific organelles in the plant endomembrane system. First, immunogold electron microscopy (EM) with specific antibodies for known functional proteins can be used as markers to identify the ultrastructure of the target organelle. For example, using antibodies against the vacuolar sorting receptor

(VSR) proteins that predominantly localized to the PVCs (Li et al., 2002), PVCs were identified as MVBs in tobacco BY-2 cells (Tse et al., 2004). Second, established organelle reporters can be used to define the subcellular localization of newly identified protein via their co-expression in the same cells for direct comparison. Selective examples include Golgi identification using various fluorescent reporters such as MAN1-GFP (Nebenfuhr et al., 1999), GONST1-YFP (Baldwin et al., 2001; Tse et al., 2004) and Sar1-YFP (daSilva et al., 2004) as well as TGN definition with SYP41, SYP42 and SYP61 (Uemura et al., 2004; Foresti and Denecke, 2008; Robert et al., 2008), the vacuolar ATPase subunit VHA-a1 (Dettmer et al., 2006) and the rice SCAMP1 (Lam et al., 2007b). Third, visible changes of fluorescent protein-marked organelles in response to treatments with drugs such as wortmannin or brefeldin A (BFA) have also been useful for organelle identification and protein localization. For instance, vacuolation of GFP-VSR-positive punctate PVCs in response to wortmannin treatment has been used as one of the reliable criteria for defining PVCs or endosomes in plant cells (Tse et al., 2004; Jaillais et al., 2006; Miao et al., 2006; Delhaize et al., 2007; Jaillais et al., 2008; Miao et al., 2008). Such wortmannin-induced enlargement of PVCs/MVBs observed by confocal microscope has been further verified by immunogold EM studies where enlarged MVBs were observed in cells treated with wortmannin (Tse et al., 2004; Miao et al., 2006; Wang et al., 2007). In addition, it seems that the effects of wortmannin on PVC/MVB morphology is a general response is plants because such wortmannin-induced PVC/MVB enlargement has been observed in various plant cell types including

suspension cultured cells of BY-2, Arabidopsis and rice (Tse et al., 2004; Miao et al., 2008), root cells of Arabidopsis, tobacco and mung bean (Jaillais et al., 2006; Wang et al., 2007; Robinson et al., 2008) and seeds of Arabidopsis and mung bean (Otegui et al., 2006; Wang et al., 2007; Wang et al., 2009).

Similar to mammalian cells (Sciaky et al., 1997; Kawamoto et al., 2002), the Golgi apparatus is one of the sites of BFA action in plant cells because BFA treatment caused COPI coats to be released into cytosol rapidly and resulted in the formation of various Golgi-derived structures in various plant cells, including ER-Golgi hybrid (Nebenfuhr et al., 2002), BFA compartment or aggregate (Satiat-Jeunemaitre and Hawes, 1994; Satiat-Jeunemaitre et al., 1996; Wee et al., 1998; Baldwin et al., 2001; Tse et al., 2004) and loss of the Golgi *cis*-cisternae (Hess et al., 2000). BFA also caused morphological changes of endosomal compartments in plant cells. For example, in Arabidopsis root cells, BFA at ~14 μg/mL (50 μM) caused endosomal compartments marked by the internalized PIN1 or PIN2 auxin transports from the PM to form aggregates that also colocalized with the internalized endosomal marker FM4-64 (Geldner et al., 2001; Baluska et al., 2002; Geldner et al., 2003; Grebe et al., 2003; Samaj et al., 2004; Dettmer et al., 2006). Similarly, an EE or TGN marked by the vacuolar ATPase subunit VHA-a1 was induced to form aggregates in the presence of BFA at ~14 μg/mL (50 μM) in Arabidopsis root cells (Dettmer et al., 2006). These BFA-induced aggregates were thus considered to be endosomes whereas Golgi remained unchanged in the presence of BFA (Richter et al., 2007; Chow et al., 2008).

In tobacco BY-2 cells, the BFA effect is more complicated as both secretory organelle Golgi apparatus (Tse et al., 2004) and the endocytic compartment TGN/EE (Lam et al., 2007b) are sensitive to BFA and form aggregates in response to BFA treatment. Since the secretory organelles and the endocytic compartments have been mostly studied one and another in plant cells (Lam et al., 2007a), the nature and relationship between these BFA-induced Golgi-derived and TGN/EE-derived aggregates in the same plant cells remain elusive.

We have previously used the rice SCAMP1 (**S**ecretory **ca**rrier **m**embrane **p**rotein 1) (SCAMP1) as a probe to study plant endocytosis (Lam et al., 2007b). In transgenic tobacco BY-2 cells expressing the SCAMP1-YFP fusion construct, the fluorescent SCAMP1 was found to locate to the PM and a punctate organelle, as well as in the cell plate of dividing cells (Lam et al., 2008). This was subsequent identified by immunogold EM with SCAMP1 and GFP antibodies as a tubular-vesicular structure resembling TGN, which may also serve as an EE (Lam et al., 2007b). In addition, when transgenic BY-2 cells expressing the SCAMP1-YFP were treated with BFA at low concentrations (5-10 μg/mL), TGN/EE-derived aggregates were observed (Lam et al., 2007b). Similarly, in transgenic BY-2 cells expressing the Golgi markers GONST1-YFP or MAN1-GFP, BFA at 5-10 μg/mL also caused the Golgi to form similar aggregates under confocal microscope observation (Tse et al., 2004; Lam et al., 2007b).

3.2 Materials and Methods

General methods for construction and characterization of recombinant plasmids, maintenance of suspension cultured tobacco (*Nicotiana tabacum*) BY-2 cells, and the preparation and characterization of antibodies have been described previously (Tse et al., 2004; Lam et al., 2007b).

3.2.1 BFA treatment studies

For BFA treatment experiments, aliquots of BFA (stock at 2.5 mg/mL in DMSO) solution were added to give the proper final concentrations.

3.2.2 FM4-64 uptake study

Transgenic tobacco BY-2 cell lines expressing various reporters were used for FM4-64 uptake studies as described (Tse et al., 2004; Lam et al., 2007b).

3.2.3 Transient expression and confocal imaging

Transient expression with protoplasts was carried out essentially as previously described (Miao and Jiang, 2007). Confocal observation and image collection were carried out as previously described (Jiang and Rogers, 1998; Tse et al., 2004; Lam et al., 2007b).

3.3 Results

3.3.1 BFA-induced Golgi-derived aggregates were distinct from the TGN/EE-derived aggregates

To further investigate the distinct nature of the Golgi-derived and the TGN-derived BFA-induced aggregates, I carried out endocytic uptake studies using the endosomal marker FM4-64 in transgenic BY-2 cells. As shown in Figure 19, in transgenic tobacco BY-2 cells expressing the TGN/EE marker SCAMP1-YFP, the BFA-induced TGN-derived aggregates (green) were fully colocalized with the internalized FM4-64 aggregates (red) (Figure 19a), indicating the endocytic nature of TGN/EE, which is consistent with the nature of PIN-positive endosomes (Lam et al., 2007a). In contrast, when identical uptake experiments were performed in BY-2 cells expressing the Golgi markers GONST1-YFP or MAN1-GFP, the BFA-induced Golgi-derived aggregates (green, arrowhead) are largely separated from the internalized FM4-64 (red, arrow) (Figure 19b,c), which presumably representing the TGN/EE-derived BFA-induced aggregates seen in Figure 19a, even though a direct comparison between Golgi and TGN markers in the same cell is still needed to draw this conclusion.

To study the relationship between the Golgi-derived and TGN/EE-derived BFA-induced aggregates in the same cell, I next carried out transient co-expression experiments in which the two distinct Golgi or TGN/EE reporters were co-expressed in tobacco BY-2 or Arabidopsis protoplasts, followed by BFA treatment. As shown in Figure 20, in BY-2 cells co-expressing the TGN/EE marker GFP-SCAMP1 and the

cis-Golgi marker MAN1-RFP (Figure 20, panel 1), or RFP-SCAMP1 and the *trans*-Golgi marker GONST1-GFP (Figure 20, panel 3), no visible aggregation was observed in untreated cells where the two markers remained separated. However, in cells treated with BFA at 10 μg/mL for one hour, BFA-induced aggregates were obvious for both reporters, where the aggregates derived from GFP-SCAMP1 or RFP-SCAMP1 remained distinct from those of MAN1-RFP or GONST1-GFP (Figure 20, panels 2 and 4, see arrows/arrowheads as examples). Similar results were obtained when these co-expression experiments with identical TGN/EE and Golgi markers were carried out in Arabidopsis cells (Figure 21). Taken together, these results demonstrate that the BFA-induced aggregates from TGN/EE and Golgi were distinct compartments.

Since GFP-SCAMP1 localized to both PM and TGN/EE (Lam et al., 2007b), I have additionally used a second well established TGN marker RFP-SYP61 (Uemura et al., 2004; Foresti and Denecke, 2008; Robert et al., 2008) in co-expression studies. As shown in Figure 22, when co-expressed with GFP-SCAMP1 in tobacco BY-2 protoplasts, the punctate cytosolic signals of GFP-SCAMP1 and RFP-SYP61 were found to colocalize (Figure 22, panel 1). When these cells were treated with BFA at 10 μg/mL for one hour, aggregates containing both GFP-SCAMP1 and RFP-SYP61 were found (Figure 22, panel 2). Identical results were obtained in Arabidopsis cells (Figure 23, panels 1-2). Taken together, these results show that the two established TGN markers GFP-SCAMP1 and RFP-SYP61 were fully colocalized in both untreated and BFA-treated Arabidopsis and BY-2 cells.

I next performed similar studies to compare the TGN marker RFP-SYP61 with Golgi markers. As shown in Figure 22, in BY-2 cells co-expressing YFP-SYP61 and MAN1-RFP (panels 3 and 4), or RFP-SYP61 and GONST1-GFP (panels 5 and 6), no visible aggregation was observed in untreated cells where the two markers remained separated (Figure 22, panels 3 and 5). However, in cells treated with BFA at 10 μg/mL for one hour, BFA-induced aggregates were obvious for both reporters, where the BFA-induced aggregates derived from YFP-SYP61 or RFP-SYP61 were largely separated from those of MAN1-RFP or GONST1-GFP (Figure 22, panels 4 and 6). Again, similar results were obtained when identical experiments were carried out in Arabidopsis protoplasts (Figure 23, panels 3-6). Taken together, these results demonstrate that the BFA-induced aggregates from TGN/EE (marked by both GFP-SCAMP1 or RFP-SCAMP1 and YFP-SYP61 or RFP-SYP61) and Golgi apparatus (marked by MAN1-RFP and GONST1-GFP) were distinct compartments in the same BY-2 or Arabidopsis cells.

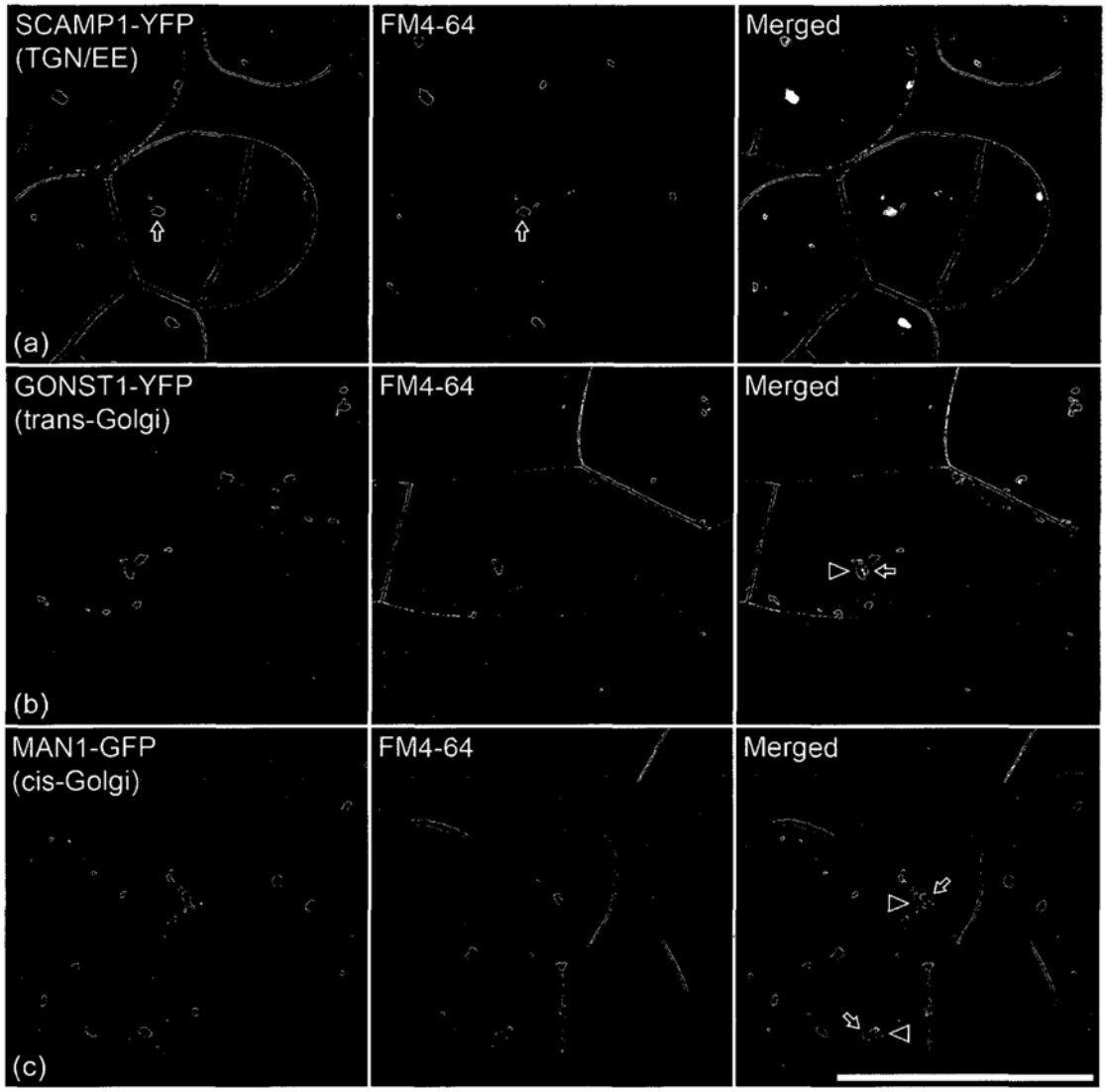

Figure 19. TGN-derived BFA-induced aggregates colocalize with the internalized endosomal marker FM4-64 dye in BY-2 cells.

Transgenic tobacco BY-2 cells expressing the TGN/EE marker SCAMP1-YFP (a) and the Golgi markers MAN1-GFP (b) or GONST1-YFP (c) were first treated with BFA at 10 μg/mL for 30 minutes, followed by FM4-64 uptake for another 30 minutes before samples were collected for confocal imaging. Arrows and arrowheads indicated examples of BFA-induced TGN/EE or Golgi aggregates respectively. Scale bar = 50 μm.

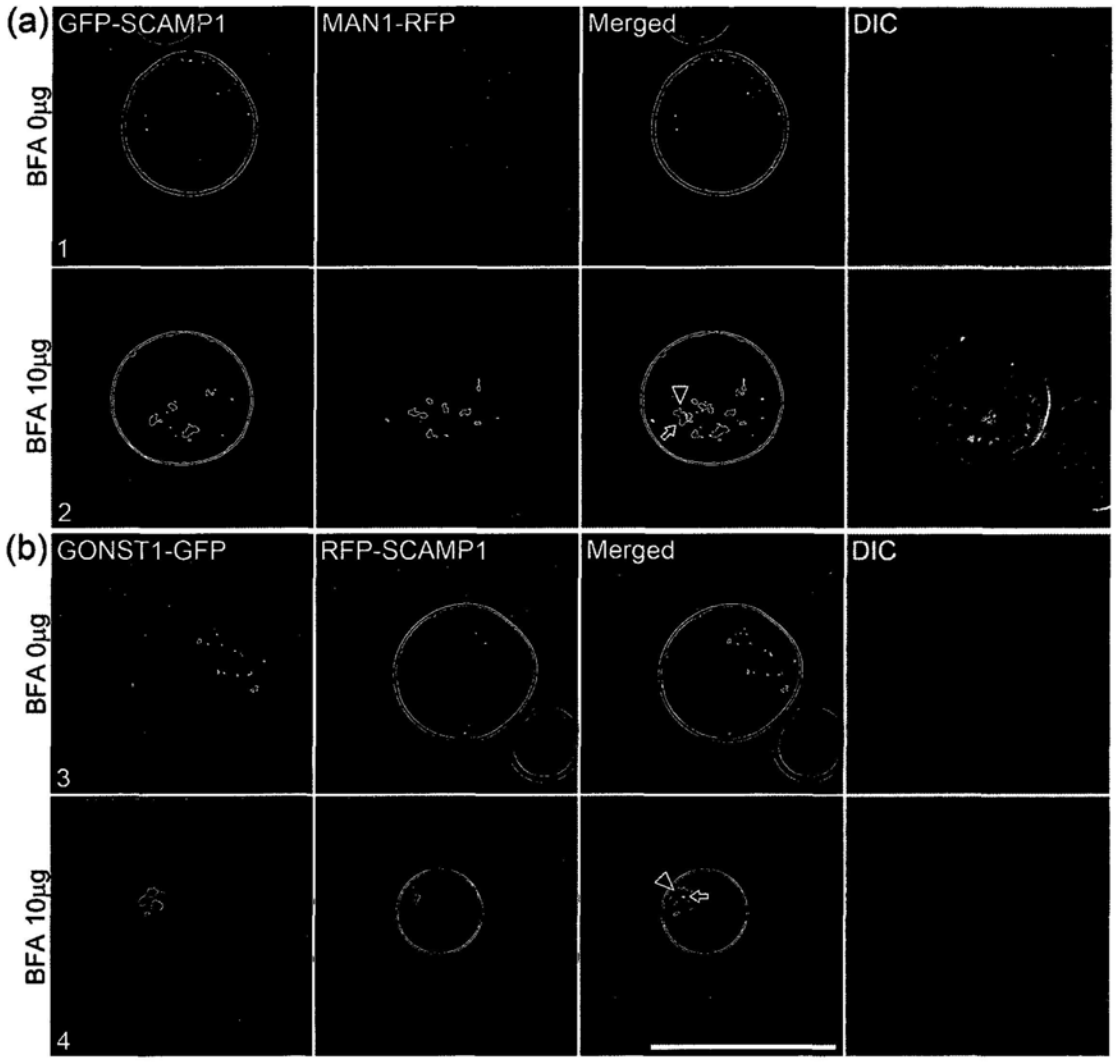

Figure 20. *In vivo* direct comparison of BFA-induced Golgi (marked by MAN1-RFP or GONST1-GFP) and TGN/EE (marked by SCAMP1) aggregates in living BY-2 cells.

Tobacco BY-2 protoplasts transiently co-expressed the TGN/EE marker SCAMP1 with the *cis*-Golgi marker MAN1-RFP (a) or the *trans*-Golgi marker GONST1-GFP (b) were first treated with BFA at 0 or 10μg/mL (as indicated) for one hour, followed by sample collections for confocal imaging. Arrows and arrowheads indicated BFA-induced TGN/EE or Golgi aggregates respectively. Scale bar = 50 μm.

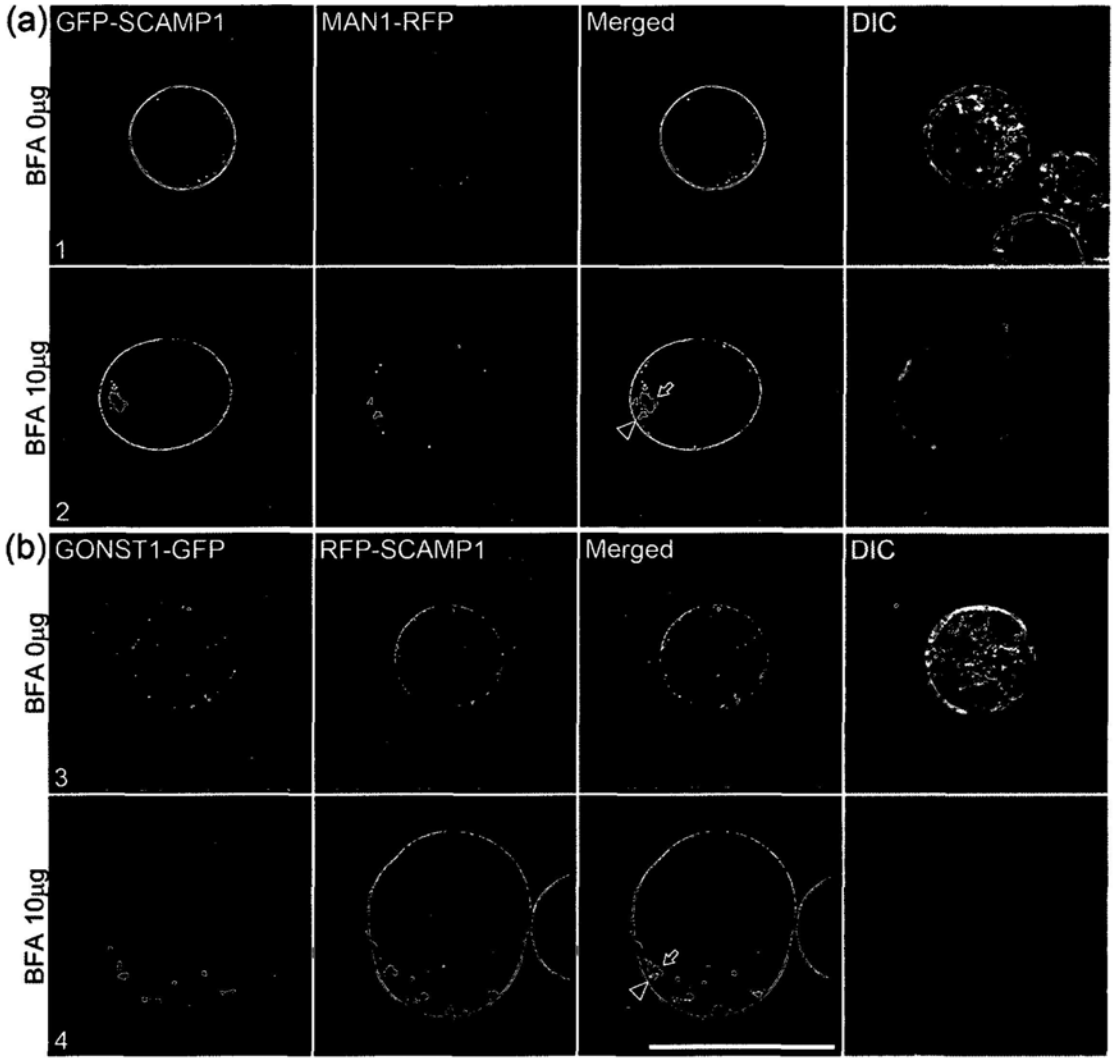

Figure 21. *In vivo* direct comparison of BFA-induced Golgi (marked by MAN1-RFP or GONST1-GFP) and TGN/EE (marked by SCAMP1) aggregates in living Arabidopsis cells.

Arabidopsis protoplasts transiently co-expressed the TGN/EE marker SCAMP1 with the *cis*-Golgi marker MAN1-RFP (a) or the *trans*-Golgi marker GONST1-GFP (b) were first treated with BFA at 0 or 10 μg/mL (as indicated) for one hour, followed by sample collections for confocal imaging. Arrows and arrowheads indicated BFA-induced TGN/EE or Golgi aggregates respectively. Scale bar = 50 μm.

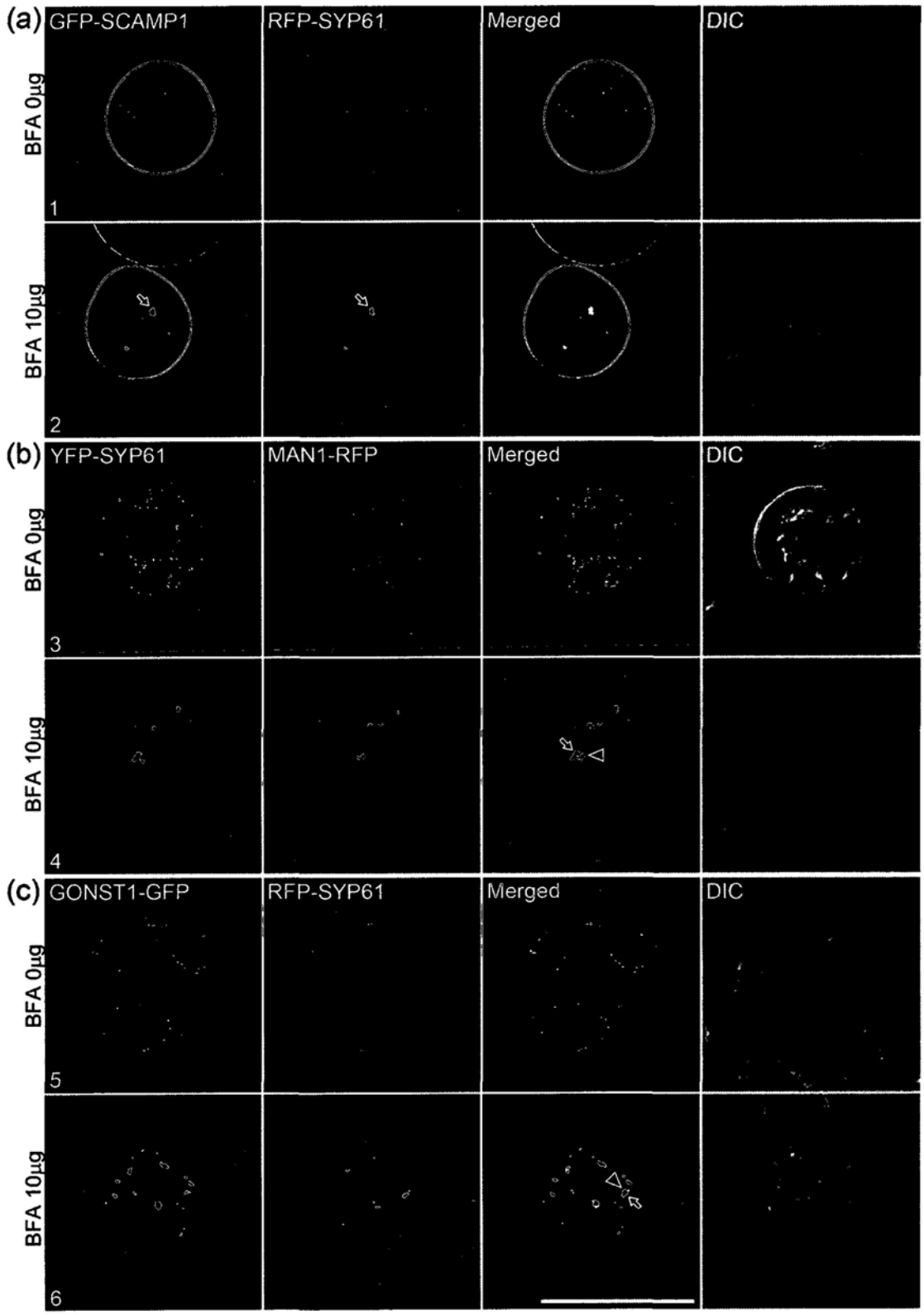
(a)
GFP-SCAMP1
RFP-SYP61
Merged
DIC
BFA 0μg
1
BFA 10μg
2
(b)
YFP-SYP61
MAN1-RFP
Merged
DIC
BFA 0μg
3
BFA 10μg
4
(c)
GONST1-GFP
RFP-SYP61
Merged
DIC
BFA 0μg
5
BFA 10μg
6

Figure 22. *In vivo* direct comparison of BFA-induced Golgi (marked by MAN1-RFP or GONST1-GFP) and TGN/EE (marked by SCAMP1 or SYP61) aggregates in living BY-2 cells.

Tobacco BY-2 protoplasts transiently co-expressed the TGN/EE marker SYP61 with GFP-SCAMP1 (a), MAN1-RFP (b) or GONST1-GFP (c) were first treated with BFA at 0 or 10μg/mL (as indicated) for one hour, followed by sample collections for confocal imaging. Arrows and arrowheads indicated BFA-induced TGN/EE or Golgi aggregates respectively. Scale bar = 50 μm.

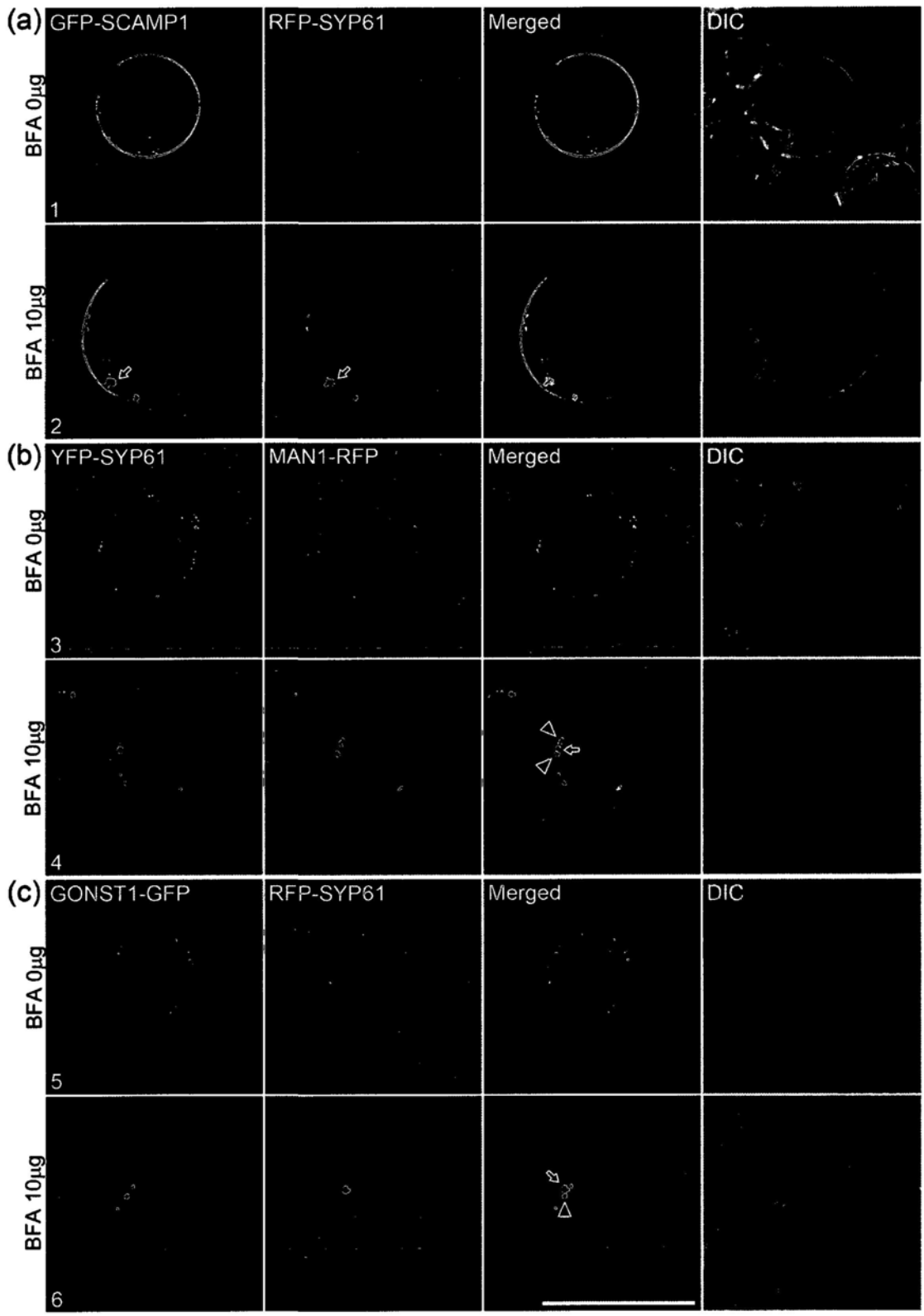
(a)
GFP-SCAMP1
RFP-SYP61
Merged
DIC
BFA 0μg
1
BFA 10μg
2
(b)
YFP-SYP61
MAN1-RFP
Merged
DIC
BFA 0μg
3
BFA 10μg
4
(c)
GONST1-GFP
RFP-SYP61
Merged
DIC
BFA 0μg
5
BFA 10μg
6

Figure 23. *In vivo* direct comparison of BFA-induced Golgi (marked by MAN1-RFP or GONST1-GFP) and TGN/EE (marked by SCAMP1 or SYP61) aggregates in living Arabidopsis cells.

Arabidopsis protoplasts transiently co-expressed the TGN/EE marker SYP61 with the GFP-SCAMP1 (a), MAN1-RFP (b) or the GONST1-GFP (c) were first treated with BFA at 0 or 10 μg/mL (as indicated) for one hour, followed by sample collections for confocal imaging. Arrows and arrowheads indicated BFA-induced TGN/EE or Golgi aggregates respectively. Scale bar = 50 μm.

3.3.2 De novo endocytic trafficking is not essential for the formation of the TGN/EE-derived aggregates

When cells co-expressing GFP-SCAMP1 and RFP-SYP61 were treated with BFA, these two TGN reporters colocalized together to the BFA-induced aggregates (Figure 22a and Figure 23a). Since tyrphostin A23 is a specific inhibitor of endocytosis whilest BFA inhibits exocytosis or recycling from TGN/EE to PM, I next wanted to find out if tyrphostin A23 would prevent GFP-SCAMP1 and/or RFP-SYP61 from reaching the TGN/EE aggregates by performing tyrphostin A23 pre-treatment for 30 min, followed by BFA treatment for another hour prior to confocal imaging. As shown in Figure 24, in BY-2 protoplasts transiently co-expressing GFP-SCAMP1 and MAN1-RFP or RFP-SYP61, pre-treatment of tyrphostin A23 prevented GFP-SCAMP1 from reaching the BFA-induced aggregates while both MAN1-RFP and RFP-SYP61 remained sensitive to subsequent BFA treatment in forming/reaching the aggregates (Figures 24a,b). In addition, pre-treatment of tyrphostin A23 also largely prevented the internalization of FM4-64 from reaching the YFP-SYP61-positive aggregates (Figure 24c), that would normally contained the same dye in cells without tyrphostin A23 treatment (e.g. Figure 19a). These results demonstrate that in the presence of the endocytosis inhibitor tyrphostin A23, BFA is still capable of inducing the formation of TGN/EE-derived (marked by RFP-SYP61) aggregates where both GFP-SCAMP1 and FM4-64 are largely excluded. Thus, de novo endocytic trafficking (as indicated by internalization of GFP-SCAMP1 and FM4-64) is not required for the formation of BFA-induced TGN/EE-derived

aggregates, even though endocytosed PM materials may substantially contribute to the aggregates. Figure 25 shows a working model for the formation of BFA-induced aggregates and the possible effects of BFA and tyrphostin A23 on the localization of SCAMPs in plant cells.

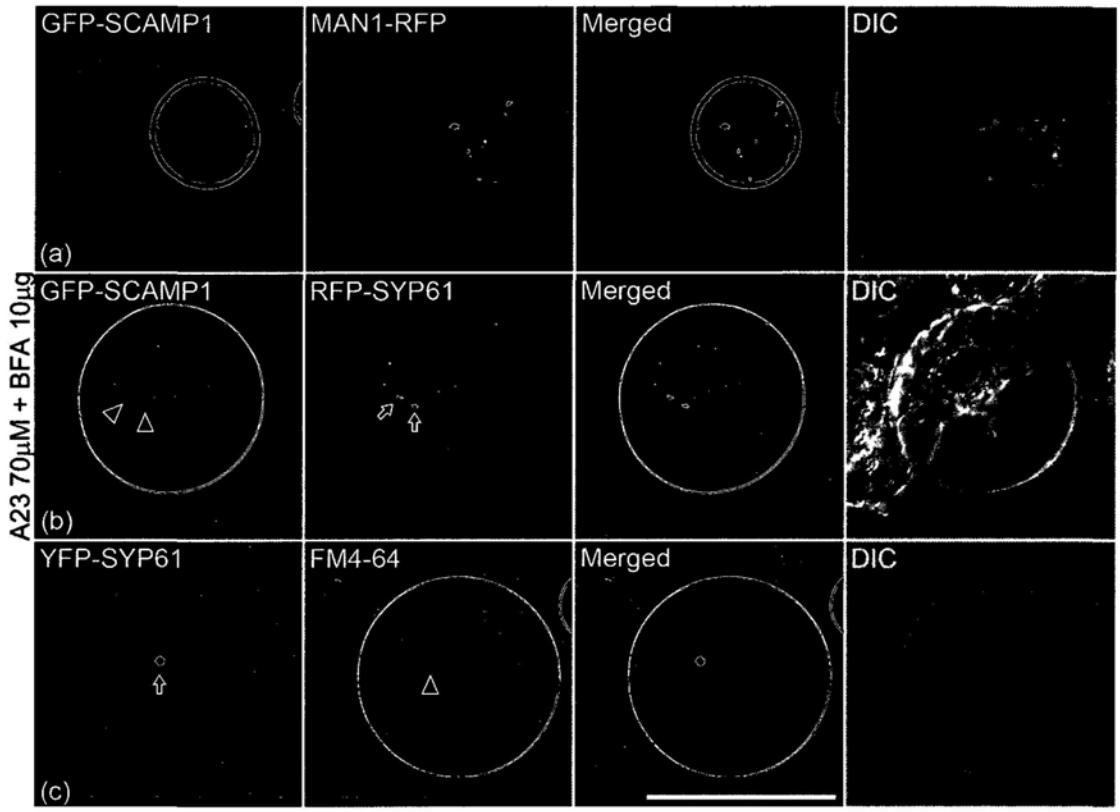

Figure 24. Tyrphostin A23 prevents BFA-induced SCAMP1 aggregation.
(a), (b) Tobacco BY-2 protoplasts transiently co-expressing GFP-SCAMP1 with MAN1-RFP or RFP-SYP61 were first pre-treated with tyrphostin A23 for 30 min, followed by BFA treatment for another 30min prior to confocal imaging.
(c) Tobacco BY-2 protoplasts expressing YFP-SYP61 were pre-treated with tyrphostin A23 for 30 min and BFA for another 30min and then followed by FM4-64 uptake for 30 min prior to confocal imaging. Scale bar = 50 μm.

3.4 Discussion

BFA has been a useful tool for organelle identification in the plant secretory and endocytic pathways. For example, the formation of BFA-induced aggregates was an indicator of Golgi apparatus in various plant cells including onion epidermic cells and tobacco BY-2 cells (Wee et al., 1998; Baldwin et al., 2001; Tse et al., 2004; Tse et al., 2006). Similarly, endosome-derived BFA aggregates or compartments were also used as an indicator for the identification of endosomal compartments in Arabidopsis root cells (Geldner et al., 2003; Dettmer et al., 2006; Jaillais et al., 2006; Jaillais et al., 2008). However, since BFA-induced aggregates derived from Golgi or endosome were morphologically similar under confocal imaging, and that the effects of BFA on various plant organelles have been studied by independent laboratories using different cell types and various BFA concentrations in either Arabidopsis root cells or other cell types over the past years, it would thus be interesting and necessary to find out the nature and possible relationship of these BFA-induced compartments in the same plant cells.

In this study, I also used tobacco BY-2 cells and Arabidopsis protoplasts expressing various fluorescent organelle reporters to study the nature of the BFA-induced compartments derived from Golgi and TGN/EE in the same plant cells, because both Golgi and TGN/EE are BFA sensitive to form aggregates in BY-2 cells (Tse et al., 2004; Tse et al., 2006; Lam et al., 2007b). When these BFA-induced aggregates from Golgi and TGN/EE were compared directly in the same cells and with the internalized endosomal marker FM4-64, they were found to be physically

distinct. In addition, the localization of SCAMP1 and FM4-64 onto the TGN/EE-derived BFA-induced aggregates was also endocytosis-dependent, because tyrphostin A23 pre-treatment specifically excludes these two markers from reaching the TGN/EE aggregates, indicating that TGN/EE aggregates could be derived from fusion of the TGN without involving much of the de novo endocytosed PM materials. Moreover, BFA could also inhibit the possible recycling pathway from TGN/EE to PM, thus causing accumulation of the newly endocytosed materials (Figure 25). Thus, the BFA-induced Golgi aggregates and TGN/EE aggregates are physically and morphologically distinct from each other in the same plant cells.

The unique response of various GFP-tagged punctate organelles to BFA treatment can also be used to define specific organelles and proteins in several ways. First, different concentrations of BFA can be used to differentiate PVC from TGN/EE and Golgi, where low concentrations of BFA (5-10 μg/mL) cause TGN/EE markers (SCAMP1 and SYP61) or Golgi markers (MAN1 and GONST1) to form aggregates whereas PVC marker (BP-80) remain unchanged but response to high concentrations of BFA (50 μg/mL) (Tse et al., 2006). Second, FM4-64 can be used to address the nature of aggregates derived from TGN/EE or Golgi. The TGN/EE aggregates are endosomal in nature that can be stained by FM4-64 in an uptake study, distinct from the secretory Golgi aggregates. Third, the endocytosis inhibitor tyrphostin A23 can be used together with BFA to understand the nature of various markers traffic to TGN. In the presence of A23, the TGN/PM recycling marker (SCAMP1) and FM4-64 were largely excluded from the BFA-induced aggregates labeled by the

TGN resident marker (SYP61). Thus, molecules that actively undergo endocytosis and recycling between TGN and PM can be differentiated from those residing in the TGN.

The TGN in plants has long time been regarded as an extension of the Golgi compartment. This notion was somehow supported by a 3D tomographic study showing that the TGN undergoes a maturation process from *trans*-most Golgi cisterna into the early TGN and finally the late TGN (Staehelin and Kang, 2008). However, when varies TGN markers (SYP61, SYP41 and SCAMP1) were directly compared the Golgi markers in the same cell, they were physically separated from each other (Uemura et al., 2004; Lam et al., 2007b; Foresti and Denecke, 2008). The plant TGN could be very closely associated or far away from the Golgi as confirmed by both confocal and EM studies (Uemura et al., 2004; Lam et al., 2007b; Foresti and Denecke, 2008). Moreover, when an endocytic tracker FM4-64 was applied to plant cells, the TGN is fast labeled with FM4-64 and thus endosomal in nature (Dettmer et al., 2006; Lam et al., 2007b; Chow et al., 2008). Here, using BFA as a tool, I again provide independent evidence that the BFA induced TGN/EE-derived aggregates are morphological and physically different from the Golgi-derived aggregates. Taken together, I conclude that the TGN in plant cells should not simply be regarded as the *trans*-most Golgi compartment but a totally different organelle.

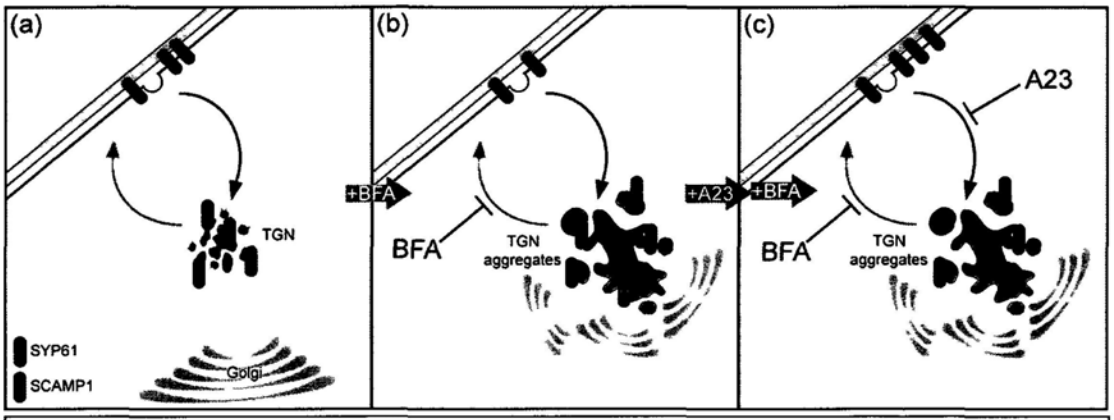

Figure 25. Possible effects of BFA and tyrphostin A23 on the localization of SCAMPs and the formation of BFA-induced TGN aggregates in plant cells.
(a) No drug treatment: SCAMP1 traffics normally from TGN to PM and internalizes from PM to TGN in cells while SYP61 resides at the TGN.
(b) BFA treatment: BFA induced both Golgi and TGN to form aggregates. Since BFA inhibits protein recycling from TGN back to the PM, causing TGN aggregation, materials including SCAMPs internalized from the PM are likely trapped into the TGN aggregates.
(c) Tyrphostin A23 treatment: A23 inhibits endocytosis while BFA prevents recycling. In the presence of BFA and A23, internalization of SCAMPs from PM is inhibited, thus excluding SCAMPs from the TGN aggregates whereas SYP61 still labels the TGN aggregates, indicating that de novo endocytic trafficking is not required for the formation of TGN aggregates. PM, plasma membrane; TGN, *trans*-Golgi network.

CHAPTER 4

Conclusions and Perspective

4.1 Conclusions from This Thesis Research

In summary, the following conclusions can be made from my thesis research:

1) Using several PM protein markers such as SCAMP1, FLS2 and AtLRR84A and protein trafficking inhibitors such as Sec12p, ARF1 mutants and ConcA as tools, I have provided direct evidence that transport of PM proteins to the PM is via an ER-Golgi-TGN pathway.
2) With detailed analysis on the sorting signals of SCAMP1, I have characterized multiple cytosolic and transmembrane sorting signals within SCAMP1 that are important for its trafficking along the secretory pathway.
3) With detailed analysis on the trafficking pathway of SCAMP1 and SCAMP1 mutants, I have placed the TGN in both ER to PM and ER to LV pathways and proposed that TGN functions as a sorting center for the three major pathways (i.e. ER to PM, ER to LV and PM to LV) in plant cells.
4) Using several Golgi (MAN1 and GONST1) and TGN (SCAMP1 and SYP61) protein markers, I show that BFA-induced aggregates derived from Golgi apparatus and TGN are morphologically distinct in plant cells. In addition, in the presence of the endocytosis inhibitor tyrphostin A23 that acts in a dosage- and time-dependent manner, SCAMP1 and FM4-64 are largely excluded from the TGN SYP61-positive BFA-induced aggregates, indicating that homotypic fusion of TGN rather than de novo endocytic trafficking is important for the formation of TGN/EE-derived BFA-induced aggregates.

Even though this thesis research has made significant contributions toward our

understanding on the trafficking mechanism of PM proteins and the nature of TGN, it only serves as the first step to further characterize the molecular machinery regulating membrane protein transport at the TGN.

Future perspectives are presented as follows.

4.2 Molecular machinery directing protein transport at the TGN

Emerging evidence suggest that TGN in plant cells is a sorting station where the three major trafficking pathways (ER to PM, ER to LV and PM to LV) converge (Lam et al., 2007b; Chow et al., 2008; Viotti et al., 2010). Trafficking of soluble proteins via the TGN depends on their sorting signals that are recognized by the membrane receptors. Soluble cargoes lacking specific sorting signals are transported via the default pathway and secreted into the extracellular space (Hadlington and Denecke, 2000). However, trafficking of membrane cargoes at the TGN is much more complicate and little is known about the molecular machinery regulating this process. Based on the current data, trafficking of single or polytopic membrane proteins via the TGN may follow different rules: For single transmembrane proteins, PM is the default location while specific transmembrane or cytosolic motifs could mediate protein transport from the TGN to PVC/LV (Brandizzi et al., 2002; daSilva et al., 2006); For polytopic transmembrane proteins, transmembrane signals are required for PM targeting while the PVC/LV are likely the default location. In future studies, forward genetics screening using polytopic (such as SCAMP1) or single (such as VSRs) transmembrane protein markers can be carried out to characterize

molecules involved in the sorting of membrane proteins at the TGN. For example, the TMD and CT of VSRs have been found to be essential and sufficient for their PVC/MVB localization and substitution of their NT with GFP has no effect on their location (Miao et al., 2008). Transgenic plants overexpressing these GFP tagged fusions can be good starting materials for future study. Theoretically, disturbance on the sorting machinery of VSRs at the TGN can cause the redistribution of VSRs from the PVC/MVB to PM since PM is the default location for single transmembrane proteins. Direct observation via the fluorescence microscopy can be done to screen the T-DNA insertion mutants.

References

Achour, L., Labbe-Jullie, C., Scott, M.G.H., and Marullo, S. (2008). An escort for GPCRs: implications for regulation of receptor density at the cell surface. Trends Pharm Sci 29, 528-535.

Alexandersson, E., Saalbach, G., Larsson, C., and Kjellbom, P. (2004). Arabidopsis plasma membrane proteomics identifies components of transport, signal transduction and membrane trafficking. Plant Cell Physiol 45, 1543-1556.

Baldwin, T.C., Handford, M.G., Yuseff, M.I., Orellana, A., and Dupree, P. (2001). Identification and characterization of GONST1, a golgi-localized GDP-mannose transporter in Arabidopsis. Plant Cell 13, 2283-2295.

Baluska, F., Hlavacka, A., Samaj, J., Palme, K., Robinson, D.G., Matoh, T., McCurdy, D.W., Menzel, D., and Volkmann, D. (2002). F-actin-dependent endocytosis of cell wall pectins in meristematic root cells. Insights from brefeldin A-induced compartments. Plant Physiol 130, 422-431.

Bard, F., and Malhotra, V. (2006). The formation of TGN-to-plasma-membrane transport carriers. Annu Rev Cell Dev Biol 22, 439-455.

Barman, S., and Nayak, D.P. (2000). Analysis of the transmembrane domain of influenza virus neuraminidase, a type II transmembrane glycoprotein, for apical sorting and raft association. J Virol 74, 6538-6545.

Brand, S.H., and Castle, J.D. (1993). SCAMP 37, a new marker within the general cell surface recycling system. EMBO J 12, 3753-3761.

Brand, S.H., Laurie, S.M., Mixon, M.B., and Castle, J.D. (1991). Secretory carrier membrane proteins 31-35 define a common protein composition among secretory carrier membranes. J Biol Chem 266, 18949-18957.

Brandizzi, F., Frangne, N., Marc-Martin, S., Hawes, C., Neuhaus, J.M., and Paris, N. (2002). The destination for single-pass membrane proteins is influenced markedly by the length of the hydrophobic domain. Plant Cell 14, 1077-1092.

Brandizzi, F., Hanton, S., daSilva, L.L.P., Boevink, P., Evans, D., Oparka, K., Denecke, J., and Hawes, C. (2003). ER quality control can lead to retrograde transport from the ER lumen to the cytosol and the nucleoplasm in plants. Plant J 34, 269-281.

Bulbarelli, A., Sprocati, T., Barberi, M., Pedrazzini, E., and Borgese, N. (2002). Trafficking of tail-anchored proteins: transport from the endoplasmic reticulum to the plasma membrane and sorting between surface domains in polarised epithelial cells. J Cell Sci 115, 1689-1702.

Castle, A., and Castle, D. (2005). Ubiquitously expressed secretory carrier

membrane proteins (SCAMPs) 1-4 mark different pathways and exhibit limited constitutive trafficking to and from the cell surface. J Cell Sci 118, 3769-3780.

Chatre, L., Wattelet-Boyer, V., Melser, S., Maneta-Peyret, L., Brandizzi, F., and Moreau, P. (2009). A novel di-acidic motif facilitates ER export of the syntaxin SYP31. J Exp Bot 60, 3157-3165.

Chow, C.M., Neto, H., Foucart, C., and Moore, I. (2008). Rab-A2 and Rab-A3 GTPases define a trans-golgi endosomal membrane domain in Arabidopsis that contributes substantially to the cell plate. Plant Cell 20, 101-123.

Coffin, W.F., Geiger, T.R., and Martin, J.M. (2003). Transmembrane domains 1 and 2 of the latent membrane protein 1 of Epstein-Barr virus contain a lipid raft targeting signal and play a critical role in cytostasis. J Virol 77, 3749-3758.

daSilva, L.L., Foresti, O., and Denecke, J. (2006). Targeting of the plant vacuolar sorting receptor BP80 is dependent on multiple sorting signals in the cytosolic tail. Plant Cell 18, 1477-1497.

daSilva, L.L., Snapp, E.L., Denecke, J., Lippincott-Schwartz, J., Hawes, C., and Brandizzi, F. (2004). Endoplasmic reticulum export sites and Golgi bodies behave as single mobile secretory units in plant cells. Plant Cell 16, 1753-1771.

De Matteis, M.A., and Luini, A. (2008). Exiting the Golgi complex. Nat Rev Mol Cell Biol 9, 273-284.

Delhaize, E., Gruber, B.D., Pittman, J.K., White, R.G., Leung, H., Miao, Y., Jiang, L., Ryan, P.R., and Richardson, A.E. (2007). A role for the AtMTP11 gene of Arabidopsis in manganese transport and tolerance. Plant J 51, 198-210.

Dettmer, J., Hong-Hermesdorf, A., Stierhof, Y.D., and Schumacher, K. (2006). Vacuolar H+-ATPase activity is required for endocytic and secretory trafficking in Arabidopsis. Plant Cell 18, 715-730.

Dunbar, L.A., Aronson, P., and Caplan, M.J. (2000). A transmembrane segment determines the steady-state localization of an ion-transporting adenosine triphosphatase. J Cell Biol 148, 769-778.

Dunkel, M., Latz, A., Schumacher, K., Wuller, T., Becker, D., and Hedrich, R. (2008). Targeting of Vacuolar Membrane Localized Members of the TPK Channel Family. Mol Plant 1, 938-949.

Fernandez-Chacon, R., Achiriloaie, M., Janz, R., Albanesi, J.P., and Sudhof, T.C. (2000). SCAMP1 function in endocytosis. J Biol Chem 275, 12752-12756.

Fernandez-Chacon, R., Alvarez de Toledo, G., Hammer, R.E., and Sudhof, T.C. (1999). Analysis of SCAMP1 function in secretory vesicle exocytosis by

means of gene targeting in mice. J Biol Chem 274, 32551-32554.

Foresti, O., and Denecke, J. (2008). Intermediate organelles of the plant secretory pathway: identity and function. Traffic 9, 1599-1612.

Foresti, O., daSilva, L.L., and Denecke, J. (2006). Overexpression of the Arabidopsis syntaxin PEP12/SYP21 inhibits transport from the prevacuolar compartment to the lytic vacuole in vivo. Plant Cell 18, 2275-2293.

Geldner, N., Friml, J., Stierhof, Y.D., Jurgens, G., and Palme, K. (2001). Auxin transport inhibitors block PIN1 cycling and vesicle trafficking. Nature 413, 425-428.

Geldner, N., Anders, N., Wolters, H., Keicher, J., Kornberger, W., Muller, P., Delbarre, A., Ueda, T., Nakano, A., and Jurgens, G. (2003). The Arabidopsis GNOM ARF-GEF mediates endosomal recycling, auxin transport, and auxin-dependent plant growth. Cell 112, 219-230.

Gohre, V., Spallek, T., Haweker, H., Mersmann, S., Mentzel, T., Boller, T., de Torres, M., Mansfield, J.W., and Robatzek, S. (2008). Plant pattern-recognition receptor FLS2 is directed for degradation by the bacterial ubiquitin ligase AvrPtoB. Curr Biol 18, 1824-1832.

Grebe, M., Xu, J., Mobius, W., Ueda, T., Nakano, A., Geuze, H.J., Rook, M.B., and Scheres, B. (2003). Arabidopsis sterol endocytosis involves actin-mediated trafficking via ARA6-positive early endosomes. Curr Biol 13, 1378-1387.

Haas, T.J., Sliwinski, M.K., Martinez, D.E., Preuss, M., Ebine, K., Ueda, T., Nielsen, E., Odorizzi, G., and Otegui, M.S. (2007). The Arabidopsis AAA ATPase SKD1 is involved in multivesicular endosome function and interacts with its positive regulator LYST-INTERACTING PROTEIN5. Plant Cell 19, 1295-1312.

Hadlington, J.L., and Denecke, J. (2000). Sorting of soluble proteins in the secretory pathway of plants. Curr Opin Plant Biol 3, 461-468.

Hanton, S.L., Matheson, L.A., and Brandizzi, F. (2006). Seeking a way out: export of proteins from the plant endoplasmic reticulum. Trends Plant Sci 11, 335-343.

Hanton, S.L., Matheson, L.A., Chatre, L., Rossi, M., and Brandizzi, F. (2007). Post-Golgi protein traffic in the plant secretory pathway. Plant Cell Rep 26, 1431-1438.

Hanton, S.L., Renna, L., Bortolotti, L.E., Chatre, L., Stefano, G., and Brandizzi, F. (2005). Diacidic motifs influence the export of transmembrane proteins from the endoplasmic reticulum in plant cells. Plant Cell 17, 3081-3093.

Hawes, C., Osterrieder, A., Hummel, E., and Sparkes, I. (2008). The plant ER-Golgi interface. Traffic 9, 1571-1580.

Hess, M.W., Muller, M., Debbage, P.L., Vetterlein, M., and Pavelka, M. (2000). Cryopreparation provides new insight into the effects of brefeldin A on the structure of the HepG2 Golgi apparatus. J Struct Biol 130, 63-72.

Hinz, G., Colanesi, S., Hillmer, S., Rogers, J.C., and Robinson, D.G. (2007). Localization of vacuolar transport receptors and cargo proteins in the Golgi apparatus of developing Arabidopsis embryos. Traffic 8, 1452-1464.

Hong, M., Zhou, F.F., and You, G.F. (2004). Critical amino acid residues in transmembrane domain 1 of the human organic anion transporter hOAT1. J Biol Chem 279, 31478-31482.

Hong, Z., Jin, H., Tzfira, T., and Li, J.M. (2008). Multiple Mechanism-Mediated Retention of a Defective Brassinosteroid Receptor in the Endoplasmic Reticulum of Arabidopsis. Plant Cell 20, 3418-3429.

Hubner, K., Windoffer, R., Hutter, H., and Leube, R.E. (2002). Tetraspan vesicle membrane proteins: synthesis, subcellular localization, and functional properties. Int Rev Cytol 214, 103-159.

Hwang, I. (2008). Sorting and anterograde trafficking at the Golgi apparatus. Plant Physiol 148, 673-683.

Jaillais, Y., Fobis-Loisy, I., Miege, C., and Gaude, T. (2008). Evidence for a sorting endosome in Arabidopsis root cells. Plant J 53, 237-247.

Jaillais, Y., Fobis-Loisy, I., Miege, C., Rollin, C., and Gaude, T. (2006). AtSNX1 defines an endosome for auxin-carrier trafficking in Arabidopsis. Nature 443, 106-109.

Jiang, L., and Rogers, J.C. (1998). Integral membrane protein sorting to vacuoles in plant cells: evidence for two pathways. J Cell Biol 143, 1183-1199.

Kawamoto, K., Yoshida, Y., Tamaki, H., Torii, S., Shinotsuka, C., Yamashina, S., and Nakayama, K. (2002). GBF1, a guanine nucleotide exchange factor for ADP-ribosylation factors, is localized to the cis-golgi and involved in membrane association of the COPI coat. Traffic 3, 483-495.

Kirsch, T., Paris, N., Butler, J.M., Beevers, L., and Rogers, J.C. (1994). Purification and Initial Characterization of a Potential Plant Vacuolar Targeting Receptor. Proc Natl Acad Sci USA 91, 3403-3407.

Kleine-Vehn, J., Leitner, J., Zwiewka, M., Sauer, M., Abas, L., Luschnig, C., and Friml, J. (2008). Differential degradation of PIN2 auxin efflux carrier by retromer-dependent vacuolar targeting. Proc Natl Acad Sci USA 105, 17812-17817.

Komatsu, S. (2008). Plasma membrane proteome in Arabidopsis and rice. Proteomics 8, 4137-4145.

Lam, S.K., Tse, Y.C., Robinson, D.G., and Jiang, L. (2007a). Tracking down the

elusive early endosome. Trends Plant Sci 12, 497-505.

Lam, S.K., Cai, Y., Hillmer, S., Robinson, D.G., and Jiang, L.W. (2008). SCAMPs highlight the developing cell plate during cytokinesis in tobacco BY-2 cells. Plant Physiol 147, 1637-1645.

Lam, S.K., Siu, C.L., Hillmer, S., Jang, S., An, G., Robinson, D.G., and Jiang, L. (2007b). Rice SCAMP1 defines clathrin-coated, trans-golgi-located tubular-vesicular structures as an early endosome in tobacco BY-2 cells. Plant Cell 19, 296-319.

Lam, S.K., Cai, Y., Tse, Y.C., Wang, J., Pimpl, P., Chan, H.Y.E., Xia, J., and Jiang, L.W. (2009). The BFA-induced compartments from Golgi apparatus and trans-Golgi network/early endosome are morphologically distinct in plant cells. Plant J 60, 865-881.

Langhans, M., Marcote, M.J., Pimpl, P., Virgili-Lopez, G., Robinson, D.G., and Aniento, F. (2008). In vivo trafficking and localization of p24 proteins in plant cells. Traffic 9, 770-785.

Lee, J., and Sugden, B. (2007). Membrane leucine heptad contributes to trafficking, signaling, and transformation by latent membrane protein 1. J Virol 81, 9121-9130.

Lefebvre, B., Batoko, H., Duby, G., and Boutry, M. (2004). Targeting of a Nicotiana plumbaginifolia H+ -ATPase to the plasma membrane is not by default and requires cytosolic structural determinants. Plant Cell 16, 1772-1789.

Letourneur, F., and Cosson, P. (1998). Targeting to the endoplasmic reticulum in yeast cells by determinants present in transmembrane domains. J Biol Chem 273, 33273-33278.

Li, Y.B., Rogers, S.W., Tse, Y.C., Lo, S.W., Sun, S.S., Jauh, G.Y., and Jiang, L. (2002). BP-80 and homologs are concentrated on post-Golgi, probable lytic prevacuolar compartments. Plant Cell Physiol 43, 726-742.

Liu, C.W., Corboy, M.J., DeMartino, G.N., and Thomas, P.J. (2003). Endoproteolytic activity of the proteasome. Science 299, 408-411.

Mancias, J.D., and Goldberg, J. (2005). Exiting the endoplasmic reticulum. Traffic 6, 278-285.

Marmagne, A., Rouet, M.A., Ferro, M., Rolland, N., Alcon, C., Joyard, J., Garin, J., Barbier-Brygoo, H., and Ephritikhine, G. (2004). Identification of new intrinsic proteins in Arabidopsis plasma membrane proteome. Mol Cell Proteomics 3, 675-691.

Marshall, R.S., Jolliffe, N.A., Ceriotti, A., Snowden, C.J., Lord, J.M., Frigerio, L., and Roberts, L.M. (2008). The role of CDC48 in the retro-translocation

of non-ubiquitinated toxin substrates in plant cells. J Biol Chem 283, 15869-15877.

Martin, P.E.M., Blundell, G., Ahmad, S., Errington, R.J., and Evans, W.H. (2001). Multiple pathways in the trafficking and assembly of connexin 26, 32 and 43 into gap junction intercellular communication channels. J Cell Sci 114, 3845-3855.

Mellman, I., and Warren, G. (2000). The road taken: past and future foundations of membrane traffic. Cell 100, 99-112.

Meusser, B., Hirsch, C., Jarosch, E., and Sommer, T. (2005). ERAD: the long road to destruction. Nat Cell Biol 7, 766-772.

Miao, Y., and Jiang, L. (2007). Transient expression of fluorescent fusion proteins in protoplasts of suspension cultured cells. Nat Protoc 2, 2348-2353.

Miao, Y., Yan, P.K., Kim, H., Hwang, I., and Jiang, L. (2006). Localization of green fluorescent protein fusions with the seven Arabidopsis vacuolar sorting receptors to prevacuolar compartments in tobacco BY-2 cells. Plant Physiol 142, 945-962.

Miao, Y., Li, K.Y., Li, H.Y., Yao, X., and Jiang, L. (2008). The vacuolar transport of aleurain-GFP and 2S albumin-GFP fusions is mediated by the same pre-vacuolar compartments in tobacco BY-2 and Arabidopsis suspension cultured cells. Plant J 56, 824-839.

Mikosch, M., Hurst, A.C., Hertel, B., and Homann, U. (2006). Diacidic motif is required for efficient transport of the K+ channel KAT1 to the plasma membrane. Plant Physiol 142, 923-930.

Muller, J., Piffanelli, P., Devoto, A., Miklis, M., Elliott, C., Ortmann, B., Schulze-Lefert, P., and Panstruga, R. (2005). Conserved ERAD-like quality control of a plant polytopic membrane protein. Plant Cell 17, 149-163.

Nakatsukasa, K., Huyer, G., Michaelis, S., and Brodsky, J.L. (2008). Dissecting the ER-associated degradation of a misfolded polytopic membrane protein. Cell 132, 101-112.

Nebenfuhr, A., Ritzenthaler, C., and Robinson, D.G. (2002). Brefeldin A: deciphering an enigmatic inhibitor of secretion. Plant Physiol 130, 1102-1108.

Nebenfuhr, A., Gallagher, L.A., Dunahay, T.G., Frohlick, J.A., Mazurkiewicz, A.M., Meehl, J.B., and Staehelin, L.A. (1999). Stop-and-go movements of plant Golgi stacks are mediated by the acto-myosin system. Plant Physiol 121, 1127-1142.

Nufer, O., Kappeler, F., Guldbrandsen, S., and Hauri, H.P. (2003). ER export of

ERGIC-53 is controlled by cooperation of targeting determinants in all three of its domains. J Cell Sci 116, 4429-4440.

Nuhse, T.S., Bottrill, A.R., Jones, A.M., and Peck, S.C. (2007). Quantitative phosphoproteomic analysis of plasma membrane proteins reveals regulatory mechanisms of plant innate immune responses. Plant J 51, 931-940.

Otegui, M.S., and Spitzer, C. (2008). Endosomal functions in plants. Traffic 9, 1589-1598.

Otegui, M.S., Herder, R., Schulze, J., Jung, R., and Staehelin, L.A. (2006). The proteolytic processing of seed storage proteins in Arabidopsis embryo cells starts in the multivesicular bodies. Plant Cell 18, 2567-2581.

Phillipson, B.A., Pimpl, P., daSilva, L.L., Crofts, A.J., Taylor, J.P., Movafeghi, A., Robinson, D.G., and Denecke, J. (2001). Secretory bulk flow of soluble proteins is efficient and COPII dependent. Plant Cell 13, 2005-2020.

Pimpl, P., Hanton, S.L., Taylor, J.P., Pinto-daSilva, L.L., and Denecke, J. (2003). The GTPase ARF1p controls the sequence-specific vacuolar sorting route to the lytic vacuole. Plant Cell 15, 1242-1256.

Pimpl, P., Movafeghi, A., Coughlan, S., Denecke, J., Hillmer, S., and Robinson, D.G. (2000). In situ localization and in vitro induction of plant COPI-coated vesicles. Plant Cell 12, 2219-2236.

Pimpl, P., Taylor, J.P., Snowden, C., Hillmer, S., Robinson, D.G., and Denecke, J. (2006). Golgi-mediated vacuolar sorting of the endoplasmic reticulum chaperone BiP may play an active role in quality control within the secretory pathway. Plant Cell 18, 198-211.

Preuss, M.L., Serna, J., Falbel, T.G., Bednarek, S.Y., and Nielsen, E. (2004). The Arabidopsis Rab GTPase RabA4b localizes to the tips of growing root hair cells. Plant Cell 16, 1589-1603.

Reggiori, F., Black, M.W., and Pelham, H.R.B. (2000). Polar transmembrane domains target proteins to the interior of the yeast vacuole. Mol Biol Cell 11, 3737-3749.

Richter, S., Voss, U., and Jurgens, G. (2009). Post-golgi traffic in plants. Traffic 10, 819-828.

Richter, S., Geldner, N., Schrader, J., Wolters, H., Stierhof, Y.D., Rios, G., Koncz, C., Robinson, D.G., and Jurgens, G. (2007). Functional diversification of closely related ARF-GEFs in protein secretion and recycling. Nature 448, 488-492.

Robatzek, S., Chinchilla, D., and Boller, T. (2006). Ligand-induced endocytosis of the pattern recognition receptor FLS2 in Arabidopsis. Gene Dev 20, 537-542.

Robert, S., Chary, S.N., Drakakaki, G., Li, S.D., Yang, Z.B., Raikhel, N.V., and

Hicks, G.R. (2008). Endosidin1 defines a compartment involved in endocytosis of the brassinosteroid receptor BRI1 and the auxin transporters PIN2 and AUX1. Proc Natl Acad Sci USA 105, 8464-8469.

Robinson, D.G., Albrecht, S., and Moriysu, Y. (2004). The V-ATPase inhibitors concanamycin A and bafilomycin A lead to Golgi swelling in tobacco BY-2 cells. Protoplasma 224, 255-260.

Robinson, D.G., Jiang, L., and Schumacher, K. (2008). The endosomal system of plants: charting new and familiar territories. Plant Physiol 147, 1482-1492.

Romisch, K. (2005). Endoplasmic reticulum-associated degradation. Annu Rev Cell Dev Biol 21, 435-456.

Ronchi, P., Colombo, S., Francolini, M., and Borgese, N. (2008). Transmembrane domain-dependent partitioning of membrane proteins within the endoplasmic reticulum. J Cell Biol 181, 105-118.

Samaj, J., Baluska, F., Voigt, B., Schlicht, M., Volkmann, D., and Menzel, D. (2004). Endocytosis, actin cytoskeleton, and signaling. Plant Physiol 135, 1150-1161.

Sanderfoot, A.A., Ahmed, S.U., Marty-Mazars, D., Rapoport, I., Kirchhausen, T., Marty, F., and Raikhel, N.V. (1998). A putative vacuolar cargo receptor partially colocalizes with AtPEP12p on a prevacuolar compartment in Arabidopsis roots. Proc Natl Acad Sci USA 95, 9920-9925.

Satiat-Jeunemaitre, B., and Hawes, C. (1994). G.A.T.T. (A General Agreement on Traffic and Transport) and Brefeldin A in Plant Cells. Plant Cell 6, 463-467.

Satiat-Jeunemaitre, B., Cole, L., Bourett, T., Howard, R., and Hawes, C. (1996). Brefeldin A effects in plant and fungal cells: something new about vesicle trafficking? J Microsc 181, 162-177.

Sato, K., and Nakano, A. (2007). Mechanisms of COPII vesicle formation and protein sorting. Febs Lett 581, 2076-2082.

Sato, K., Sato, M., and Nakano, A. (2003). Rer1p, a retrieval receptor for ER membrane proteins, recognizes transmembrane domains in multiple modes. Mol Biol Cell 14, 3605-3616.

Schamel, W.W.A., Kuppig, S., Becker, B., Gimborn, K., Hauri, H.P., and Reth, M. (2003). A high-molecular-weight complex of membrane proteins BAP29/BAP31 is involved in the retention of membrane-bound IgD in the endoplasmic reticulum. Proc Natl Acad Sci USA 100, 9861-9866.

Schoberer, J., Vavra, U., Stadlmann, J., Hawes, C., Mach, L., Steinkellner, H., and Strasser, R. (2009). Arginine/lysine residues in the cytoplasmic tail promote ER export of plant glycosylation enzymes. Traffic 10, 101-115.

Sciaky, N., Presley, J., Smith, C., Zaal, K.J., Cole, N., Moreira, J.E., Terasaki,

M., Siggia, E., and Lippincott-Schwartz, J. (1997). Golgi tubule traffic and the effects of brefeldin A visualized in living cells. J Cell Biol 139, 1137-1155.

Seaman, M.N. (2008). Endosome protein sorting: motifs and machinery. Cell Mol Life Sci 65, 2842-2858.

Sieben, C., Mikosch, M., Brandizzi, F., and Homann, U. (2008). Interaction of the K(+)-channel KAT1 with the coat protein complex II coat component Sec24 depends on a di-acidic endoplasmic reticulum export motif. Plant J 56, 997-1006.

Staehelin, L.A., and Kang, B.H. (2008). Nanoscale architecture of endoplasmic reticulum export sites and of Golgi membranes as determined by electron tomography. Plant Physiol 147, 1454-1468.

Takano, J., Miwa, K., Yuan, L., von Wiren, N., and Fujiwara, T. (2005). Endocytosis and degradation of BOR1, a boron transporter of Arabidopsis thaliana, regulated by boron availability. Proc Natl Acad Sci USA 102, 12276-12281.

Tanaka, H., Kitakura, S., De Rycke, R., De Groodt, R., and Friml, J. (2009). Fluorescence imaging-based screen identifies ARF GEF component of early endosomal trafficking. Curr Biol 19, 391-397.

Toyooka, K., Goto, Y., Asatsuma, S., Koizumi, M., Mitsui, T., and Matsuoka, K. (2009). A mobile secretory vesicle cluster involved in mass transport from the Golgi to the plant cell exterior. Plant Cell 21, 1212-1229.

Tsai, B., Ye, Y.H., and Rapoport, T.A. (2002). Retro-translocation of proteins from the endoplasmic reticulum into the cytosol. Nat Rev Mol Cell Bio 3, 246-255.

Tse, Y.C., Lo, S.W., Hillmer, S., Dupree, P., and Jiang, L. (2006). Dynamic response of prevacuolar compartments to brefeldin a in plant cells. Plant Physiol 142, 1442-1459.

Tse, Y.C., Mo, B., Hillmer, S., Zhao, M., Lo, S.W., Robinson, D.G., and Jiang, L. (2004). Identification of multivesicular bodies as prevacuolar compartments in Nicotiana tabacum BY-2 cells. Plant Cell 16, 672-693.

Uemura, T., Ueda, T., Ohniwa, R.L., Nakano, A., Takeyasu, K., and Sato, M.H. (2004). Systematic analysis of SNARE molecules in Arabidopsis: dissection of the post-Golgi network in plant cells. Cell Struct Funct 29, 49-65.

Viotti, C., Bubeck, J., Stierhof, Y.D., Krebs, M., Langhans, M., Berg, W.V.E., Dongen, W.V., Richter, S., Geldner, N., Takano, J., Jurgens, G., Vries, S.C., Robinson, D.G., and Schumacher, K. (2010). Endocytic and Secretory Traffic in Arabidopsis Merge in the Trans-Golgi Network/Early Endosome, an Independent and Highly Dynamic Organelle. Plant Cell, in press.

Wang, J., Suen, P.K., Xu, Z.F., and Jiang, L. (2009). A 64 kDa sucrose binding protein is membrane-associated and tonoplast-localized in developing mung bean seeds. J Exp Bot 60, 629-639.

Wang, J., Li, Y., Lo, S.W., Hillmer, S., Sun, S.S., Robinson, D.G., and Jiang, L. (2007). Protein mobilization in germinating mung bean seeds involves vacuolar sorting receptors and multivesicular bodies. Plant Physiol 143, 1628-1639.

Wang, J.M., Zhang, L.L., Yao, Y., Viroonchatapan, N., Rothe, E., and Wang, Z.Z. (2002). A transmembrane motif governs the surface trafficking of nicotinic acetylcholine receptors. Nature Neurosci 5, 963-970.

Wee, E.G., Sherrier, D.J., Prime, T.A., and Dupree, P. (1998). Targeting of active sialyltransferase to the plant Golgi apparatus. Plant Cell 10, 1759-1768.

Zelazny, E., Miecielica, U., Borst, J.W., Hemminga, M.A., and Chaumont, F. (2008). An N-terminal diacidic motif is required for trafficking of the maize aquaporins ZmPIP2;4 and ZmPIP2;5 to the plasma membrane. Plant J 57, 346-355

Zheng, H., Camacho, L., Wee, E., Batoko, H., Legen, J., Leaver, C.J., Malho, R., Hussey, P.J., and Moore, I. (2005). A Rab-E GTPase mutant acts downstream of the Rab-D subclass in biosynthetic membrane traffic to the plasma membrane in tobacco leaf epidermis. Plant Cell 17, 2020-2036.

List of Publications

1. Lam, S.K., **Cai, Y.**, Tse, Y.C., Wang, J., Law, A.H., Pimpl, P., Chan, H.Y., Xia, J., and Jiang, L. (2009). BFA-induced compartments from the Golgi apparatus and trans-Golgi network/early endosome are distinct in plant cells. Plant J 60, 865-881. **(Co-first author)**

2. Wang, J., **Cai, Y.**, Miao, Y., Lam, S.K., and Jiang, L. (2009). Wortmannin induces homotypic fusion of plant prevacuolar compartments. J Exp Bot 60, 3075-3083.

3. Lam, S.K., **Cai, Y.**, Hillmer, S., Robinson, D.G., and Jiang, L. (2008). SCAMPs highlight the developing cell plate during cytokinesis in tobacco BY-2 cells. Plant Physiol 147, 1637-1645.